NOTICE

The quality of this microform is heavily dependent upon the quality of the original thesis submitted for microfilming. Every effort has been made to ensure the highest quality of reproduction possible.

If pages are missing, contact the university which granted the degree.

Some pages may have indistinct print especially if the original pages were typed with a poor typewriter ribbon or if the university sent us an inferior photocopy.

Reproduction in full or in part of this microform is governed by the Canadian Copyright Act, R.S.C. 1970, c. C-30, and subsequent amendments.

AVIS

La qualité de cette microforme dépend grandement de la qualité de la thèse soumise au microfilmage. Nous avons tout fait pour assurer une qualité supérieure de reproduction.

S'il manque des pages, veuillez communiquer avec l'université qui a conféré le grade.

La qualité d'impression de certaines pages peut laisser à désirer, surtout si les pages originales ont été dactylographiées à l'aide d'un ruban usé ou si l'université nous a fait parvenir une photocopie de qualité inférieure.

La reproduction, même partielle, de cette microforme est soumise à la Loi canadienne sur le droit d'auteur, SRC 1970, c. C-30, et ses amendements subséquents.

RIDE PERFORMANCE OF LATERAL SEAT SUSPENSIONS WITH DYNAMIC VIBRATION ABSORBERS IN OFF-ROAD VEHICLES

Youcai Chen

A Thesis

In

The Department

Of

Mechanical Engineering

Presented In Partial Fulfillment Of The Requirements
For The Master Of Engineering At
Concordia University
Montréal, Québec, Canada

December, 1990

ISBN 0-315-64693-4

RIDE PERFORMANCE OF LATERAL SEAT SUSPENSIONS WITH DYNAMIC VIBRATION ABSORBERS IN OFF-ROAD VEHICLES

ABSTRACT

Youcai Chen

The lateral vibration of off-road vehicles has been found to be quite severe and needs to be isolated. The lateral ride performance through a passive seat suspension can not be adequately improved due to the very low excitation frequency. In this investigation, three different schemes of lateral seat suspensions with vibration absorbers are proposed and their performances are evaluated. Influence of absorber parameters and primary system damping ratio on the motion response of both driver and absorber mass are investigated through parametric study as well as parameter optimization. The trade-off between the acceleration and the relative displacement response is investigated through sensitivity study. Results show that a passive lateral seat suspension with a dynamic vibration absorber can produce significant attenuation of lateral vibration with small increase in relative displacement response of the driver mass. Lateral seat suspensions with vibration absorber provide approximately 80% vibration attenuation in acceleration PSD response for the driver mass compared to an optimal lateral seat suspension without an absorber. Also, the vibration isolation performance with absorber is comparable or even slightly better than a system with optimal cab and seat suspensions. Among the three types of vibration absorbers for the

seat suspension, the three-element absorber provides marginally better vibration isolation performance over the others. The suspension with dual absorbers can also effectively reduce the vibration response of vehicle operator at the tuned frequency without much deterioration of ride performance at other excitation frequencies and is slightly better than a suspension system with a single conventional absorber. The lateral suspension with proper selection of absorber tuning ratio can simultaneously reduce the acceleration and the relative displacement response of the driver mass. In order to achieve a good compromise between the ride performance and the weight of the resultant system, the absorber mass ratio should be chosen less than 0.4.

ACKNOWLEDGEMENTS

The author is greatly indebted to his supervisor, Dr. S.Sankar for suggesting the project and providing continued encouragement, guidance and support during the course of this endeavour.

The author wishes to express his sincere thanks to the CONCAVE personnel for their assistance and time during the investigation.

The financial support from the CONCAVE Research Centre is gratefully acknowledged.

Montréal, Canada

December, 1990 Y.Chen

TABLE OF CONTENTS

CHAPTER 3

Lateral Seat Suspension with a Single Absorber

LIST OF FIGURES

LIST OF TABLES

NOMENCLATURE

a	Acceleration, m/s^2
b_{i1}, b_{i2}	Intercept of the ISO Recommended RMS Acceleration Limits for FDP in Transverse Vibrations
C_a	Absorber damping coefficient, N·s/m
C_c	Critical damping coefficient, N·s/m
C_1	Main system damping coefficient, N·s/m
C_2	Absorber damping coefficient, N·s/m
C_3	Absorber damping coefficient, N·s/m
D	Sign of the derivative $\frac{d}{dt}$
f	Excitation frequency, Hz
f_u, f_l	Upper and lower cut-off frequency, Hz
K_a	Absorber stiffness ratio, N/m
K_{a1}, K_{a2}	Absorber stiffness ratio, N/m
K_1	Main system stiffness ratio, N/m
M_a	Absorber mass, Kg
M_1	Seat and driver mass, Kg
M_2, M_3	Absorber mass, Kg
m_{i1}, m_{i2}	Slope of the ISO Recommended RMS Acceleration Limits for FDP in Transverse Vibrations
Q	Absorber stiffness ratio
$S_y(\omega)$	Acceleration power spectral density
$S_{\dot{y}}(\omega)$	Displacement power spectral density
T_1	Absolute transmissibility of driver mass, Y_1/Y_o
T_{r1}	Relative transmissibility of driver mass, Y_1-Y_o/Y_o
T_{r2}	Relative transmissibility of absorber mass, Y_2-Y_o/Y_o
$W(f_1)$	Weighting factor

Y_o	Lateral displacement input
$\ddot{Y}_o$	Lateral acceleration input
Y_{r1}	Relative displacement response of the driver mass, Y_1-Y_o
Y_{r2}	Relative displacement response of the absorber mass, Y_2-Y_o
Y_1	Absolute displacement response of the driver mass
$\ddot{Y}_1$	Absolute acceleration response of the driver mass
Y_2	Absolute displacement response of the absorber mass
Y_3	Absolute displacement response of the absorber mass
α	Absorber tuning ratio, ω_a/ω_1
α_1	Absorber tuning ratio, ω_2/ω_1
α_2	Absorber tuning ratio, ω_3/ω_1
ξ_1	main system damping ratio
ξ_2	Absorber damping ratio
ξ_3	Absorber damping ratio
ω	Angular frequency of the lateral excitations
ω_1	Natural frequency of the primary system
ω_2	Natural frequency of the vibration absorber
ω_3	Natural frequency of the vibration absorber
ω_a	Natural frequency of the vibration absorber
μ	Absorber mass ratio, M_a/M_1
μ_1	Absorber mass ratio, M_{a1}/M_1
μ_2	Absorber mass ratio, M_{a2}/M_1
Δ	denominator of transmissibility functions
β	Absorber mass ratio, M_{a1}/M_{a2}

CHAPTER 1

Introduction

1.1 General Introduction

In recent years, the importance of providing better ride comfort and safety for off-road vehicle operators has been increasingly emphasized. As the size and power of vehicles increase for high speed operations, comfort features become important factors in determining operator's work performance. Ride comfort associated with vehicle vibrations has become particular concern of off-road vehicle designer's.

The ride quality of off-road vehicles is a measure of a degree of comfort for the operator so as to enable the operator to retain suitable control of the vehicle and perhaps its ancillary devices. Although the term ride quality could include such factors as seat spacing, temperature, air quality, humidity, and noise levels, it has generally come to refer to the vibration environment to which drivers are exposed to.

The vibration levels experienced by off-road vehicle drivers have long been recognized to be severe[1 - 5]. The drivers have been exposed to the excessive vibration in all of the three translational modes — vertical, longitudinal, and lateral. The rotational modes of vibrations were also found to be severe. The agricultural tractor vibrations are of low excitation frequencies and have significant effect on human performance, comfort, and health. For most farming operations, the vibration levels, as measured at the operator's seat, need to be reduced by roughly 60% or more in the vertical, longitudinal and lateral

directions in order to meet the safe 8-hour ISO exposure criteria[6]. It is apparent that operators of off-road vehicles must be isolated to some degree from vehicle vibrations.

Ride comfort for off-road vehicle operators depends largely upon the vibration isolation characteristics of the vehicle. Since most off-road vehicles do not have suspension at axles and are directly supported by tires which have little inherent damping, vibrations induced from terrain surfaces can be easily transmitted to the operator. Therefore, proper design of vehicle seat and/or cab suspensions are very important to achieve the operator's ride comfort.

1.2 Survey of Past Works

With the increasing concern of driver's health and productivity, research on off-road vehicle ride improvement has gained a lot of attention. To reduce operator's fatigue from shock and vibration, ergonomic considerations have become an important design criteria for vehicle development. Claar II, Buchele and Sheth[5] made a survey on the improvement of off-road vehicle ride. Improvement of vehicle ride can be achieved by the following approaches:

1) suitable tires;
2) seat suspension;
3) vehicles with operator cab suspension; and
4) vehicle with front axle and rear axle suspensions.

Each of these approaches offers respective advantages, limitations, and performance characteristics. The discussions on this was made by several

researchers[1,4,5,6,7]. Of the possible approaches, the concepts of seat suspension and cab suspension are usually preferred due to their easier adaptability and less modification to an existing vehicle design configuration[4]. Theoretically, the driver's ride comfort can be considerably improved by using seat or cab suspensions. One main difference between these two approaches is the resulting large relative displacement between the driver and vehicle instrument panel, in the case of a suspended seat. From the point of an ergonomic design, suspended cabs should be preferred because they can provide better working environment for drivers. Cab suspensions not only can attenuate the vibration level but also can provide better working environment for the driver. Since seat suspension has the advantages of simplicity and low cost, research on the improvement of seat suspension is still pursued. Besides, suspended seat can be easily added to a suspended cab to further improve the ride performance.

1.2.1 Cab Suspension

Over the past two decades, considerable research efforts have been devoted to the development, simulation and optimization of cab suspension models.

Roley[2] developed a set of computer models for the passive, active, and semi-active cab suspension systems to compare their relative performance for typical tractor cab vibrations. A four degree-of-freedom (bounce, pitch, lateral and longitudinal) cab with interchangeable passive, active and semi-active suspension elements was developed. Real time vibration acceleration measured over the NIAE(National Institute of Agricultural Engineers) smooth track were used as the input data for the computer models. The active suspension with 0.25 Hz natural frequency

provided vibration attenuation of over 90 percent for all modes. While the semi-active suspension provided 25 percent attenuation improvement compared with the passive suspension with the same natural frequency. Although active and semi-active cab suspensions provide good isolation performance, they have the disadvantage of high manufacturing cost, less reliability and demand of complex control techniques.

Refs.[4,8] presented a study on the different configurations of passive cab suspensions. Parametric study as well as optimal design have been carried out to investigate the ride improvement. It is found that the lateral ride can be significantly improved by the introduction of cab suspensions. But, it is still difficult to control the lateral vibration within ISO 8-hour fatigue decreased proficiency limit.

1.2.2 Seat Suspension

Seat suspension is the simplest and most commonly used means for vehicle shock and vibration attenuation. The majority of research work on ride improvement is related to the vertical seat suspension since the vertical vibration is the most severe one. However, the vibration level in the lateral mode has been also found to be adverse and need to be reduced[1-3].

Conventionally, seat suspensions of off-road vehicles have been based on a passive isolating method which employs a spring and a damping element as a force generator. Passive suspensions typically provide good isolation performance for high frequency vibrations. Theoretically, in passive isolation systems, amplification of vibration occurs for lower frequencies, and isolation of vibration occurs for frequencies higher than $\sqrt{2}$ times the natural frequency of the suspension system. Therefore,

in order for the passive seat suspension to perform a satisfactory vibration isolation in the low frequency range, they must have a low natural frequency. However, the natural frequency of passive suspensions varies as the inverse square root of the static deflection of the spring element. Lowering the natural frequency can result in large static and dynamic deflections that may not be acceptable in the seat suspension design. Although damping can help in reducing the dynamic deflections, it is achieved at the expense of poor isolation performance for higher excitation frequency.

Rakheja[4] presented a study on the ride improvement of the agricultural tractor via seat suspensions. In his study, the velocity-square damping and Coulomb damping were both considered. The investigation reveals that a seat suspension can successfully be employed to improve ride performance in the bounce, longitudinal, and pitch modes. Vibrations of lateral and roll modes, however, are difficult to be isolated via passive seat suspension because of the very low excitation frequencies in the lateral vibration.

Although many arrangement of adaptive dampers[9,10] have been proposed for the potential alternative of vehicle ride improvement, the attenuation of vibration is possible only when the excitation frequency is $\sqrt{2}$ greater than the natural frequency of the system. For the excitation frequency below $\sqrt{2}$ times the natural frequency, no vibration reduction (transmissibility ratio below unity) can be achieved regardless of the damping value of the passive suspension system.

Because of this design limitation of passive suspensions, active vibration isolation methods may be implemented for ride improvement. Active seat suspension employs active energy dissipating and storing

elements. In this case, the relative displacement of the suspension system is no longer directly related to its natural frequency of the suspension and hence the ride quality and suspension displacement are not in conflict. Although many configurations of active systems have been proposed for vehicle vibration controls, they are used in parallel with passive suspension because of the reliability problem. And also, they are generally expensive due to the complex control systems required.

Stikeleather et al.[11] developed an active seat suspension to isolate the operator from the low frequency vibration. It was indicated that the active suspension isolated the operator from the input frequencies ranging from 1.5 to 8 Hz, and provided approximately 65 to 75 percent acceleration attenuation. The researchers have suggested that this active suspension system should be utilized to isolate the entire operator's control platform.

Young and Suggs[12] extended Stikeleather's seat suspension to isolate the low frequency roll and pitch vibrations. The suspension system provided 70 to 80 percent vibration displacement isolation over the frequency range 1 to 2 Hz.

Kim, Hoag and Hung[13] presented a study on vertical ride simulation of passive, active and semi-active seat suspensions for off-road vehicles. Each suspension model was combined with a three degree of freedom model of the vehicle operator to formulate models of the ride systems of off-road vehicles. The input vibration for the simulation is based on the acceleration time history measured at the base of the seat suspension of the agricultural tractors during transport and moldboard plowing operations. Response acceleration levels were evaluated using the criteria based on the ISO 8-hour fatigue decreased proficiency boundary.

It was found that active seat suspension can provide good ride performance for excitations at very low frequency. Semi-active suspension systems showed better ride performance than passive suspensions when input vibration had high frequency components relative to the natural frequencies of the suspension systems. Passive suspensions have mechanical simplicity and provided good ride performance for high frequency vibrations.

1.2.3 Vibration Control Via Dynamic Absorbers

Of the possible ways of reducing the undesirable vibrations, a vibration absorber provides an alternative selection for vibration control. Auxiliary masses can be attached to a vibrating system by springs and damping devices to assist in controlling the amplitude of vibration of mechanical systems[14].

From the absolute transmissibility plot of the single-degree-of-freedom model, as shown in Fig.1.1, one can easily see that the vibration isolation is achievable only if the excitation frequency is $\sqrt{2}$ higher than the natural frequency. For excitation frequency lower than this limit, vibration isolation is impossible regardless of the damping ratio of the suspension system.

In order to reduce the undesirable vibration in the excitation frequency range below $\sqrt{2}$ times the natural frequency, vibration absorbers are attached to the primary system to assist the vibration control. Basically, the attachment of a vibration absorber will modify the dynamic behaviour of the primary system and make the vibration isolation of low frequency excitations possible. Vibration absorbers have been described as "devices" that can be added to a system to reduce the

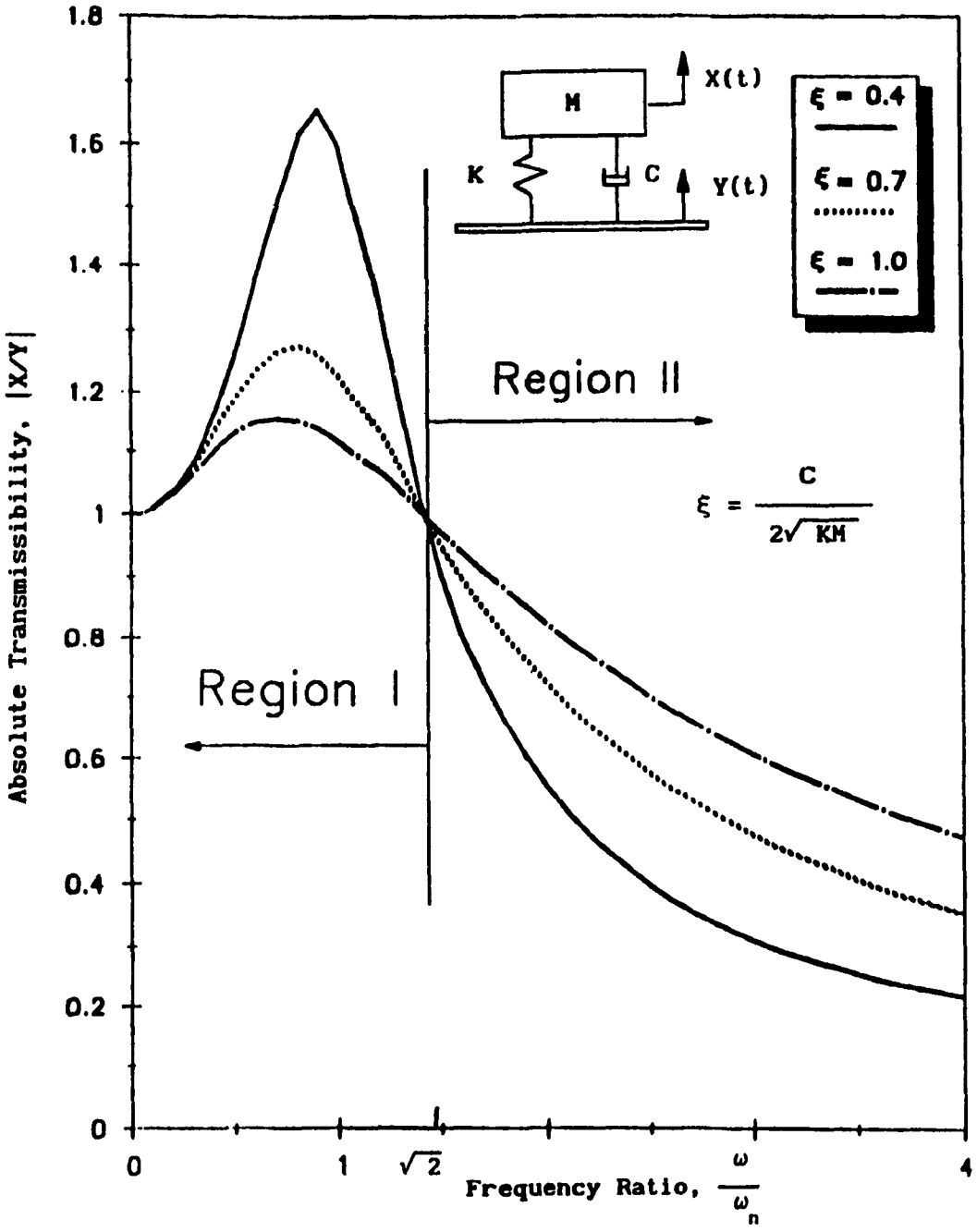

Fig.1.1 The Absolute Transmissibility Plot of A Single-Degree-of-Freedom Model

vibration amplitude by introducing equal and opposite dynamic forces and/or by introducing damping to dissipate energy.

The majority of the applications of vibration absorbers have been the case where excessively large amplitude of motion response of the primary system takes place due to light damping and coincident of excitation frequency to the system's natural frequency[15-21]. When the modification of primary system is impractical or not economical, dynamic absorbers are considered to be an excellent solution. If the primary system is excited by a force or displacement that has a constant frequency, or in some cases by an excitation force that is a constant multiple of rotational speed, then it is possible to modify the vibration pattern of the primary system and to reduce its amplitude significantly by the use of dynamic absorber that is tuned to the frequency of the excitation. By introducing damping to the absorber system, it is possible to obtain a good broad band response.

Ormondroyd and Den Hartog analyzed the case of damped vibration absorber attached to an undamped main system. The computation of optimal system design parameters subjected to force disturbance was discussed in detail in Den Hartog's book[15]. The optimization was carried out so as to minimize the maximum displacement response of the main system in frequency domain.

The optimization of the spring and damper rates for a dynamic absorber applied to a force excited and damped primary system was presented in [16,17]. Thompson[16] used frequency locus method to establish a tuning function which enables the optimal natural frequency for the absorber to be determined. The optimum damping ratio for the absorber can be found directly once the optimum tuning frequency has been

obtained. Randall, Halsted, and Taylor[17] solved the same problem by numerical search method. Computational graphs that determine the optimal linear vibration absorber for linear damped primary systems were presented. With independent system parameters specified, the computational graphs can be used to find the response amplitudes as well as the optimal absorber characteristics.

Puksand[18] studied the optimum conditions for damped absorbers for variable speed systems with rotating or reciprocating unbalances. Frequency locus methods were used for establishing the equations for optimum tuning and damping of the vibration absorber so as to minimize the displacement response.

Kojima and Saito[19] studied forced vibrations of a simply supported beam having an attached non-linear dynamic vibration absorber and excited by sinusoidal motion of its supporting base. The optimum tuning and optimum damping for the absorber are obtained by the simplex method.

Soon and Lee[20] studied the optimal design of linear and nonlinear vibration absorbers for damped systems subjected to sinusoidal force excitation. Minimization of the displacement and velocity response in the frequency domain has been taken as objectives.

Jordanov and Cheshankov[21] studied the optimal design of linear and nonlinear dynamic vibration absorbers. The minimization of the vibration response has been carried out for damped as well as undamped force excited primary systems with linear and nonlinear spring characteristics. Six optimization criteria by which the response is minimized over narrow and broad frequency bands were examined.

Although the application of absorber for reducing undesirable vibration follows a long history, very little effort has been devoted to

vehicle vibration control. Ghoneim and Metwalli[22] studied the optimum vehicle suspension with a damped absorber. A two-degree-of-freedom linear model, subjected to random guideway disturbance, is adopted. Optimization is based upon the rms tire-terrain force, constrained by the rms sprung mass acceleration.

Some of the applications of absorber to vehicle vibration control was also reported by Hunt in his book[23]. Shotwell[24] applied the tuned and damped dynamic absorber to attenuate the vibration of earth-moving machines that are primarily excited by irregularities in the roadbed surface. Absorber performance in terms of dynamic scraper load reduction was evaluated by means of strain measurements. The dynamic load amplitudes were reduced by over 50 percent with absorber in action. Inoh and Aisaka[25] studied the application of absorber to heavy-duty trucks. The investigations are closely related to the improvement of driving comfort and reduction of driving fatigue. They used the engine as the absorber and tuned the engine mounting stiffness for minimum vertical displacement of the cab.

1.3 Objectives and Outline of the Thesis

The vibration level experienced by off-road vehicle drivers is very severe and need to be reduced in all vibration modes. Among these modes of vibrations, the lateral vibration has identified to be the most difficult to isolate because of the low excitation frequency. In the present investigation, improvement of the lateral ride performance is investigated by means of vibration absorbers attached to the passive seat suspension.

In the traditional absorber design, the following assumptions are usually being made:

1) the primary system is undamped or lightly damped; and

2) the excitation inputs are assumed to have same amplitude over a wide excitation frequency range.

These assumptions, however, are inappropriate for the present investigation. Firstly, intensive lateral excitation occurs at low frequencies, and hence primary seat suspension with heavy damping is advantageous. Secondly, the terrain induced excitations are rarely of the property of equal amplitude. They are usually limited to a specific frequency range and are of varying amplitudes. Since the input amplitudes are varying, the severity of vibration responses cannot be totally understood from the transmissibility response and the characteristics of vibration input data must also be fully considered. Although the optimal parameters of absorbers have been proposed by several researchers either by computer searching methods or by frequency root locus methods[16-21], they are only limited to the problems considered and are hardly optimal in any practical sense because of the assumptions they made in their study.

In this investigation, the characteristics of the lateral excitations is fully considered. Different absorber arrangements are analyzed and simulated to suggest potential ways of improving lateral ride vibration.

In chapter 2, a study on the time history representation of acceleration PSD spectrum is carried out. For this investigation, acceleration PSD as measured at the cab floor[2] is used as the representative input excitation for converting into time series

representation, namely, the acceleration, velocity and displacement time series representation. Chapter 3 presents a parametric study of a seat suspension with a single absorber. Mathematical models of the lateral seat suspension with a single absorber are developed and parametric study is carried out to investigate the influences of system parameters on the lateral ride performance. Chapter 4 presents a study on the ride performance of seat suspension with dual absorbers. A parametric study is also conducted to suggest better absorber design for the lateral ride improvement. The parametric optimization is carried out in chapter 5 to investigate the influence of the relative displacement constraint on the ride performance. The effect of the absorber mass on the lateral ride is probed through sensitivity study.

Finally, in chapter 6, the ride performance of different suspension systems are compared and conclusions are made. Some future works are also recommended.

CHAPTER 2

The Characteristics of the Lateral Excitation Input and Its Time History Representation

2.1 Introduction

The vibration level experienced by the off-road vehicle driver depends on both the excitation input and the transmissibility characteristics of the suspension system. In order to effectively reduce the terrain-induced vibration transmitted to the driver, suspensions at the seat and/or cab are necessary. To achieve this goal, a good knowledge of the vehicle vibration excitation input to the vehicle is necessary.

In order to simulate the vehicle performance with accuracy and fidelity, the input excitation data must be representative of typical off-road terrains and working conditions. The intense efforts in the field measurements have led to the standardization of the terrain induced excitation data for simulation. In frequency domain, power spectral density has been used to describe terrain-induced disturbances. The International Organization for Standardization[26] has proposed approximate expressions describing bounce acceleration PSD required for tractor seat testing. However, acceleration input data in other vibration modes has not been available in the ISO standard. Matthews[1] constructed a test track at National Institute of Agricultural Engineers (NIAE), Silsoe, England, to represent the agricultural terrains. The artificial track has been widely accepted in Europe as the representative of agricultural terrain. In this investigation, lateral excitation input

data which is measured by Roley[2] from the Silsoe track is adopted. It is presented in the form of acceleration PSD and is shown in Fig.2.1. The input acceleration PSD of lateral mode indicates that the lateral acceleration excitation occurs in the dominant frequency range of 0.6-1.6 Hz with acceleration PSD peak value occuring approximately at 1 Hz.

2.2 Description of the Lateral Excitation in Terms of Displacement PSD

In order to evaluate the relative displacement response, the understanding of the absolute displacement input at the cab floor is also desirable. This is achieved by using the relationship between acceleration PSD and absolute displacement PSD [27], which is:

$$S_{\ddot{y}}(\omega) = \omega^4 S_y(\omega) \quad . \tag{2.1}$$

The input displacement PSD of lateral mode vibration is plotted in Fig.2.2, it indicates excessively high displacement input PSD at the very low frequencies and relatively low displacement input PSD for frequencies higher than 0.2 Hz.

2.3 Time History Representations of a Given Spectrum

Terrain-induced vibration is characterized by the power spectral density. This representation is justified by the central role which spectra occupies in the theory of random vibrations. Their importance comes from the simple form of the input-output relations for spectral density for a linear system subjected to random excitation. However, the power spectral density representation will be unable to explicitly characterize the temporal amplitudes of input data, and further, the time

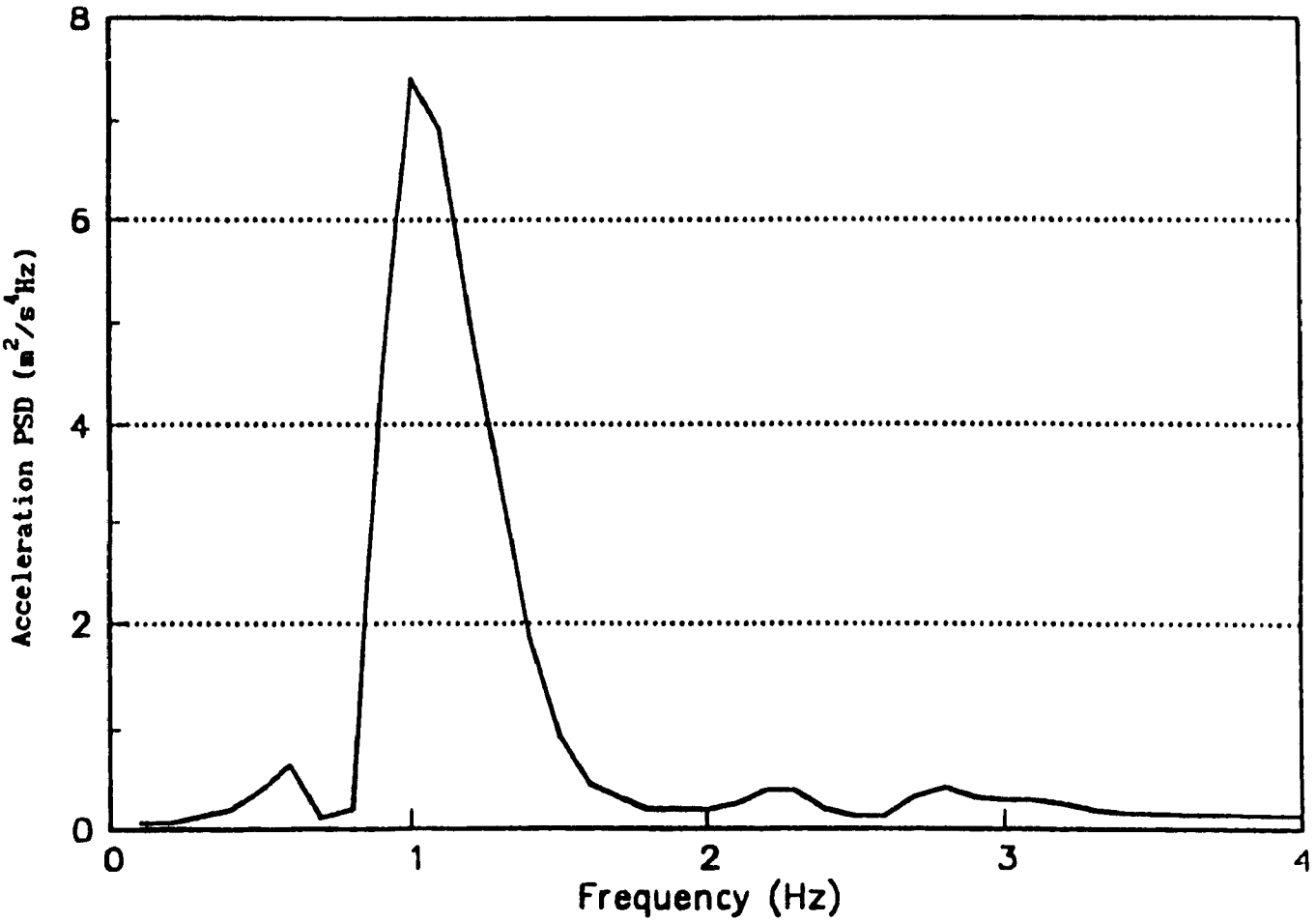

Fig.2.1 Lateral Acceleration Input PSD [2]

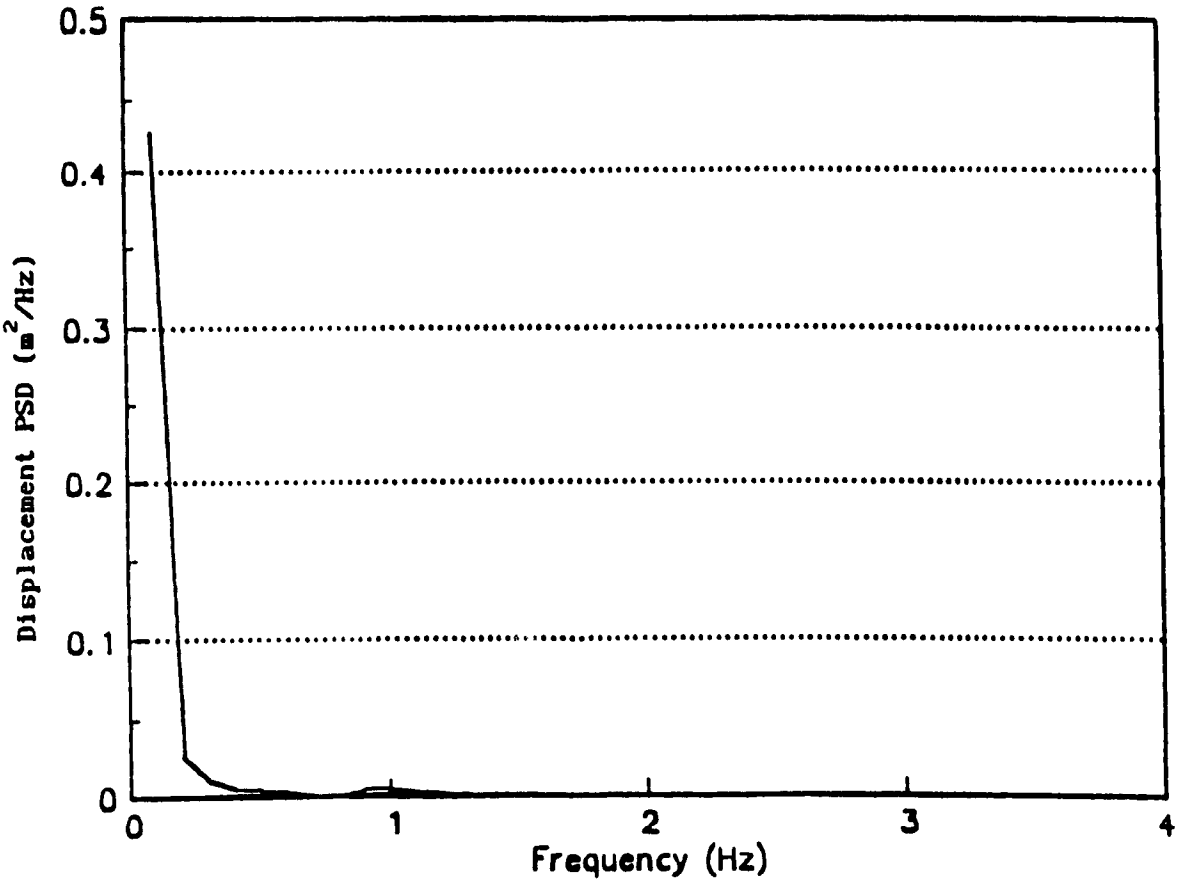

Fig.2.2 Lateral Displacement Input PSD

series representation of the random terrain will be useful in the dynamic simulation of nonlinear vehicle system. Although some studies in vehicle simulation have employed direct recording of the terrain profile as the representative time domain input excitation for the simulation, this approach is characterized by its high computing cost and complexity. In order to simplify the computation, a number of methods for generating time histories of a given spectra have been introduced [4,28]. It has been concluded that the power spectral density for a typical terrain surface can be represented approximately by the sum of sine wave series. Such time series will statistically match a given spectrum.

The procedure of converting the acceleration power spectral density into a time history of sine wave series can be described as the following:

1. Calculate the peak acceleration amplitude at center frequency f_i

$$a(f_i) = \sqrt{2}\sqrt{\int_{f_l}^{f_u} S_{\ddot{y}}(f_i)df} \tag{2.2}$$

where

f_l, f_u are the lower and upper frequency limits

$S_y(f_i)$ is the power spectral density

2 Represent time history as sum of sine waves[29]

$$a(t) = \sum_{i=1}^{N} (-1)^i a(f_i)\sin(2\pi f_i t) \tag{2.3}$$

If the description of $S_y(f_i)$ is not available in a close mathematical form, $a(f_i)$ can be computed from the approximation:

a) obtain the root mean square value of input acceleration, $\bar{a}(f_i)$ using the equation

$$\bar{a}(f_1) = \sqrt{\bar{S}_{\ddot{y}}(f_1)\Delta f} \tag{2.4}$$

where

$\bar{S}_{\ddot{y}}(f_1)$ is the average acceleration PSD

Δf is the frequency bandwidth.

b) calculate the peak acceleration amplitudes using the following relation

$$a(f_1) = \sqrt{2}\,\bar{a}(f_1) \tag{2.5}$$

The ISO 2631 standard[26] specifies vibration limits for reduced comfort, fatigue decreased proficiency and health impairment, expressing the amplitude of the weighted root-mean-square (RMS) acceleration that could be tolerated at each one-third octave frequency band comprised between 1 and 80 Hz. Fig.2.3 shows the ISO recommended fatigue decreased proficiency limits for transverse vibrations.

In order to compare the ride performance with the ISO recommended fatigue decreased proficiency limit, the input acceleration is evaluated over finite bands of one-third octave width. The relationship between the bandwidth Δf and the center frequency f_o is obtained from the following derivation:

Let f_1 and f_u be the lower and upper cut-off frequencies respectively, then for a 1/3 octave bandwidth, we have

$$f_u/f_1 = \sqrt[3]{2} \tag{2.6}$$

if the central frequency is f_o

$$f_1 f_u = f_o^2 \tag{2.7}$$

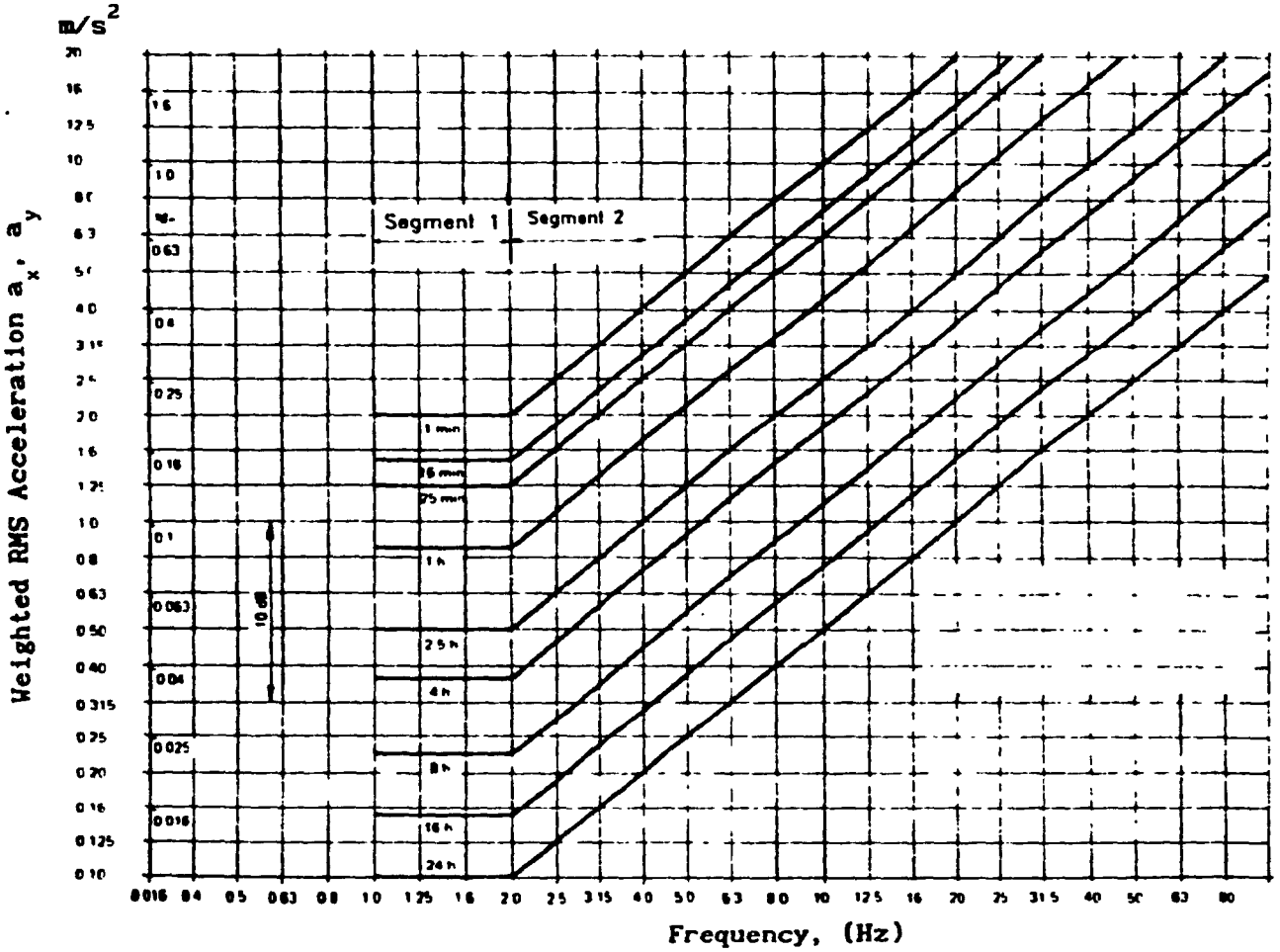

Fig.2.3 The ISO recommended transverse acceleration limits of the fatigue-decreased proficiency boundary[26]

and the bandwidth is

$$\Delta f = 0.23 f_0 \tag{2.8}$$

where $\Delta f = f_u - f_l$

Table 2.1 gives a list of the lower and upper frequency limits for each central frequency f_0. Using the tabulated frequency bandwidth and applying the procedure outlined above, the peak amplitudes of acceleration for the discrete frequencies are shown in Fig.2.4. It can be easily seen that the maximum of the peak acceleration amplitude occurs at the frequency 1.1 Hz.

From the information of input acceleration amplitudes, the amplitudes of input velocity and input displacement can be easily determined using the following relations:

$$a(f_i) = 2\Pi f_i V(f_i) \tag{2.9}$$

$$a(f_i) = 4\Pi^2 f_i^2 Y(f_i) \tag{2.10}$$

where

$V(f_i)$ is the amplitude of the velocity at excitation frequency f_i

$Y(f_i)$ is the amplitude of the displacement at excitation frequency f_i

The amplitudes of the input velocity and displacement are plotted against frequency in Figs.2.5 and 2.6. The maximum of the peak value for the velocity input occurs approximately at the excitation frequency 1.1.

2.4 Summary

In this chapter, the lateral acceleration input PSD is represented by acceleration, velocity and displacement time series over finite bands

Table 2.1 Numerical Values for One-Third Octave Frequency Relation

Centre Frequency, Hz	Lower Frequency, Hz	Upper Frequency, Hz	Effective Bandwidth, Hz
f_c	f_l	f_u	Δf
0.1	0.0893	0.112	0.023
0.2	0.1786	0.224	0.046
0.3	0.2679	0.336	0.069
0.4	0.3571	0.448	0.092
0.5	0.4464	0.560	0.115
0.6	0.5357	0.672	0.138
0.7	0.6250	0.784	0.161
0.8	0.7143	0.896	0.184
0.9	0.8036	1.008	0.207
1.0	0.8929	1.120	0.230
1.1	0.9821	1.232	0.253
1.2	1.0714	1.344	0.276
1.3	1.1607	1.456	0.299
1.4	1.2500	1.568	0.322
1.5	1.3393	1.680	0.345
1.6	1.4286	1.792	0.368
1.7	1.5179	1.904	0.391
1.8	1.6071	2.016	0.414
1.9	1.6964	2.128	0.437
2.0	1.7857	2.240	0.460
2.1	1.8750	2.352	0.483
2.2	1.9643	2.464	0.506
2.3	2.0536	2.576	0.529
2.4	2.1429	2.688	0.552
2.5	2.2321	2.800	0.575
2.6	2.3214	2.912	0.598
2.7	2.4107	3.024	0.621
2.8	2.5000	3.136	0.644
2.9	2.5893	3.248	0.667
3.0	2.6786	3.360	0.690
3.1	2.7679	3.472	0.713
3.2	2.8571	3.584	0.736
3.3	2.9464	3.696	0.759
3.4	3.0357	3.808	0.782
3.5	3.1250	3.920	0.805
3.6	3.2143	4.032	0.828

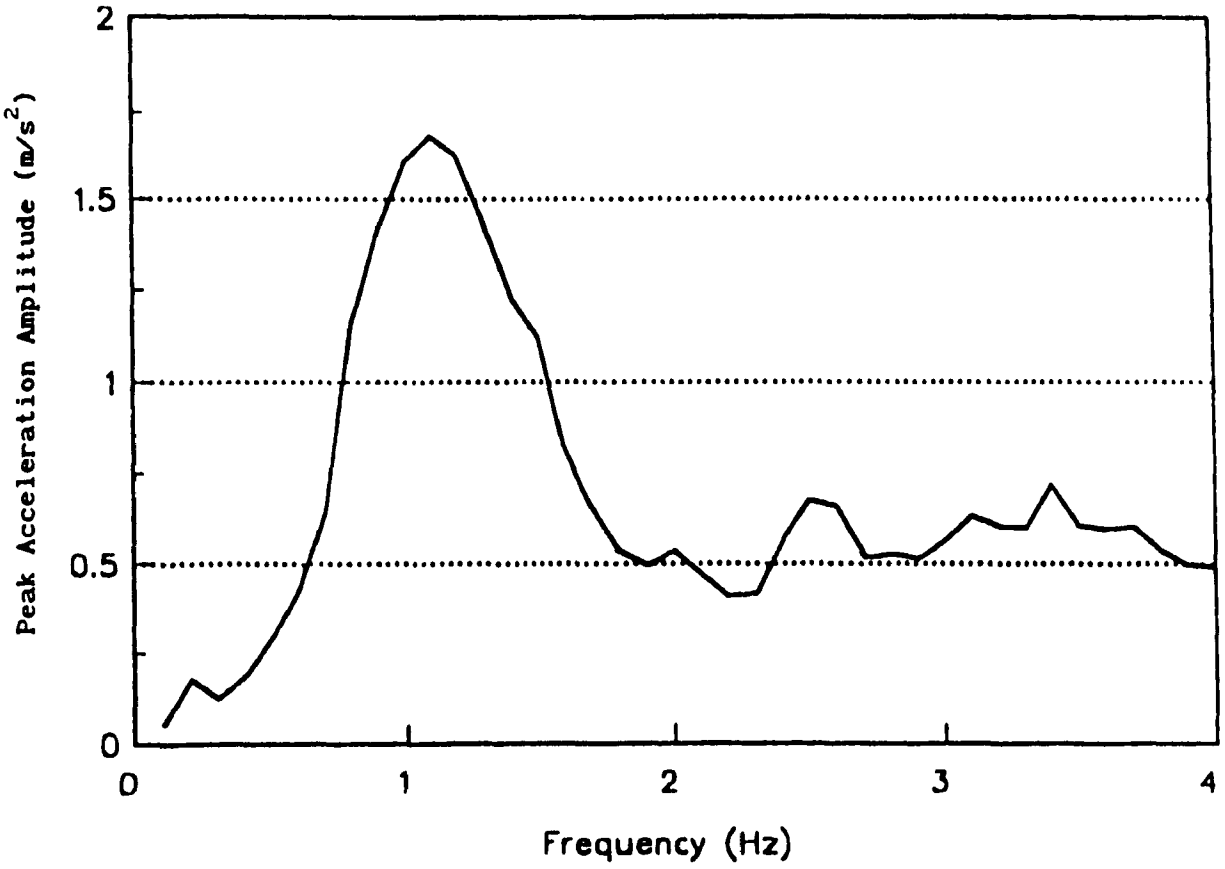

Fig.2.4 Acceleration Time Series Representation of the Lateral Excitation

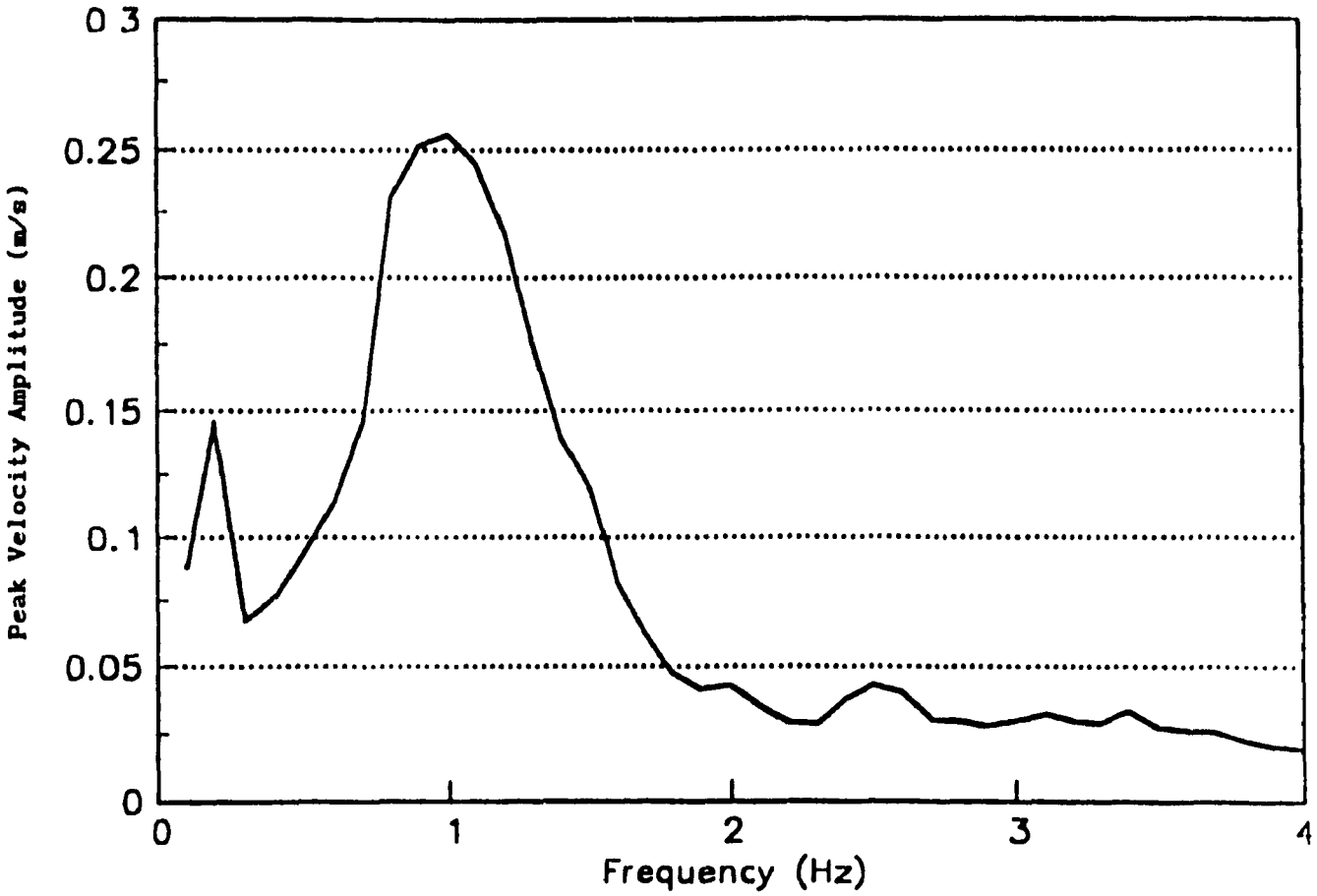

Fig. 2.5 Velocity Time Series Representation of the Lateral Excitation

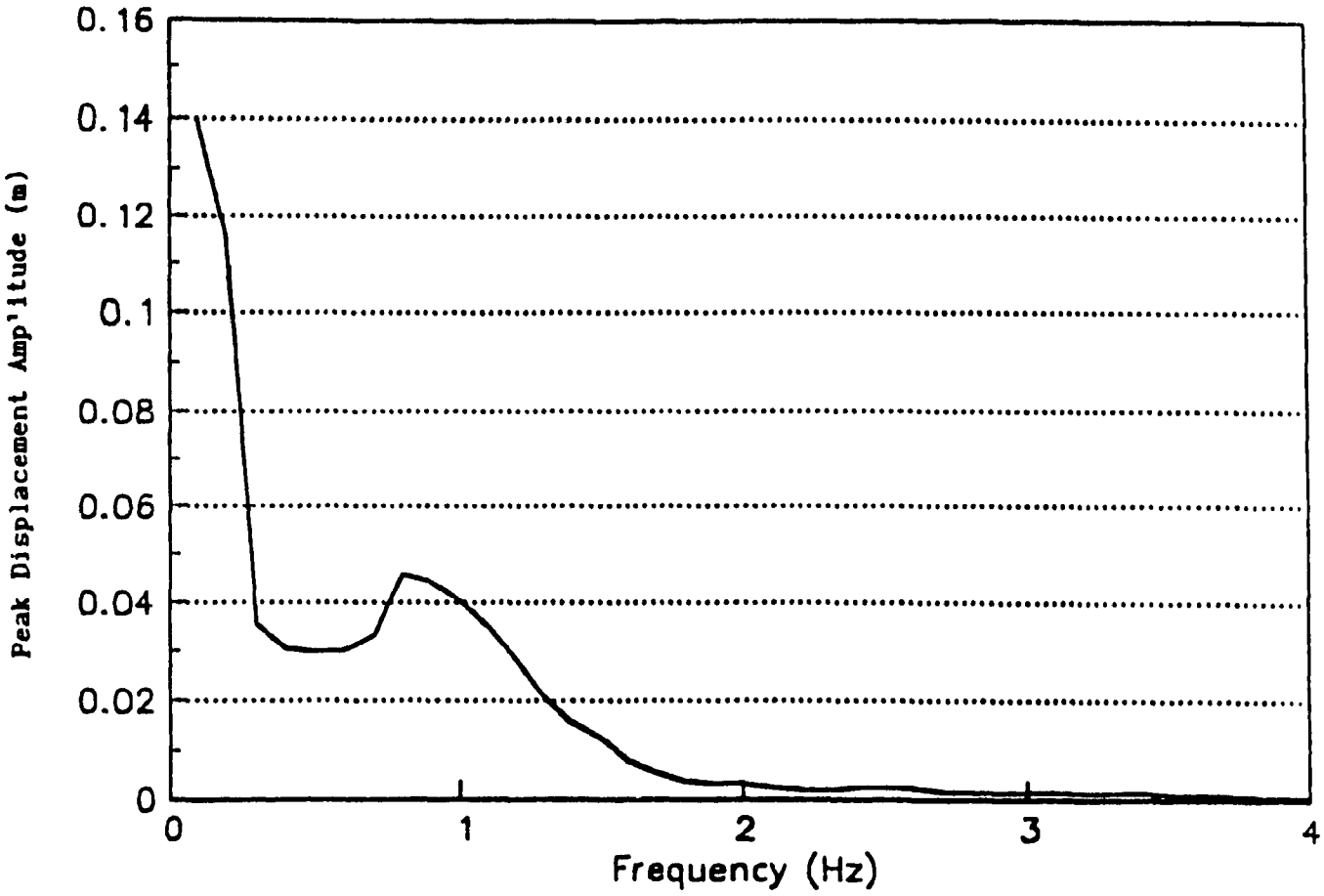

Fig. 2.6 Displacement Time Series Representation of the Lateral Excitation

of one-third octave width. The presentations reveal the characteristics as well as the severity of lateral inputs in terms of amplitude and frequency.

CHAPTER 3

Lateral Seat Suspension with a Single Absorber

3.1 Introduction

The vehicle seat is the driver's working platform. The main objective of seat suspension design is to provide good riding comfort to driver as well as good control of vehicle. Earlier vehicles have basically a rigidly supported steel pan as seats. Such a simple seat offers very little shock and vibration isolation and thus very harsh ride. Modern seat suspension designs have employed complex linkage mechanism to obtain effective shock and vibration isolation.

In practice, the majority of seat suspensions are usually limited to vibration attenuation of vertical mode. The lateral movement of driver seat is considered to be fixed and thus the terrain induced lateral vibrations are directly transmitted to the driver mass. In order to investigate the possibility of lateral and/or longitudinal ride improvement for off-road vehicle, refs.[3,4] studied seat isolators in the longitudinal and lateral modes. The schematic configurations are shown in Fig.3.1. The longitudinal and lateral isolators consist of a platform supported on a set of linear bearings with a spring and a shock absorber. Bounce suspension seat can be mounted on the sprung platform to form a suspension system capable of isolating the driver along the three translational coordinates. Parametric study as well as parameter optimization were fully conducted[4]. Figs.3.2 and 3.3 show the simulation results for an optimal seat suspension with lateral isolator. It is demonstrated that the passive lateral seat suspension alone

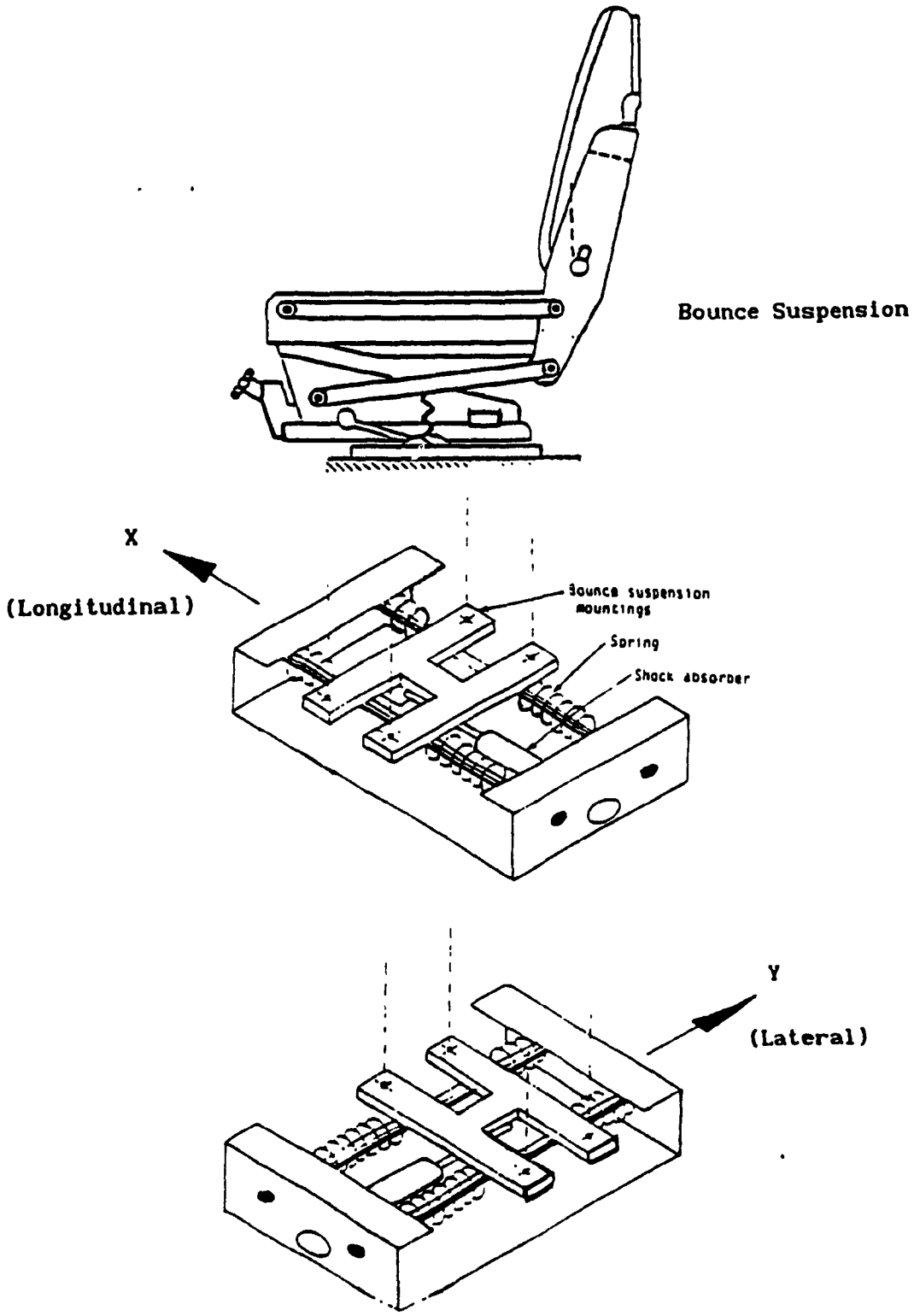

Fig.3.1 The Schematic of a Multi-Mode Seat Suspension[3,4]

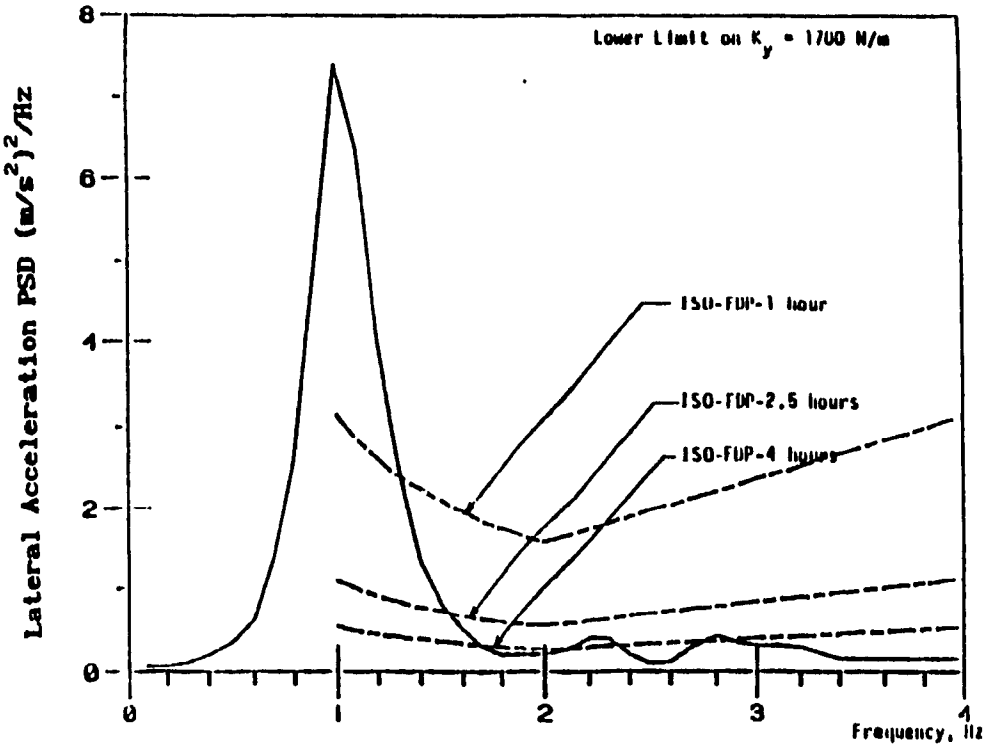

Fig.3.2 Lateral Acceleration Response of the Driver Mass with the Optimum Lateral Seat Suspension[4]

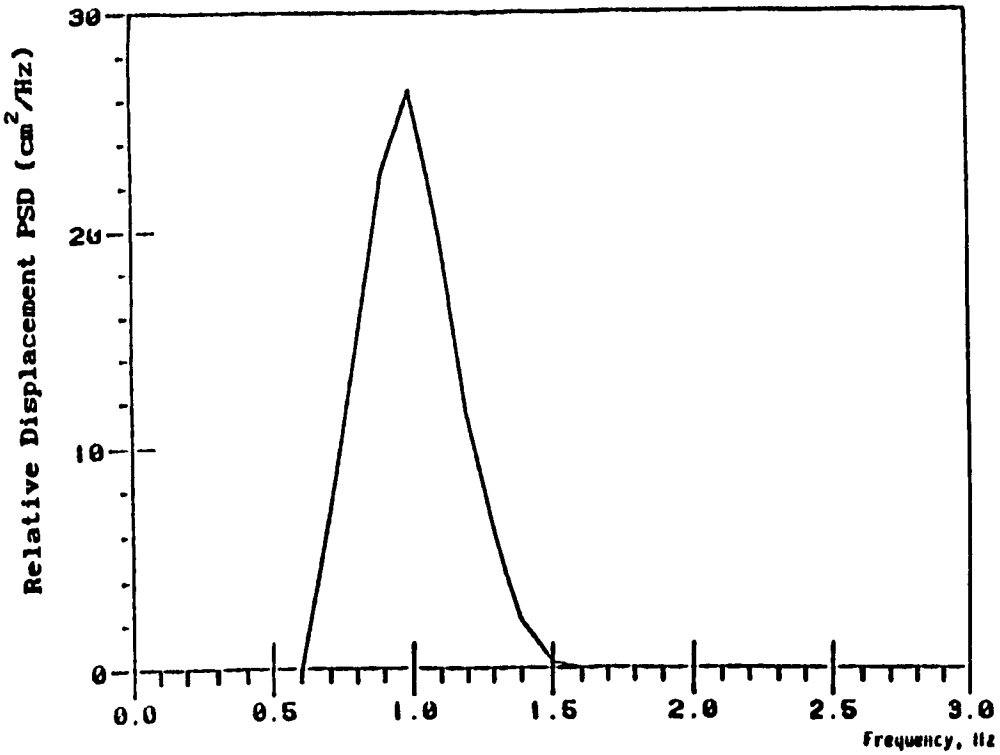

Fig.3.3 Relative Displacement Response of the Driver Mass with the Optimum Lateral Seat Suspension[4]

provides very little lateral vibration attenuation because of the limitation on the allowable relative displacement response. Recognizing the disadvantage of passive seat suspension, they continued to study the performance of different arrangements of cab and cab-seat suspensions[30]. Fig.3.4 shows the cab-seat model and the acceleration PSD response of the driver mass with optimal suspension parameters for a cab with only bounce seat suspension. The acceleration PSD response of the driver mass for a cab with bounce and lateral seat suspensions is shown in Fig.3.5. The results demonstrated that cab suspension with lateral seat isolator provides good ride performance.

It has been shown in the previous chapter that terrain-induced lateral excitation of off-road vehicle is characterized by its low excitation frequency. Isolation of such low frequency vibration requires very soft seat suspension design. An extremely soft seat suspension will cause an excessively large relative displacement response and can lead to inefficiencies in operator's performance. In this study, lateral seat suspension with a vibration absorber will be investigated for its potential in lateral ride improvement. Investigation of lateral seat suspension with dual absorbers will be presented in the next chapter.

For this study, the mathematical model as presented in [3] is developed for the primary lateral seat suspension. However, for investigating the dynamic behaviour of vibration absorber, the proposed model assumes the damping element to be a viscous damper instead of Coulomb and velocity squared dampers. Fig.3.6 shows the lateral primary seat suspension system, which consists of seat and driver mass M_1, spring with stiffness rate K_1, and viscous damper with damping coefficient C_1.

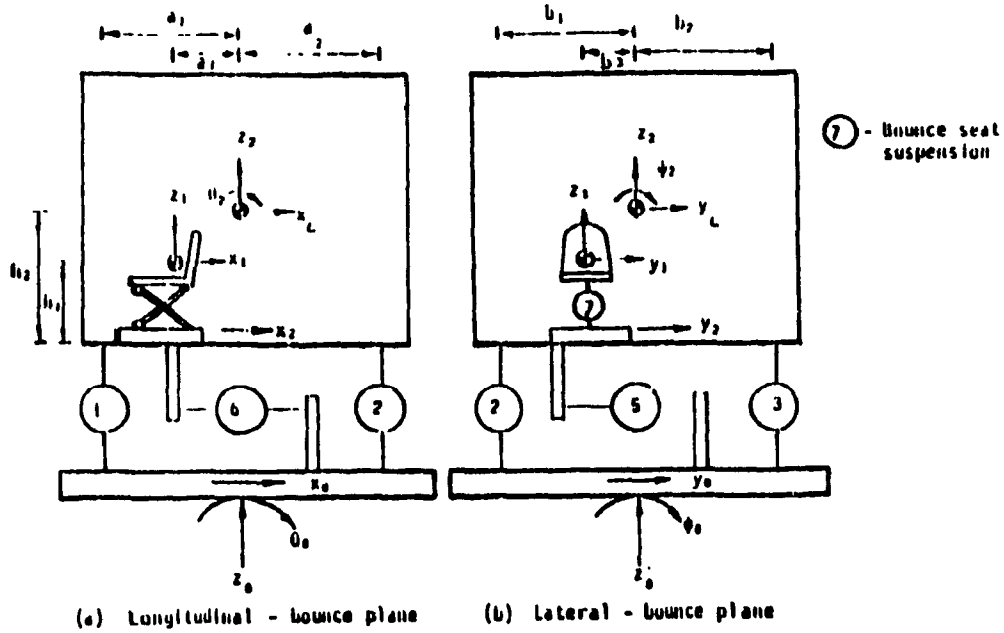

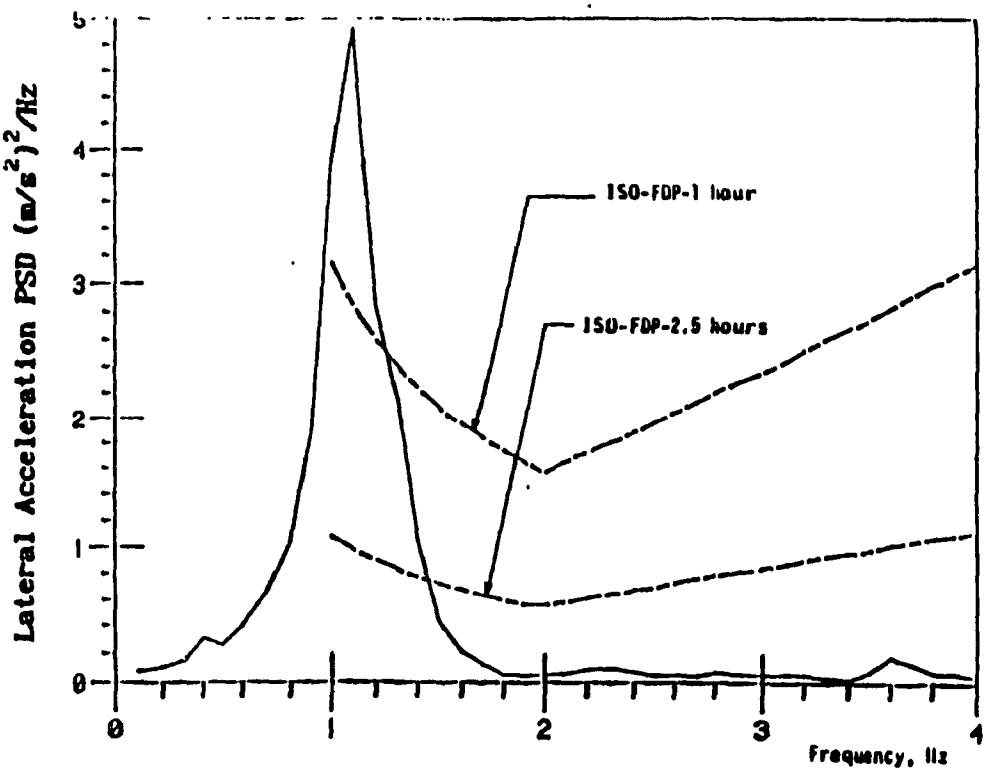

Fig.3.4 A 5 DOF Cab-Seat Model (Cab and Bounce Seat Suspension) and the Acceleration Response of the Driver Mass[4]

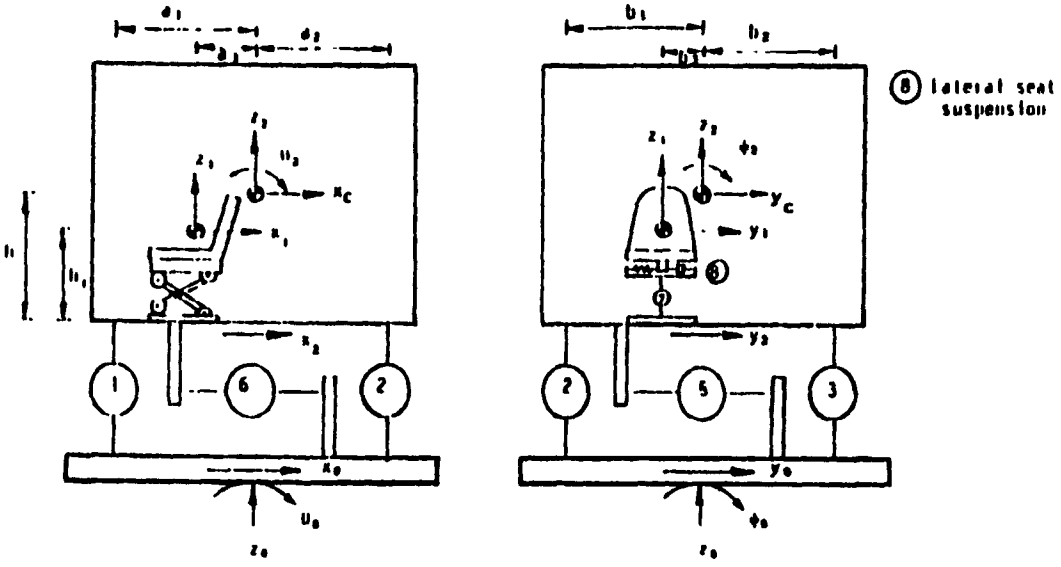

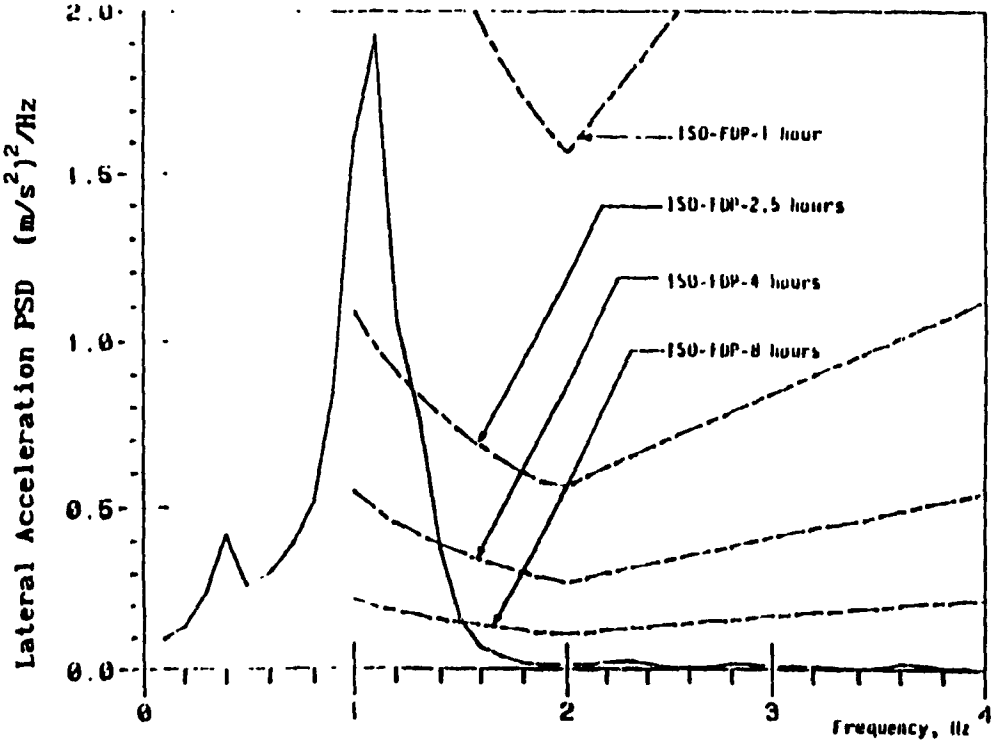

Fig.3.5 A 6 DOF Cab-Seat Model (Cab, Bounce and Lateral Seat Suspension) and the Lateral Acceleration Response of the Driver Mass[4]

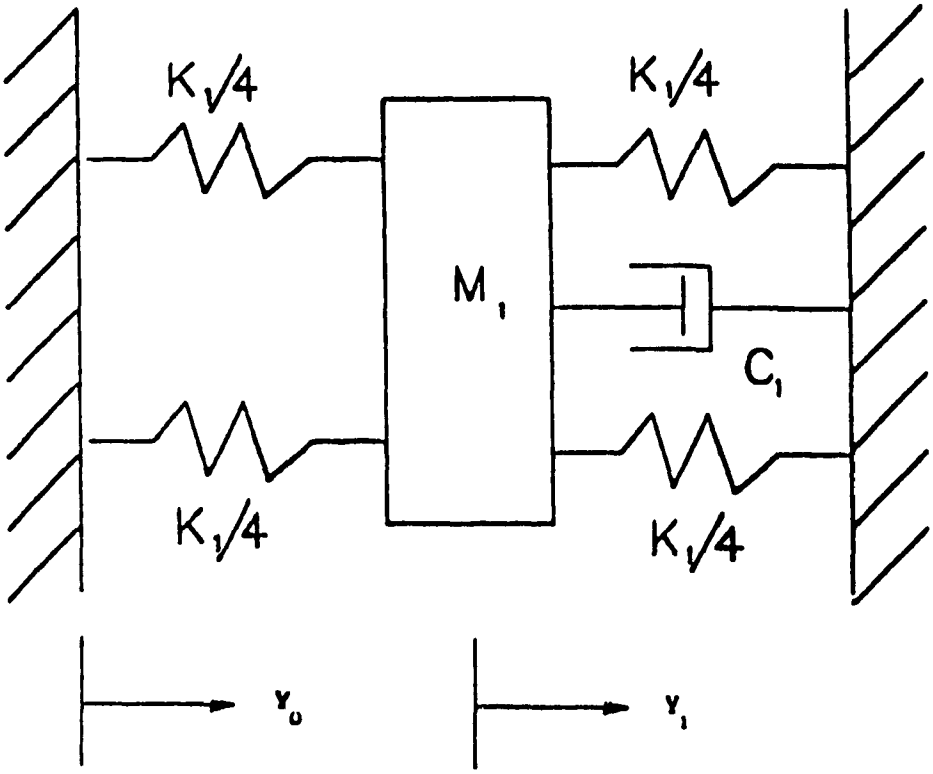

Fig.3.6 The Lateral Primary Seat Suspension

3.2 Lateral Seat Suspension with a Conventional Absorber

The application of absorber for vibration control has been recognized for a long time. In the conventional absorber design, the amplitude of input excitation is usually taken as a constant over the frequency range of interest, and the parameters of vibration absorber are selected in such way that the transmissibility peak in the excitation frequency is minimized. In the case of the lateral seat suspension design for off-road vehicle, the lateral excitation amplitude is frequency dependent. Hence, it is obvious that the traditional approach, will not be able to evaluate directly the ride performance of the lateral seat suspension. Ride performance can be evaluated only if the characteristics of the input excitations are also fully considered. In this investigation, consideration is given to the frequency dependent amplitude characteristics of the lateral excitation input.

3.2.1 Equations of Motion

The lateral seat suspension incorporated with a conventional vibration absorber is shown in Fig.3.7. The vibration absorber consists of a secondary mass M_a, a spring with stiffness coefficient K_a and a viscous damper with damping coefficient C_a. The equations of motion of the suspension system can be expressed as:

$$M_1\ddot{Y}_1+C_1(\dot{Y}_1-\dot{Y}_0)+K_1(Y_1-Y_0)+C_a(\dot{Y}_1-\dot{Y}_2)+K_a(Y_1-Y_2) = 0 \qquad (3.1)$$

$$M_a\ddot{Y}_2+C_a(\dot{Y}_2-\dot{Y}_1)+K_a(Y_2-Y_1) = 0 \qquad (3.2)$$

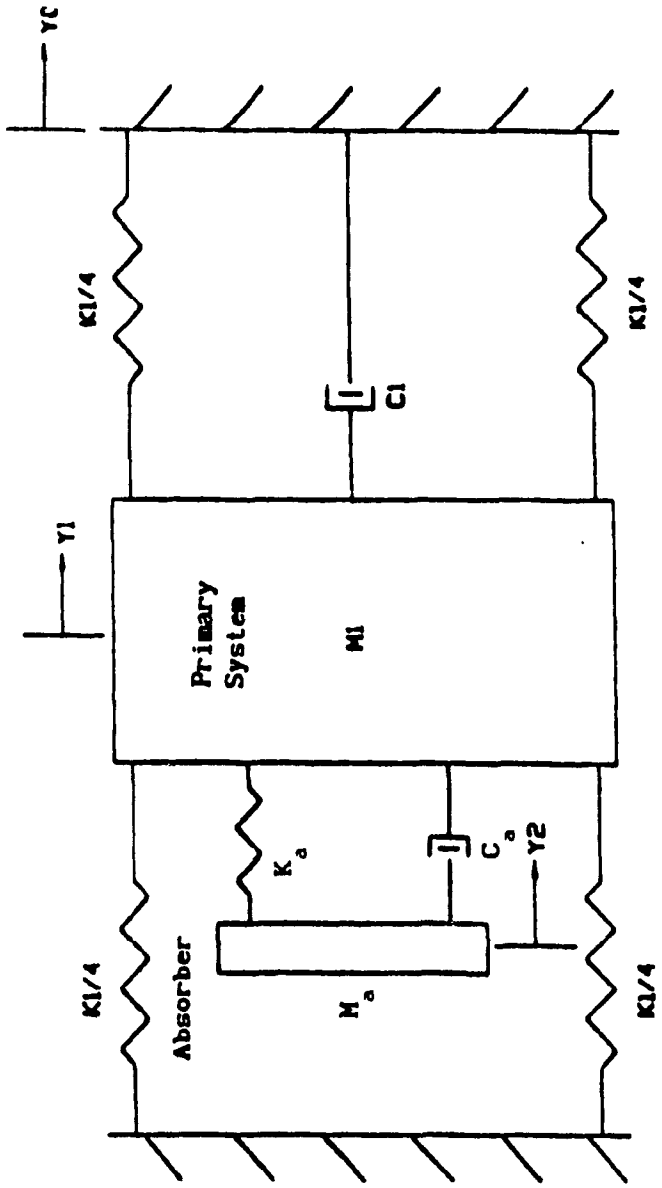

Fig.3.7 The Lateral Seat Suspension with a Conventional Absorber

Now introducing the following notations:

$$K_1/M_1 = \omega_1^2 \qquad K_a/M_a = \omega_2^2 \qquad M_a/M_1 = \mu$$

$$C_1/2\sqrt{K_1 M_1} = \xi_1 \qquad C_a/2\sqrt{K_a M_a} = \xi_2 \tag{3.3}$$

Eqns.(3.1) and (3.2) are rewritten as follows:

$$\ddot{Y}_1 + 2\xi_1\omega_1(\dot{Y}_1-\dot{Y}_0)+2\xi_2\omega_2\mu(\dot{Y}_1-\dot{Y}_2)+\omega_1^2(Y_1-Y_o)+\mu\omega_2^2(Y_1-Y_2) = 0 \tag{3.4}$$

$$\ddot{Y}_2 + 2\xi_2\omega_2(\dot{Y}_2-\dot{Y}_1)+\omega_2^2(Y_2-Y_1) = 0 \tag{3.5}$$

Complex frequency response functions $T_{\ddot{y}_1}(j\omega)$ of absolute acceleration, $\ddot{Y}_1(t)$, and $T_{y_{r1}}(j\omega)$ and $T_{y_{r2}}(j\omega)$ of relative displacements, Y_{r1} ($Y_{r1}=Y_1-Y_0$) and Y_{r2} ($Y_{r2}=Y_2-Y_o$) respectively, are given as follows:

Absolute acceleration transmissibility of the driver mass, $T_{\ddot{y}_1}(j\omega)$,

$$T_{\ddot{y}_1}(j\omega) = \frac{\ddot{Y}_1}{\ddot{Y}_o}$$

$$= \frac{[-j2\omega^3\xi_1\omega_1-\omega^2(\omega_1^2+4\xi_1\xi_2\omega_1\omega_2)+j\omega(2\xi_1\omega_1\omega_2^2+2\xi_2\omega_2\omega_1^2)+\omega_1^2\omega_2^2]}{\Delta} \tag{3.6}$$

Relative displacement transmissibility of the driver mass, $T_{y_{r1}}(j\omega)$,

$$T_{y_{r1}}(j\omega) = \frac{Y_{r1}}{Y_o}$$

$$= \frac{\omega^4-j\omega^3(1+\mu)2\xi_2\omega_2-(1+\mu)\omega_2^2\omega^2}{\Delta} \tag{3.7}$$

Relative displacement transmissibility of the absorber mass, $T_{y_{r2}}(j\omega)$,

$$T_{y_{r2}}(j\omega) = \frac{Y_{r2}}{Y_o}$$

$$= \frac{-j2\xi_1\omega_1\omega^3 - \omega_1^2\omega^2}{\Delta} \tag{3.8}$$

where the denominator in all cases is

$$\Delta = \omega^4 - j\omega^3[2\xi_1\omega_1 + 2(1+\mu)\xi_2\omega_2] - \omega^2[\omega_1^2 + (1+\mu)\omega_2^2 + 4\xi_1\xi_2\omega_1\omega_2]$$
$$+ j\omega[2\xi_1\omega_1\omega_2^2 + 2\xi_2\omega_2\omega_1^2] + \omega_1^2\omega_2^2 \tag{3.9}$$

The relative displacement responses of the driver mass and absorber mass are found to be:

$$Y_{r1}(j\omega) = T_{y_{r1}}(j\omega)Y_o(j\omega) \tag{3.10}$$

$$Y_{r2}(j\omega) = T_{y_{r2}}(j\omega)Y_o(j\omega) \tag{3.11}$$

The acceleration response PSD of the linear system is:

$$S_o(j\omega) = T_{\ddot{y}_1}(j\omega)T^*_{\ddot{y}_1}(j\omega)S_i(j\omega) \tag{3.12}$$

where

$S_i(j\omega)$ is the power spectral density of the input excitation,

$T_{\ddot{y}_1}(j\omega)$ is the complex acceleration frequency response function and

$T^*_{\ddot{y}_1}(j\omega)$ is its conjugate function.

3.3 Selection of Performance Indices

In order to investigate the influence of vibration absorber, performance indices as a function of acceleration and relative motion

response should be selected. Performance indices are chosen based on the peak steady-state response over the frequency range of interest. Such performance indices will be adequate to assess the performance of the suspension system. The acceleration response PSD over a frequency range provides a better basis for comparing the suspension performance with respect to the ISO specified fatigue decreased proficiency limits. The peak relative displacement response can be best used to evaluate the influence of operator's performance in the work space. In this study, the peak acceleration response PSD and the peak relative displacement response of the driver mass are both selected as performance indices. The relative displacement of absorber mass with respect to its rattle space is taken into account as a secondary performance index in order to constraint excessively large relative displacement response of absorber mass for practical consideration.

3.4 The ISO Recommended Fatigue Decreased Proficiency (FDP) Boundary

There are four physical factors of primary importance in determining the human response to vibration, namely, intensity, frequency, direction, and duration of the vibration. The ISO recommended guidance for evaluating the whole-body vibration is established based on the above-mentioned factors.

The ISO recommended data are given in terms of the weighted root-mean-square acceleration. In order to use this recommendation for the random vehicle vibration which are characterized by the power spectral density, the vibration boundary must be described in terms of the weighted average acceleration PSD $\bar{S}_{FDP}(f_o)$. This is accomplished by the following conversion equation[31]:

$$\bar{S}_{FDP}(f_o) = \frac{\bar{a}_w^2 (f_o)}{0.23 f_o} \tag{3.13}$$

where:

$\bar{a}_w$ is the ISO recommended weighted root-mean-square acceleration limit

f_o is the central frequency in Hz

From Fig.2.3, the equation describing the root-mean-square acceleration as a function of frequency is given by:

$$\bar{a}_w(f) = \begin{cases} 10^{b_{i1}} f^{m_{i1}} & \text{for } 1 \text{ Hz} < f < 2 \text{ Hz} \\ 10^{b_{i2}} f^{m_{i2}} & \text{for } 2 \text{ Hz} < f < 80 \text{ Hz} \end{cases} \tag{3.14}$$

The subscript i is used here to specify the exposure time. The second subscript 1 or 2 represent segment number 1 or 2 respectively (Fig.3.8). For the exposure times 1.0 h, 2.5 h, and 4 h, the values for b_{i1}, b_{i2}, m_{i1}, and m_{i2} are tabulated in Table 3.1. The data describing FDP boundary in terms of the weighted average acceleration PSD are plotted in Fig.3.8. The acceleration response PSD of driver mass must also be weighted to account for the influence of excitation frequency. The weighted acceleration response PSD $S_{wo}(f_i)$ is calculated in each of the one-third octave frequency band from the following:

$$S_{wo}(f_i) = W^2(f_i) S_o(f_i) \tag{3.15}$$

Duration of Exposure hours	Segment	ISO Recommended RMS Acceleration Curve	
		Slope m_i	Intercept b_i
1	1	0.0	-0.0706
	2	1.0	-0.3716
2.5	1	0.0	-0.3010
	2	1.0	-0.6020
4	1	0.0	-0.4498
	2	1.0	-0.7508

Table 3.1 Slope and Intercept of the ISO Recommended RMS Acceleration Limits for FDP in Transverse Vibrations

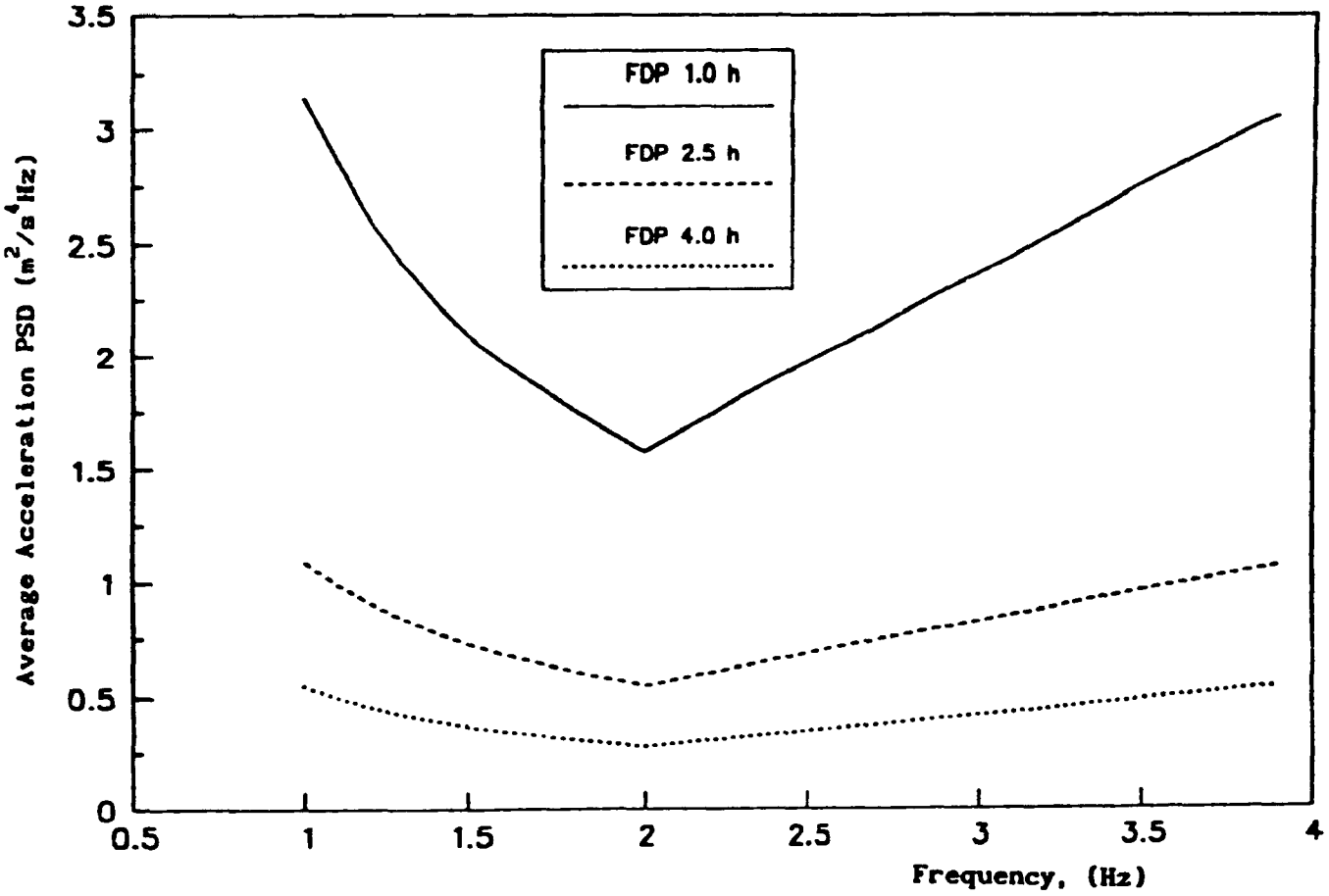

Fig.3.8 The ISO Recommended Fatigue Decreased Proficiency Limits in Terms of Average Acceleration PSD

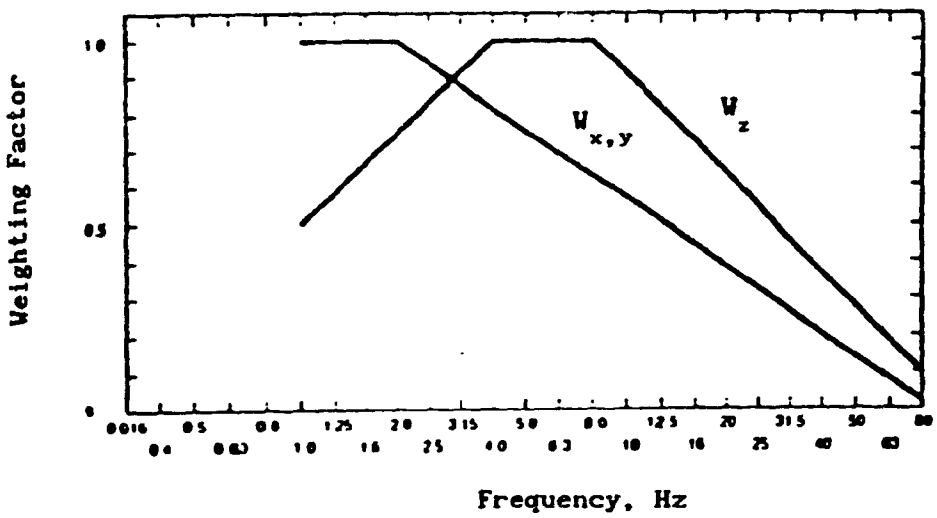

Fig.3.9 Frequency Weighting Curves Defined in ISO 2631 for Z-Axis (W_z) and X-Y Axis ($W_{x,y}$) Vibrations[26]

Where $W(f_1)$ is the ISO recommended frequency weighting factor which is shown in Fig.3.9.

3.5 Response Study of the Lateral Seat Suspension Model with a Vibration Absorber

The off-road terrain irregularities characterized by acceleration power spectral density indicate severe lateral vibration at 1.1 Hz. In order to achieve better ride performance without lowering the spring stiffness rate of the primary seat suspension, a vibration absorber is attached to the suspension system. A better understanding of the performance of such a system can be accomplished through parametric sensitivity study. The parametric sensitivity study will reveal the acceleration and relative displacement responses to variations of suspension parameters and will indicate a trend in the behaviour of various suspension parameters on the response and thus provides a basis for optimal design.

From Eqns.(3.6)-(3.12), it can be easily seen that the vibration response depends on both random input excitation and system parameters, specifically, the main system damping ratio ξ_1, absorber mass ratio μ ($\mu=M_a/M_1$), absorber tuning ratio α ($\alpha = \omega_2/\omega_1$), and absorber damping ratio ξ_2. In this investigation, the influence of each parameter on the system performance indices are studied in detail. The investigation is carried out by performing studies on both transmissibility and vibration response.

In the present study, the seat and driver mass M_1 and the spring rate of the primary suspension K_1 are assumed to be constants as given in

[4]. They are assigned the following values:

M_1 = 89.5 kg

K_1 = 1700 N/m

For parametric study of each parameter, one parameter at a time is varied and the other system parameters are taken as constants. The nominal values of the system parameters for this study are listed in Table 3.2. They are selected from several trial runs and are very close to the optimal values for the suspension parameters which are presented in chapter 5.

3.5.1 Influence of System Parameters on the Absolute Transmissibility of the Driver Mass

The Influence of the system parameters on the absolute transmissibility of the driver mass are shown in Figs.3.10 - 3.13. The results indicate that an increase of the absorber mass will widen the suppression frequency range (the suppression frequency range is defined as the frequency range which corresponds to the transmissibility below unity). The increase of absorber mass also shows a higher transmissibility peak at the low excitation frequency and a lower transmissibility peak at the higher excitation frequency. Since the first transmissibility peak is usually higher than the second one, larger absorber mass will give higher transmissibility peak. Comparing with the transmissibility without vibration absorber, the advantage of adding absorber mass is to obtain lower transmissibility values between the two transmissibility peaks. The absolute transmissibility is very sensitive to the absorber mass ratio at the neighborhood of the tuned frequency (1.1Hz). The absorber mass has little effect on the absolute

Parametric study of	Other parameters for the simulation
main system damping ratio , ξ_1	$\mu = 0.4$ $\alpha = 1.5$ $\xi_2 = 0.15$
absorber damping ratio , ξ_2	$\mu = 0.4$ $\xi_1 = 0.55$ $\alpha = 1.5$
absorber tuning ratio , α	$\mu = 0.4$ $\xi_1 = 0.55$ $\xi_2 = 0.15$
absorber mass ratio , μ	$\alpha = 1.5$ $\xi_1 = 0.55$ $\xi_2 = 0.15$

Table 3.2 The System Parameters Used For Simulations

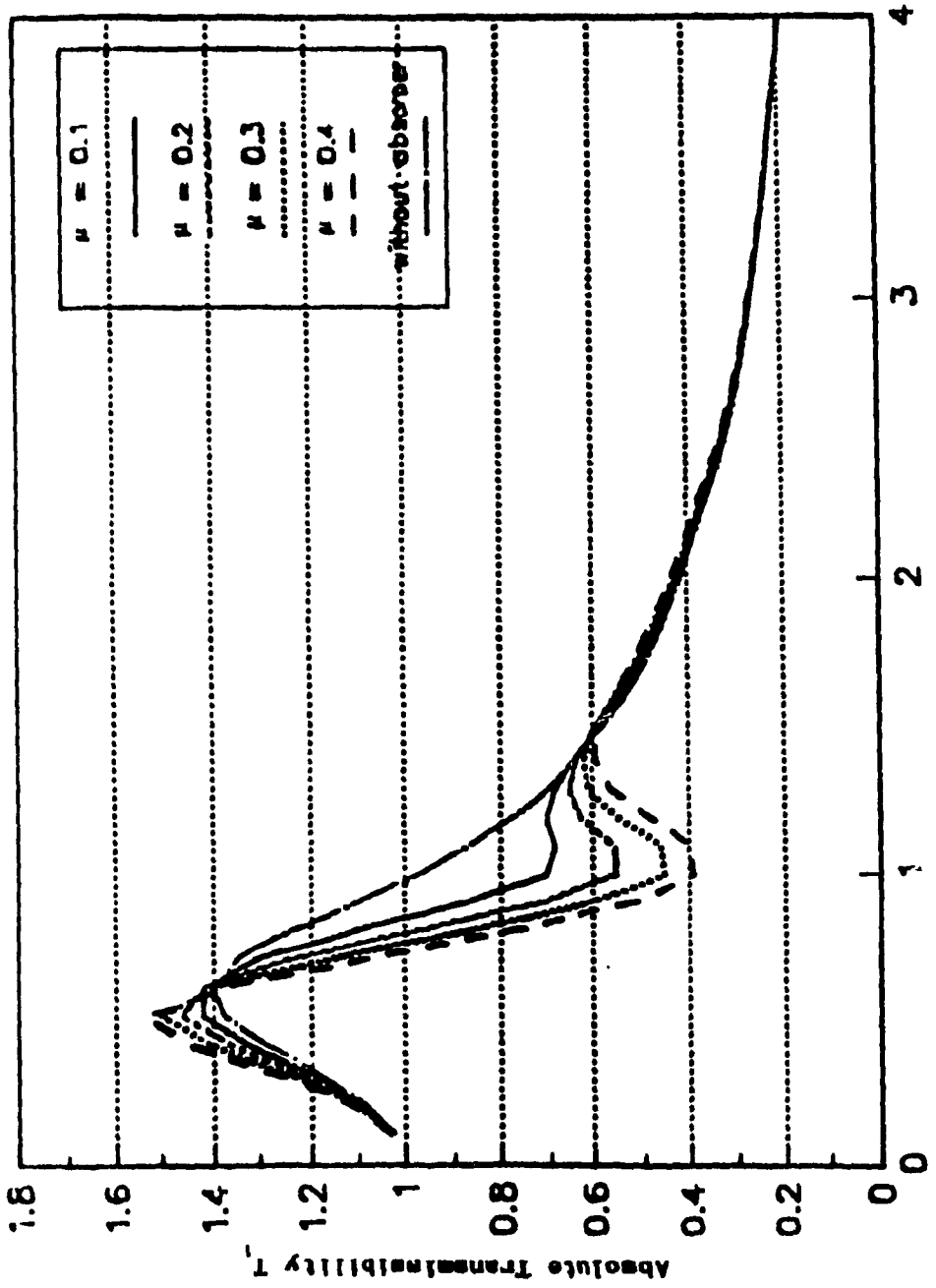

Fig.3.10 Influence of Absorber Mass on the Absolute Transmissibility of the Driver Mass

transmissibility for the excitation frequencies below 0.3 or higher than 1.5 Hz.

The effect of the main system damping on the absolute transmissibility is similar to that of a single-degree-of-freedom system. Higher damping will help in suppressing the transmissibility at low excitation frequency and will increase the transmissibility at high excitation frequency. The main difference is that, due to the addition of a vibration absorber, the frequency ratio which distinguish the performance of damping is no longer $\sqrt{2}$, but some value below this. Thus the addition of a vibration absorber will increase the suppression bandwidth.

The absolute transmissibility of driver mass with variations in absorber damping value is simulated with absorber damping ratio varying in the range of 0.05 - 0.35. The damping ratio for the simulation is assumed to be low because high damping will result in stiffening the vibration absorber and the resultant system will behave similarly as that of primary system having total mass M_1+M_a. For conventional absorber, the absorber damping ratio is usually below 0.3.

The influence of absorber damping on the absolute transmissibility is shown in Fig.3.12. The absorber damping is most effective in the neighborhood of the tuned frequency. In this frequency range, the smaller the absorber damping, the lower the absolute transmissibility of the driver mass will be. When the vibration absorber has no damping, the vibration response of the driver at the tuned frequency will be totally diminished. However, the effectiveness of vibration isolation at the neighborhood of the tuned frequency is achieved at the cost of relatively poorer isolation performance for excitation frequency away from the tuned

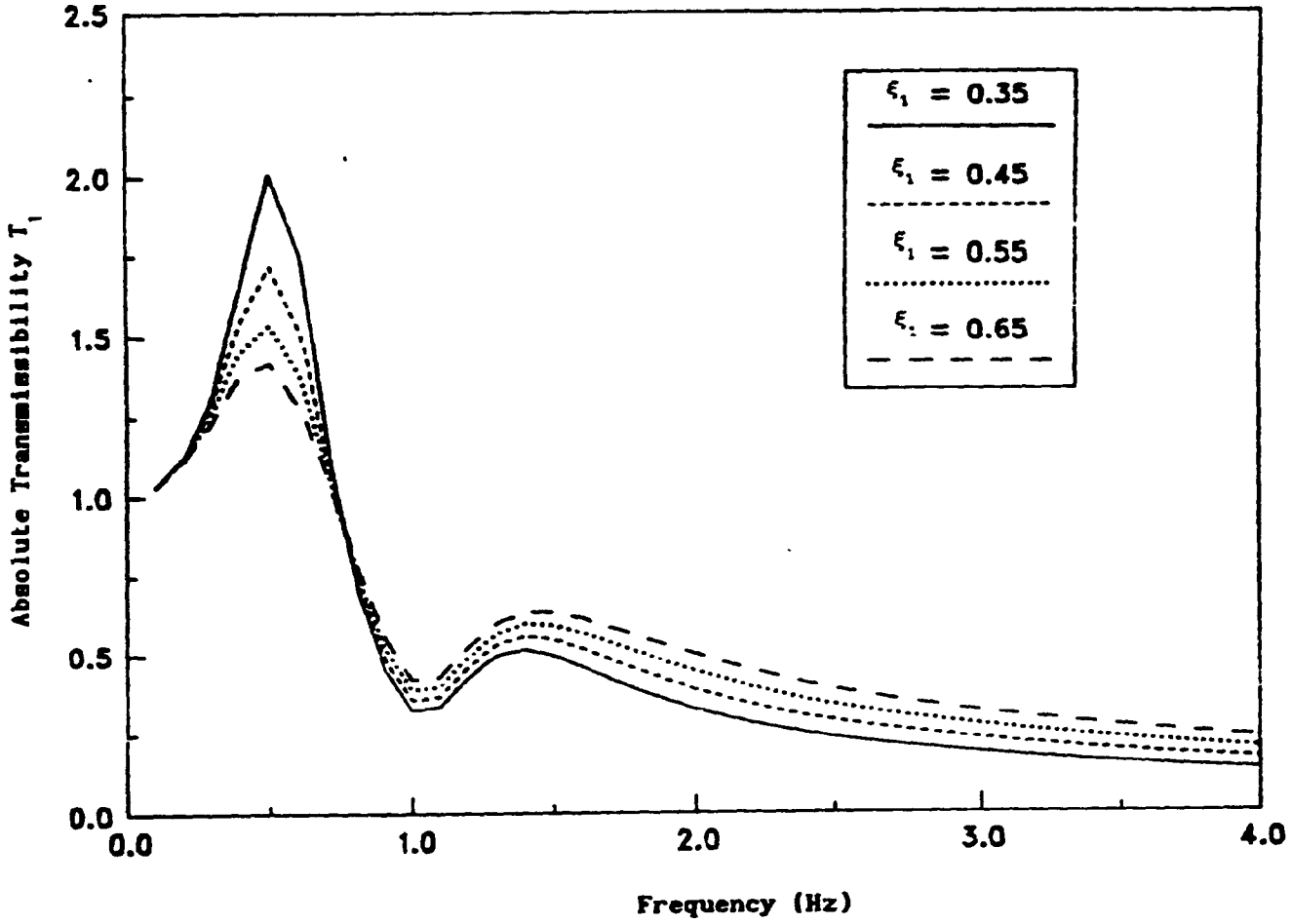

Fig.3.11 Influence of Main System Damping Ratio on the Absolute Transmissibility of the Driver Mass

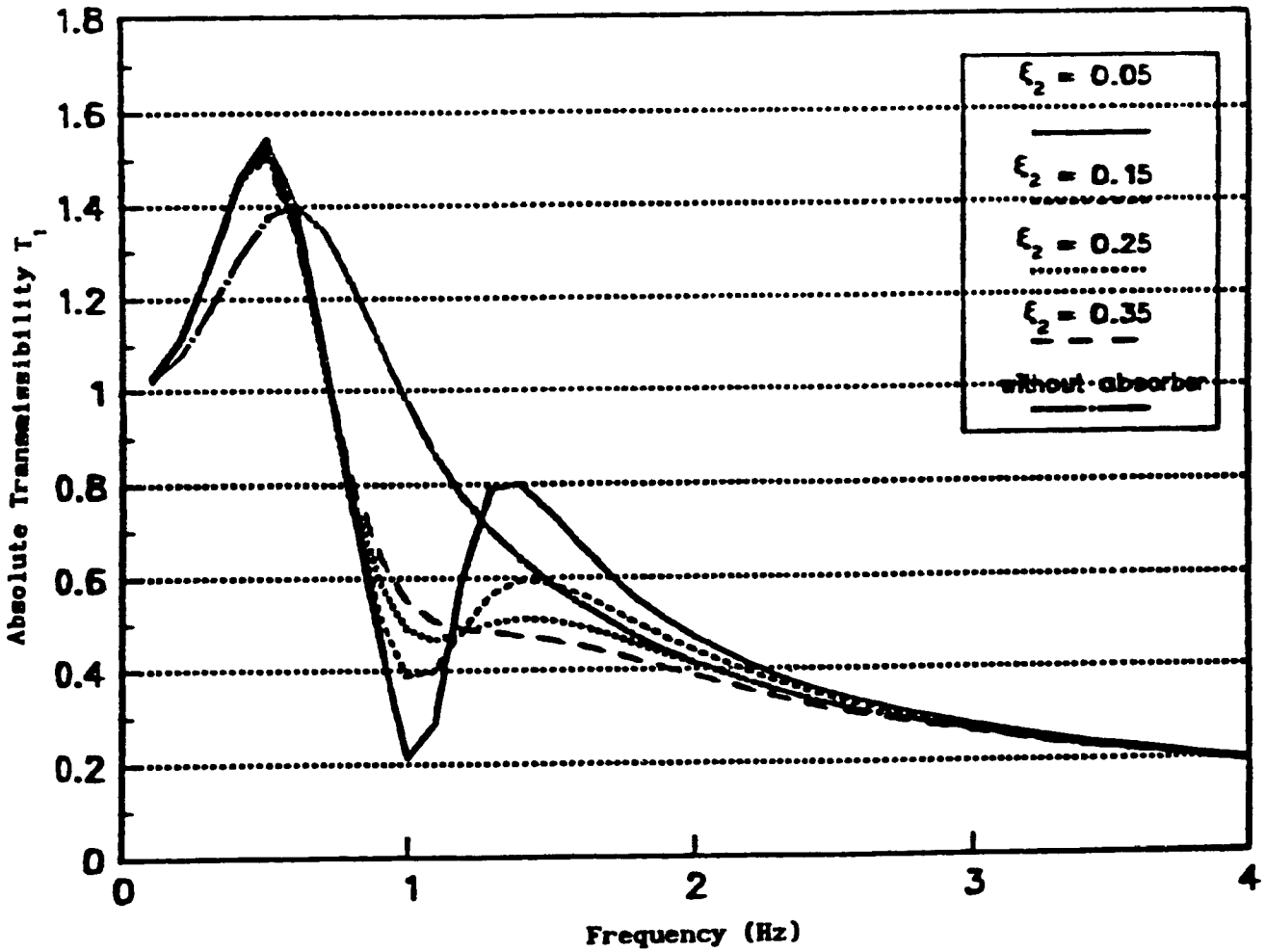

Fig.3.12 Influence of Absorber Damping Ratio on the Absolute Transmissibility of the Driver Mass

frequency, especially at the system's natural frequencies. It can also be noted that the transmissibility plot has only one peak for absorber damping ratio equal to or greater than 0.35.

The influence of the absorber tuning ratio on the transmissibility is shown Fig.3.13. The tuning ratio has little influence on the first peak of the absolute transmissibility. The increase of tuning ratio is to shift the "trough" of the transmissibility to the right (corresponding to a higher excitation frequency). It is also found that, the transmissibility is more sensitive to the absorber tuning ratio when the excitation is in the vicinity of the tuned frequency. Since vibration excitation at the tuned frequency is usually the most intensive, the transmissibility at the neighborhood of the tuned frequency generally has greater influence on the vibration response.

3.5.2 Influence of System Parameter Variations on the Acceleration PSD Response of the Driver Mass

The influence of the variations of the suspension parameters on the acceleration PSD response of the driver mass is similar to that of the absolute transmissibility. However, there are differences due to the varying excitation input amplitudes. It is well known that the vibration response depends on both the transmissibility characteristics and the excitation input. If the excitation input is constant over the frequency range, then the severity of the vibration response can be totally informed by the transmissibility. However, if the excitation input amplitudes are not constant over the frequency range, then the transmissibility alone is not capable of reflecting the real picture of

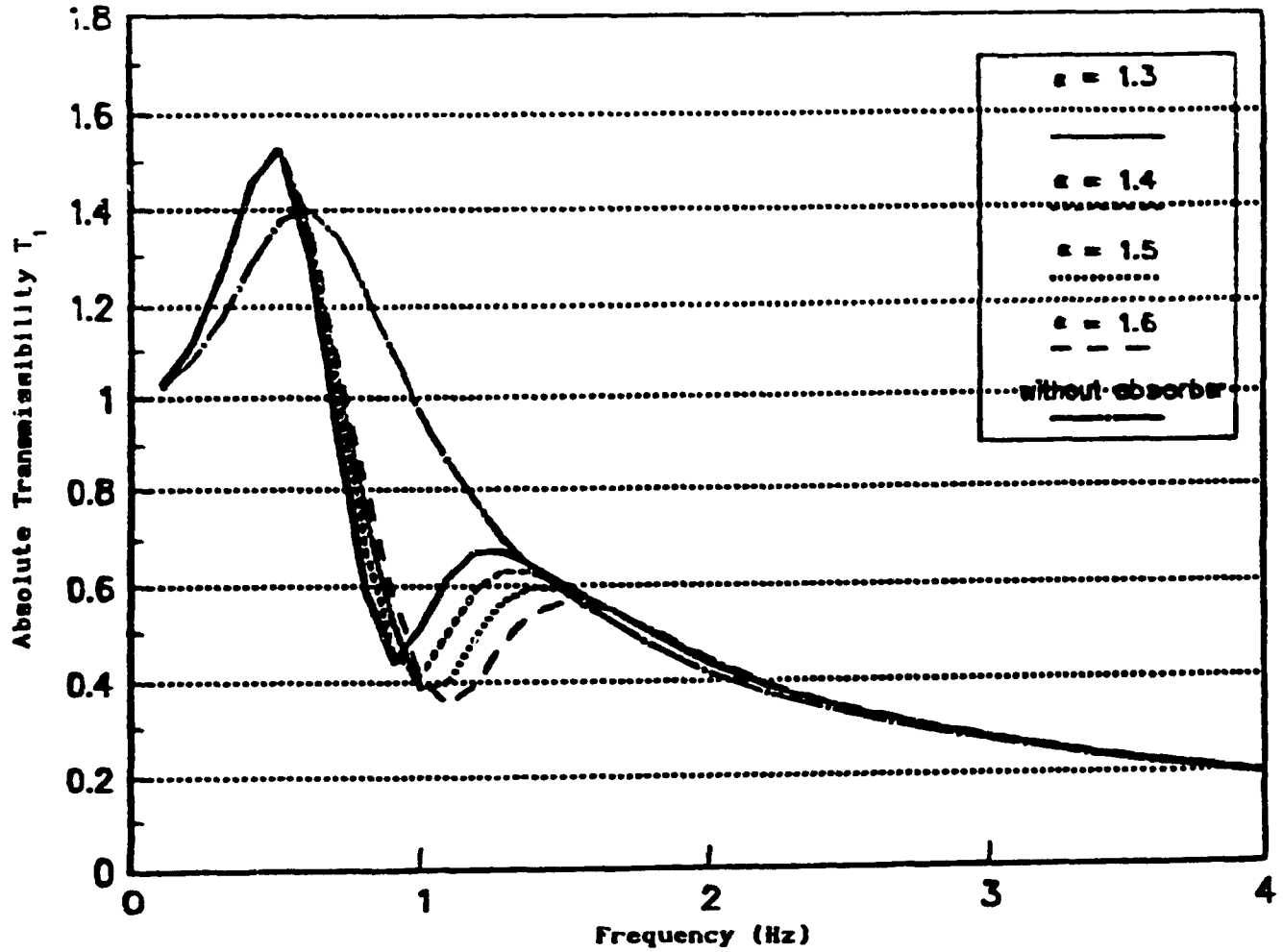

Fig.3.13 Influence of Absorber Tuning Ratio on the Absolute Transmissibility of the Driver Mass

the intensity of the vibration response. In this case, special attention must be made to the transmissibility where large vibration input occurs.

The acceleration response PSD of the driver mass, as shown in Fig.3.14 reveals that smaller absorber damping will help to reduce the acceleration response in the vicinity of the excitation to which the dynamic absorber is tuned. This performance is achieved at the expense of relatively poorer acceleration isolation for the excitation frequency away from the tuned frequency. By increasing the absorber damping, the acceleration response around the tuned frequency will be increased while the acceleration response for the excitation frequency away from the tuned frequency will be improved. The absorber damping ratio should be selected in such way that the acceleration response of the driver mass at the tuned frequency and at the system's resonant frequencies are reduced uniformly to a certain level. From the point of view of reduction of the peak level of lateral acceleration PSD, the absorber damping ratio should be selected around 0.15. In such case, the peak level of the lateral acceleration PSD can be reduced approximately to 1.37 $m^2/s^4/Hz$, about 80% vibration reduction in comparison to a seat suspension without absorber. This is a significant improvement.

Absorber tuning ratio is another important factor that has great influence on the ride performance. The selection of the absorber tuning ratio determines the "filter band". Usually, the tuned frequency is chosen either at the natural frequency of the primary system or at the excitation frequency where intensive vibration input occurs. Due to this reason, the acceleration response is very sensitive to the tuning ratio. Improper tuning ratio may cause significantly higher acceleration response.

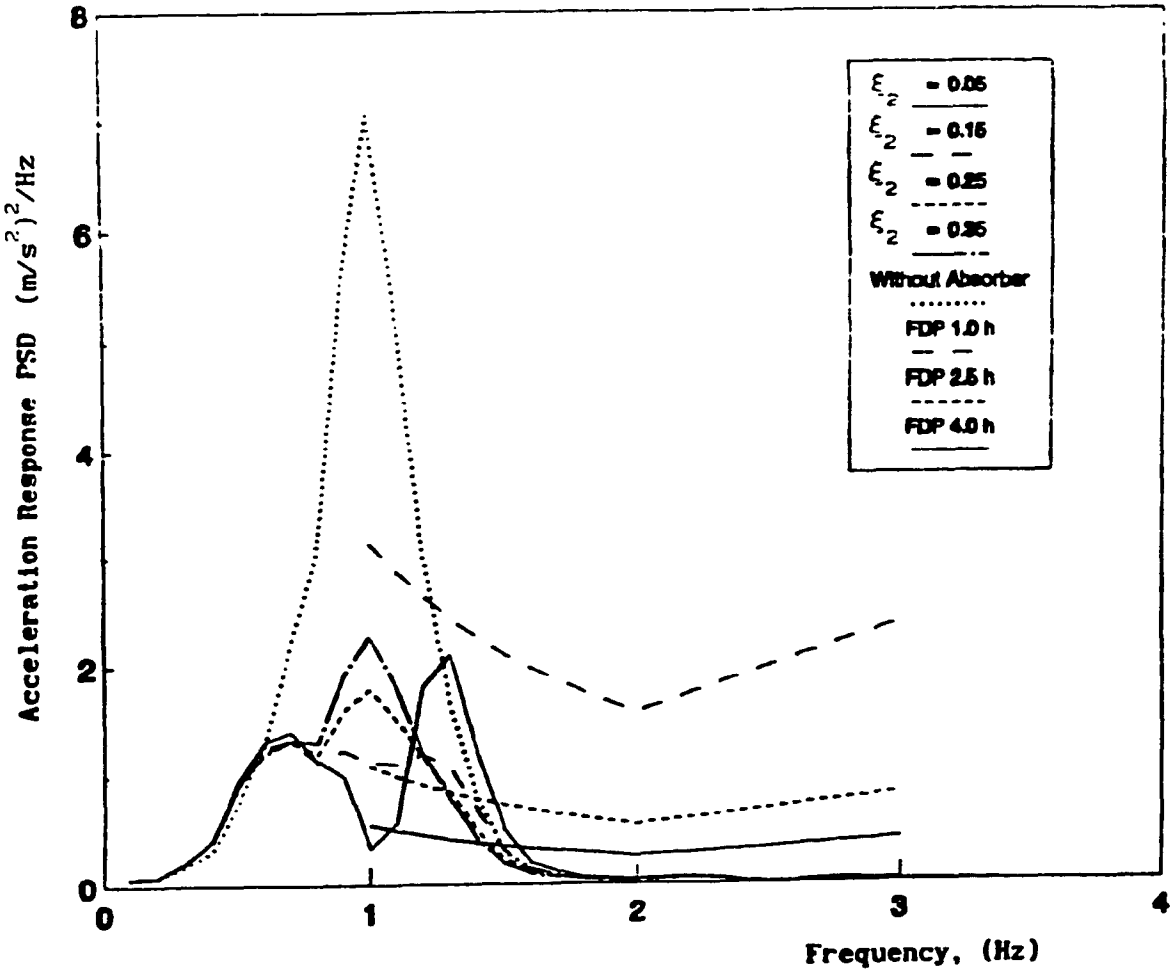

Fig.3.14 Influence of Absorber Damping Ratio on the Acceleration Response of the driver Mass

The influence of tuning ratio on the acceleration response of driver mass is shown in Fig.3.15. The simulation results indicate that the absorber tuning ratio equal to 1.5 produce better ride performance than other tuning ratios.

The role of the main system damping in the vibration isolation is to dissipate energy and thus to reduce the vibration response. In the lower excitation frequency range, the damper is mainly for dissipating energy, thus high damping will give lower acceleration response, however, in the higher excitation frequency, high damping will cause the suspension system to stiffen up, and thus deteriorates the vibration isolation performance. Since the excitation input is varying with the excitation frequency, higher transmissibility peak does not necessarily correspond to a higher peak in the acceleration response. The simulation results indicate that better ride performance is achieved when the main system damping ratio is selected around 0.55. This damping ratio offers good compromise between high and low frequency performance. The optimal value for minimizing the peak of the acceleration response PSD can be found in chapter 5.

The effect of the absorber mass on the acceleration response of the driver mass, as shown in Fig.3.17, indicates that larger mass ratio will produce smaller acceleration response. However, this statement is true only if other parameters are properly chosen. In other words, if other parameters are not correctly selected, larger mass ratio will not necessarily provide better vibration isolation. In fact, it is not always an improvement by arbitrarily increasing M_a, leaving ξ_1, ω_2 and ξ_2 unchanged. Rather, any change of a single parameter will require variation in other parameters. From the point of view of better ride

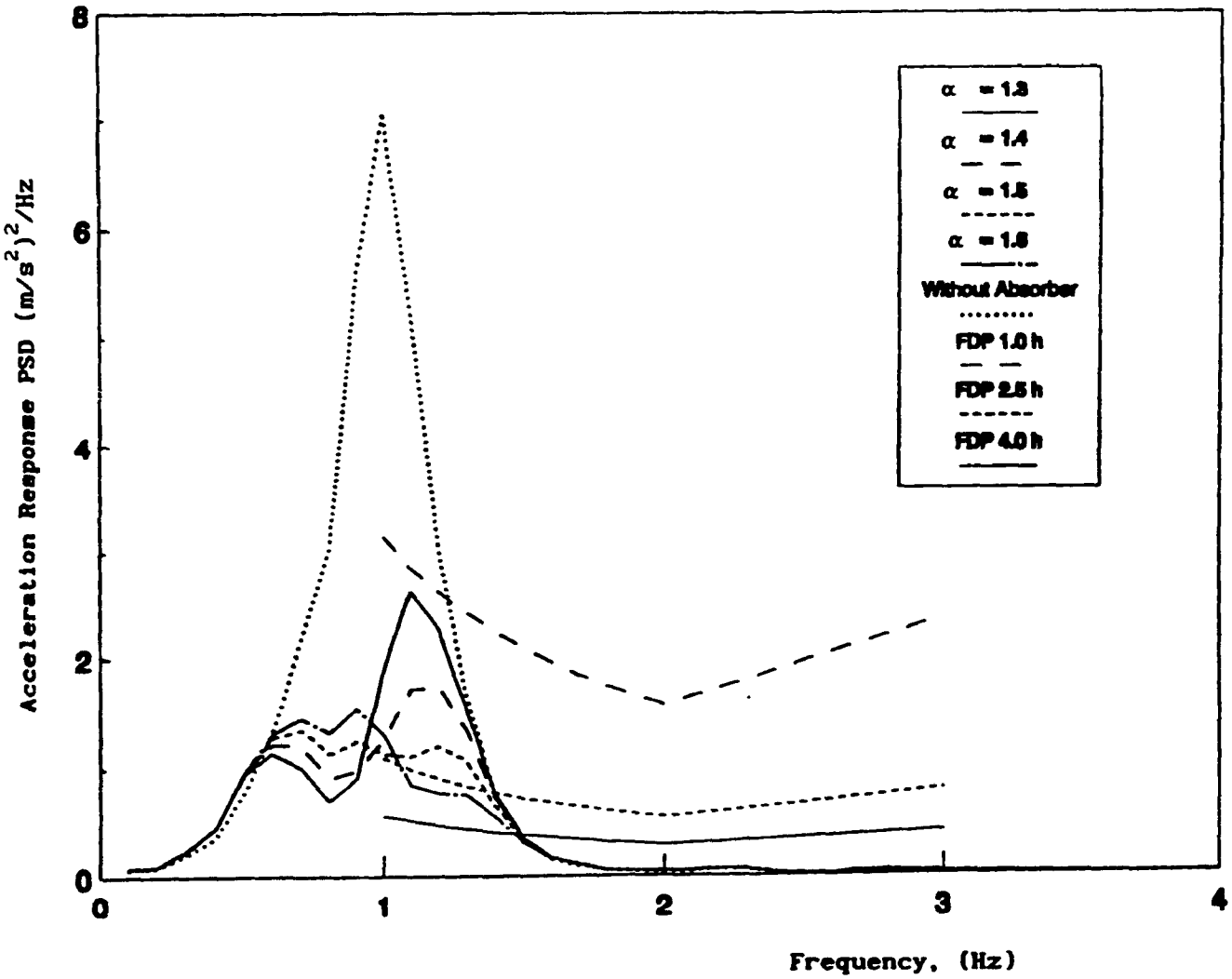

Fig.3.15 Influence of Absorber Tuning Ratio on the Acceleration Response of the Driver Mass

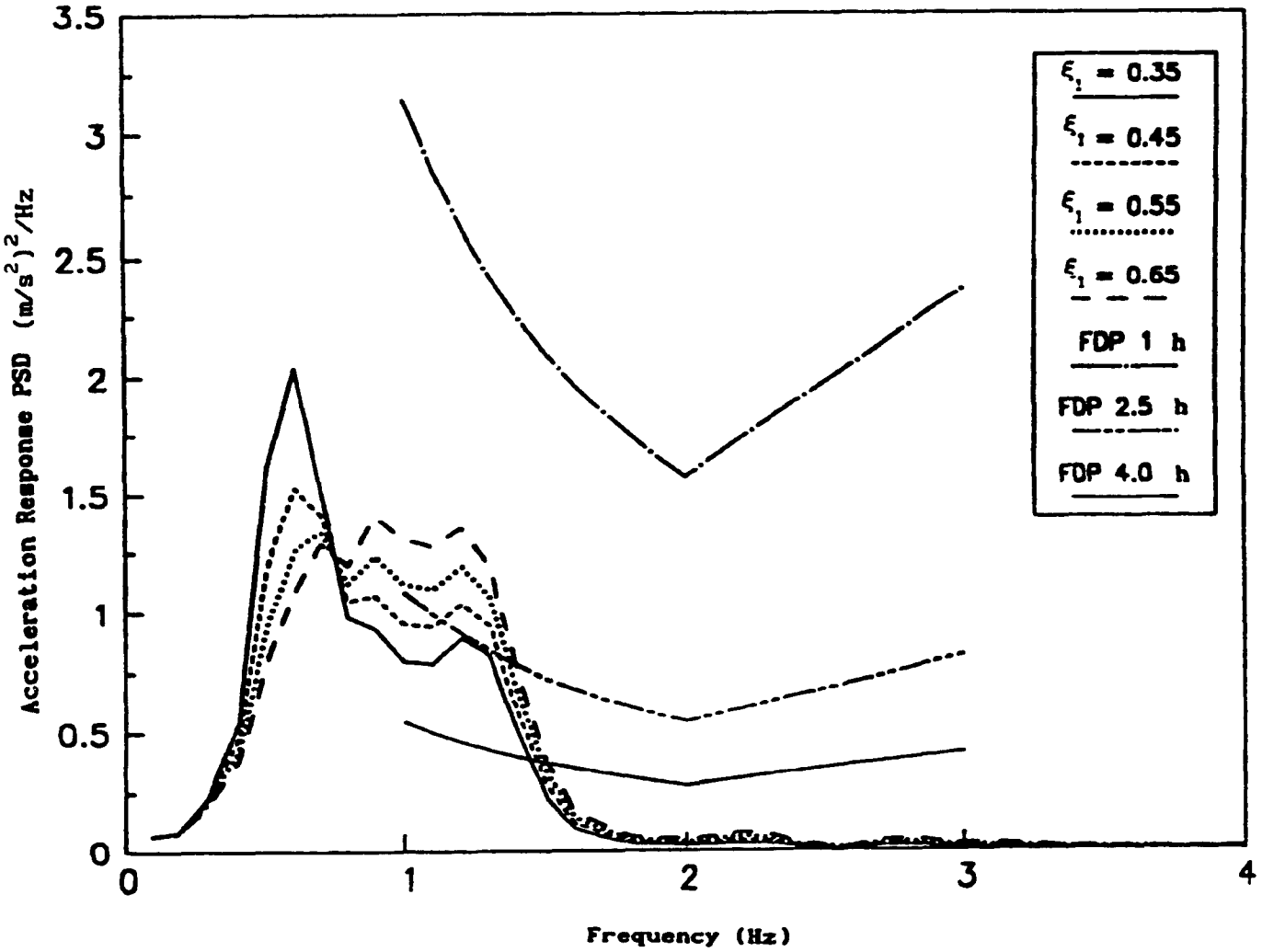

Fig.3.16 Influence of Main System Damping Ratio on the Acceleration Response of the Driver Mass

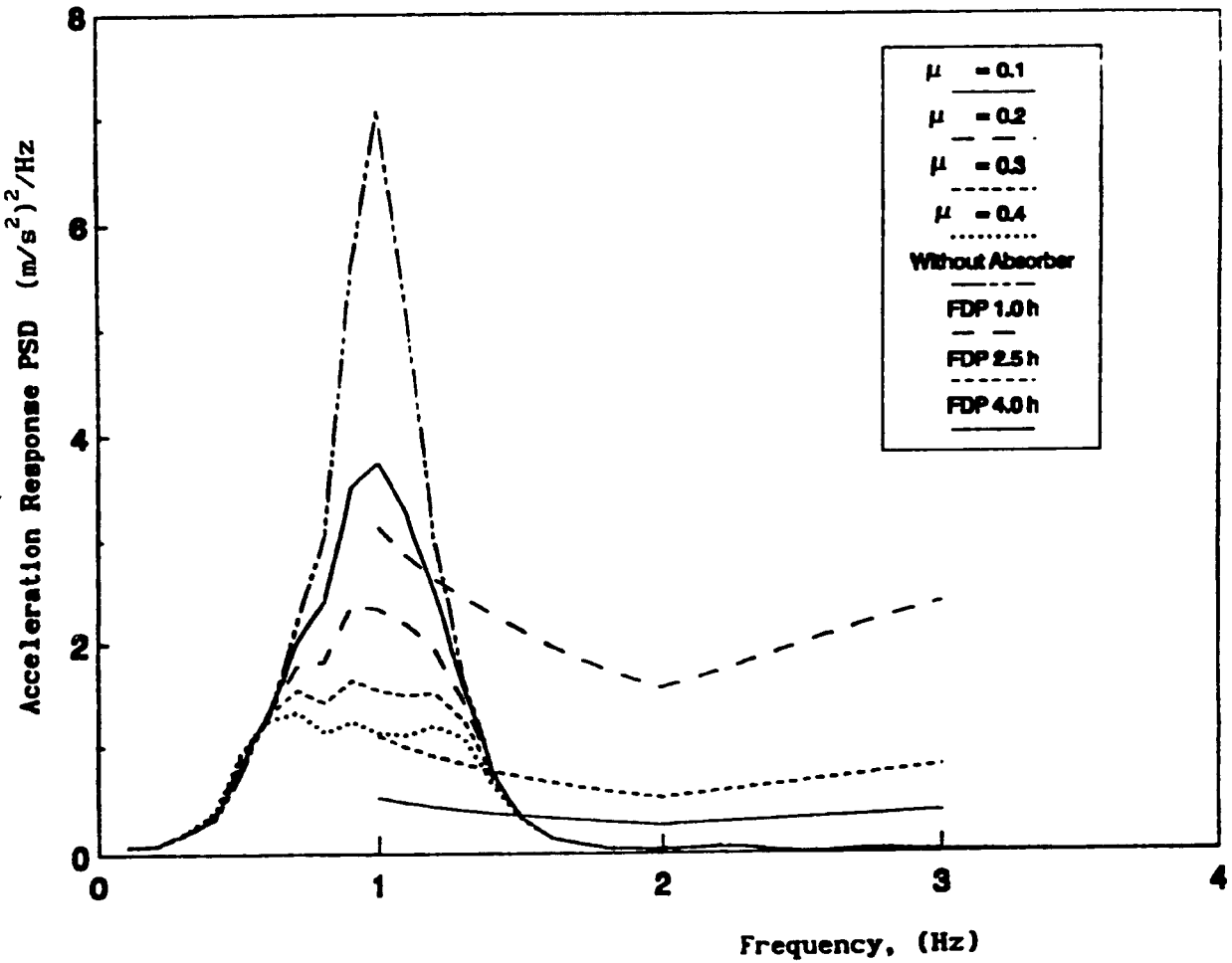

Fig.3.17 Influence of Absorber Mass on the Acceleration Response of the Driver Mass

performance, it is always desirable to have larger mass ratio. However, larger mass ratio means heavier weight of combined system which is undesirable in practice. The selection of mass ratio thus has to compromise between good vibration isolation and small weight of the resultant system.

3.5.3 Influence of System Parameter Variations on the Relative Transmissibility of Driver Mass

The influence of system parameters on the relative transmissibility is demonstrated in Figs.3 18 - 3.21. Increasing the absorber mass will produce lower relative transmissibility for the excitation frequency greater than 0.8 Hz. For the excitation frequency below 0.8 Hz, however, the transmissibility increases with greater absorber mass. Comparing the results with that of the lateral seat suspension without absorber, the addition of vibration absorber gives better isolation performance for higher excitation frequencies ($f > 0.8$ Hz), but poorer isolation performance for lower excitation frequencies ($f < 0.8$ Hz).

The influence of the absorber damping on the relative displacement transmissibility is shown in Fig.3.19. It can be seen that smaller absorber damping ratio provides better isolation performance in the neighborhood of the tuned frequency. At other excitation frequencies, higher absorber damping ratio is desirable. The results also show that higher absorber damping ratio will produce wider suppression frequency range.

The influence of the absorber tuning ratio on the relative transmissibility is shown in Fig.3.20. The effect of the absorber tuning

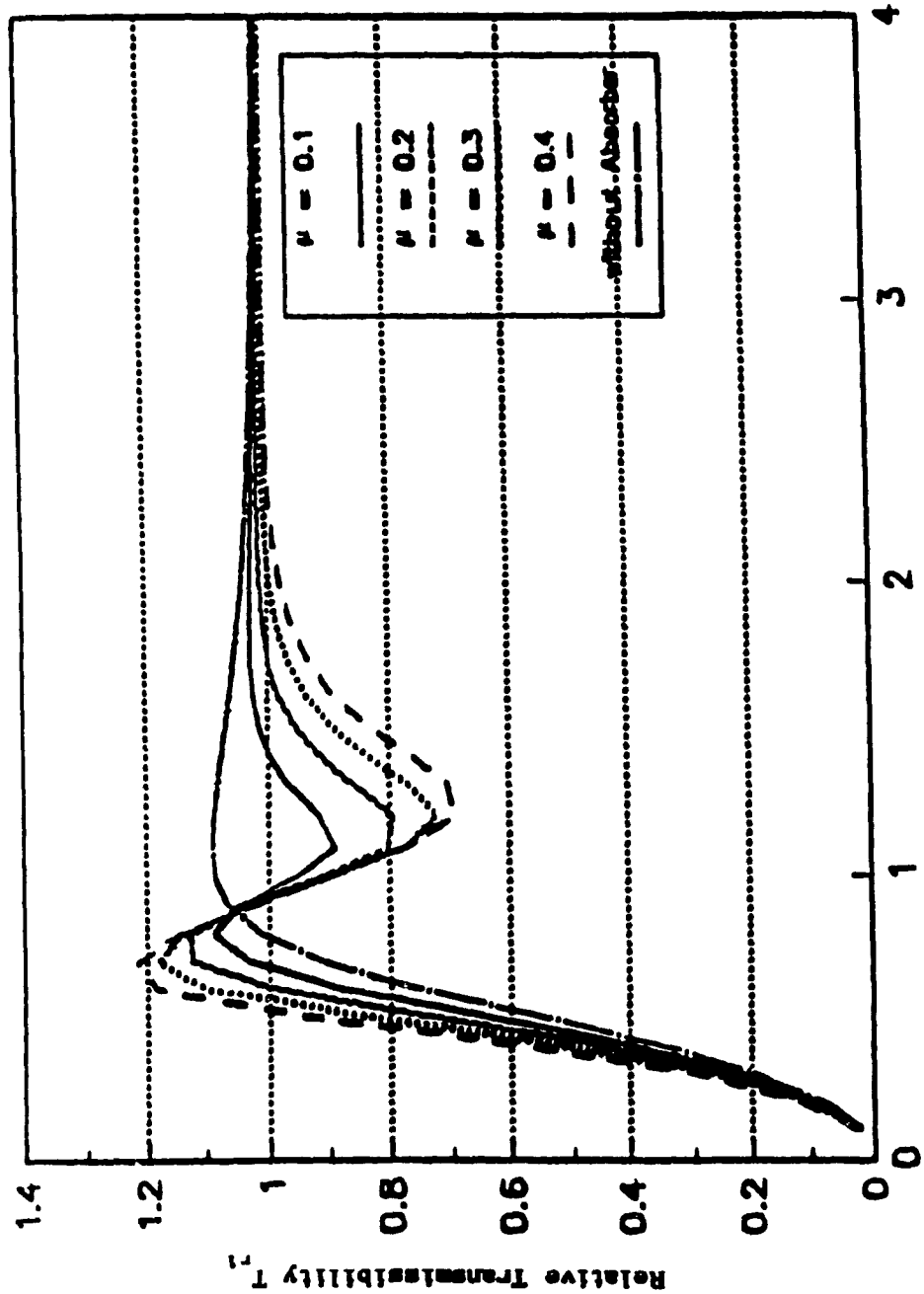

Fig.3.18 Influence of Absorber Mass on the Relative Transmissibility of the Driver Mass

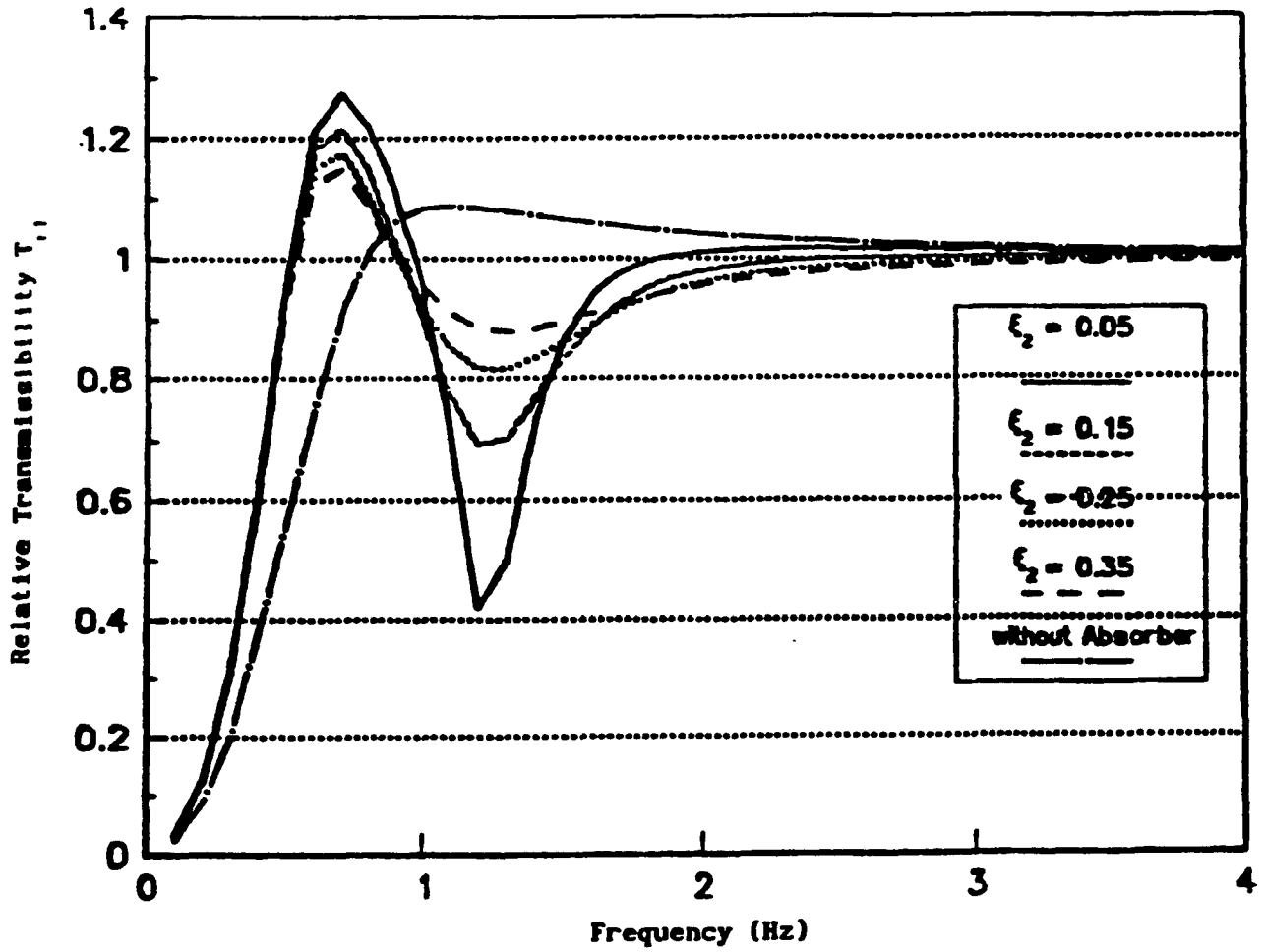

Fig.3.19 Influence of Absorber Damping Ratio on the Relative Transmissibility of the Driver Mass

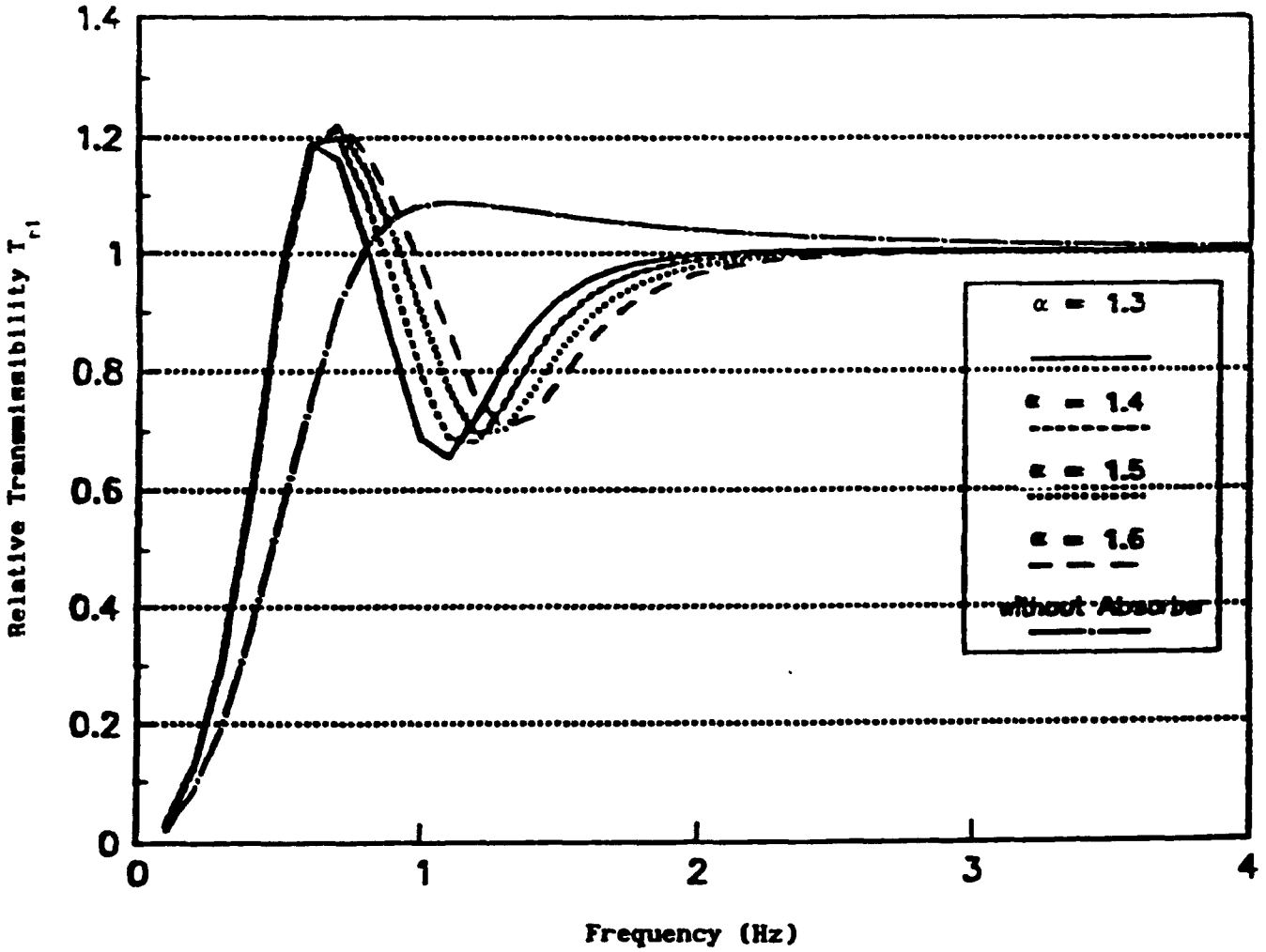

Fig.3.20 Influence of Absorber Tuning Ratio on the Relative Transmissibility of the Driver Mass

ratio on the relative transmissibility is to shift the "trough" at the tuned frequency.

The influence of the main system damping ratio on the relative transmissibility is plotted in Fig.3.21, It can be seen that higher main system damping produces lower relative transmissibility for all excitation frequencies.

3.5.4 Influence of System Parameter Variations on the Relative Displacement Response of Driver Mass

The influence of absorber damping ratio on the relative displacement response of driver mass is shown in Fig.3.22. It indicates that, unless the absorber damping ratio is very small which cause the resonance at the system's second resonant frequency, the influence of the absorber damping ratio on the relative displacement response of the driver mass is very little. The simulation results also show that the attachment of the vibration absorber will produce higher peak relative displacement response. In the case of $\xi_2 = 0.15$, the best absorber damping ratio based on acceleration response PSD of the driver mass (Fig.3.14), the peak relative displacement is approximately 0.5 cm greater than the seat suspension without absorber.

Fig.3.23 shows the influence of tuning factor on the relative displacement of the driver mass. It can be seen that smaller tuning ratio will produce lower relative displacement response. It is also interesting to find that the relative displacement response of the driver mass corresponding to $\alpha = 1.3$ is smaller than that of the lateral seat suspension without absorber. This result illustrates the possibility

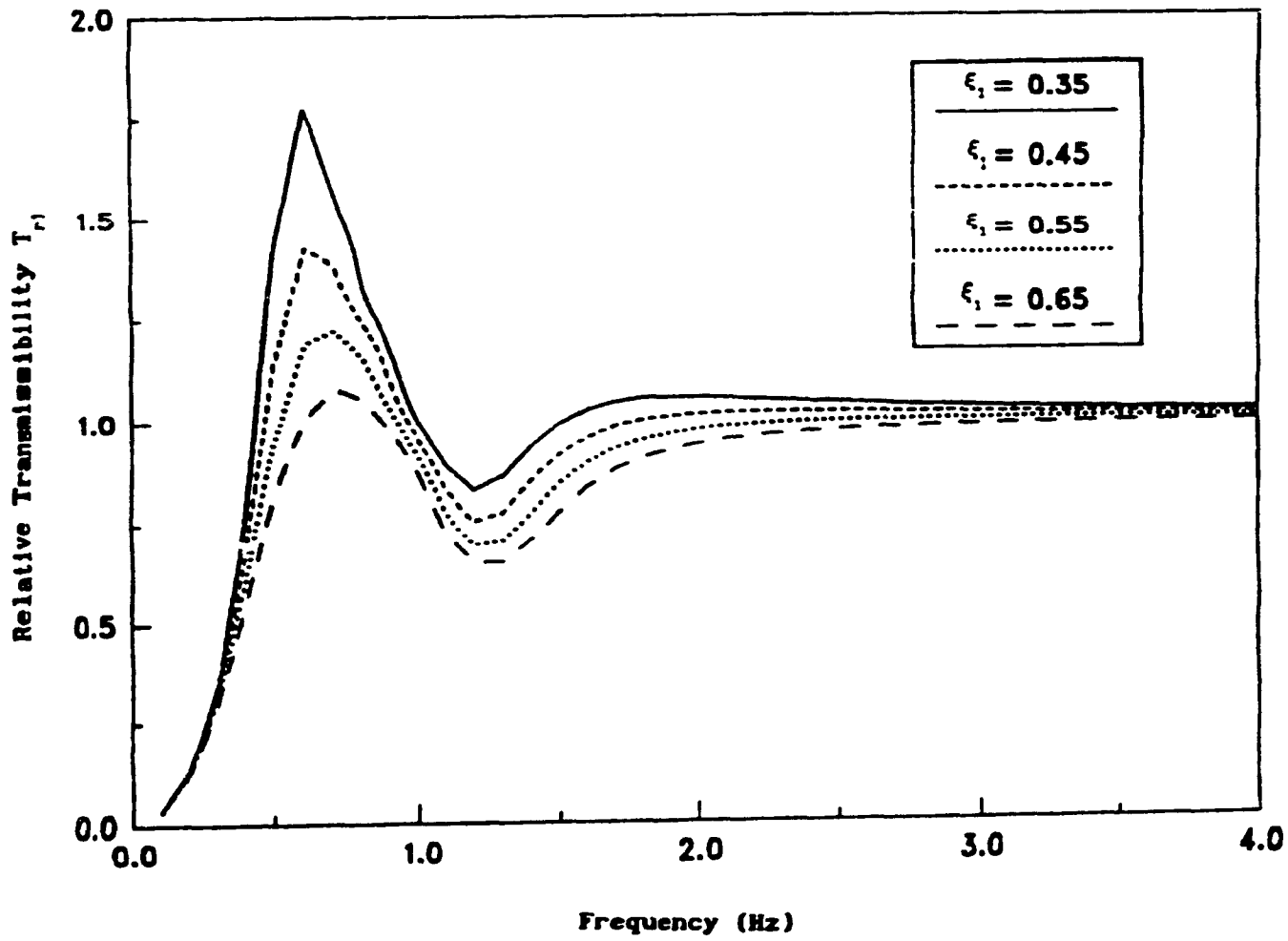

Fig.3.21 Influence of Main System Damping Ratio on the Relative Transmissibility of the Driver Mass

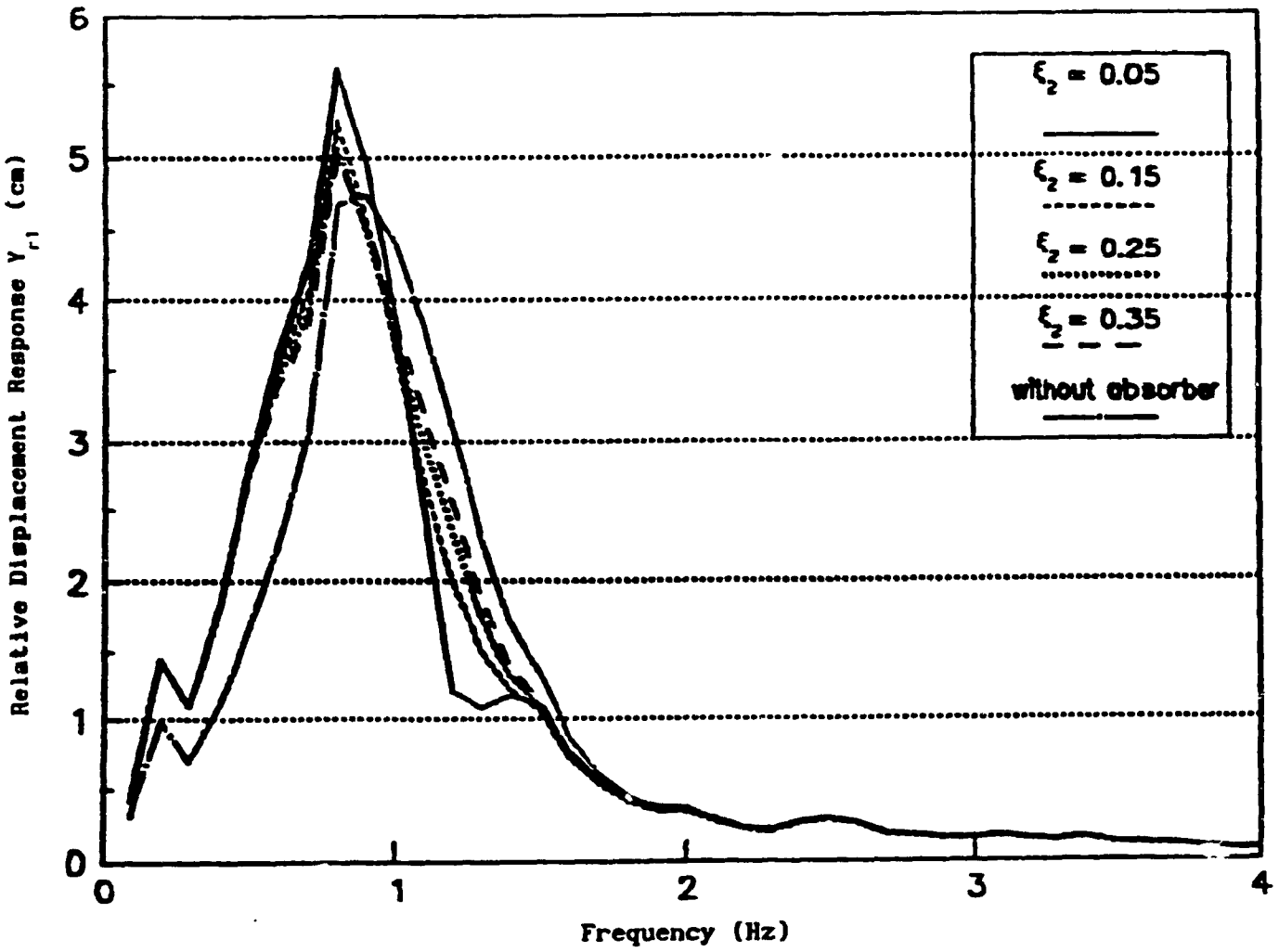

Fig.3.22 Influence of Absorber Damping Ratio on the Relative Displacement Response of the Driver Mass

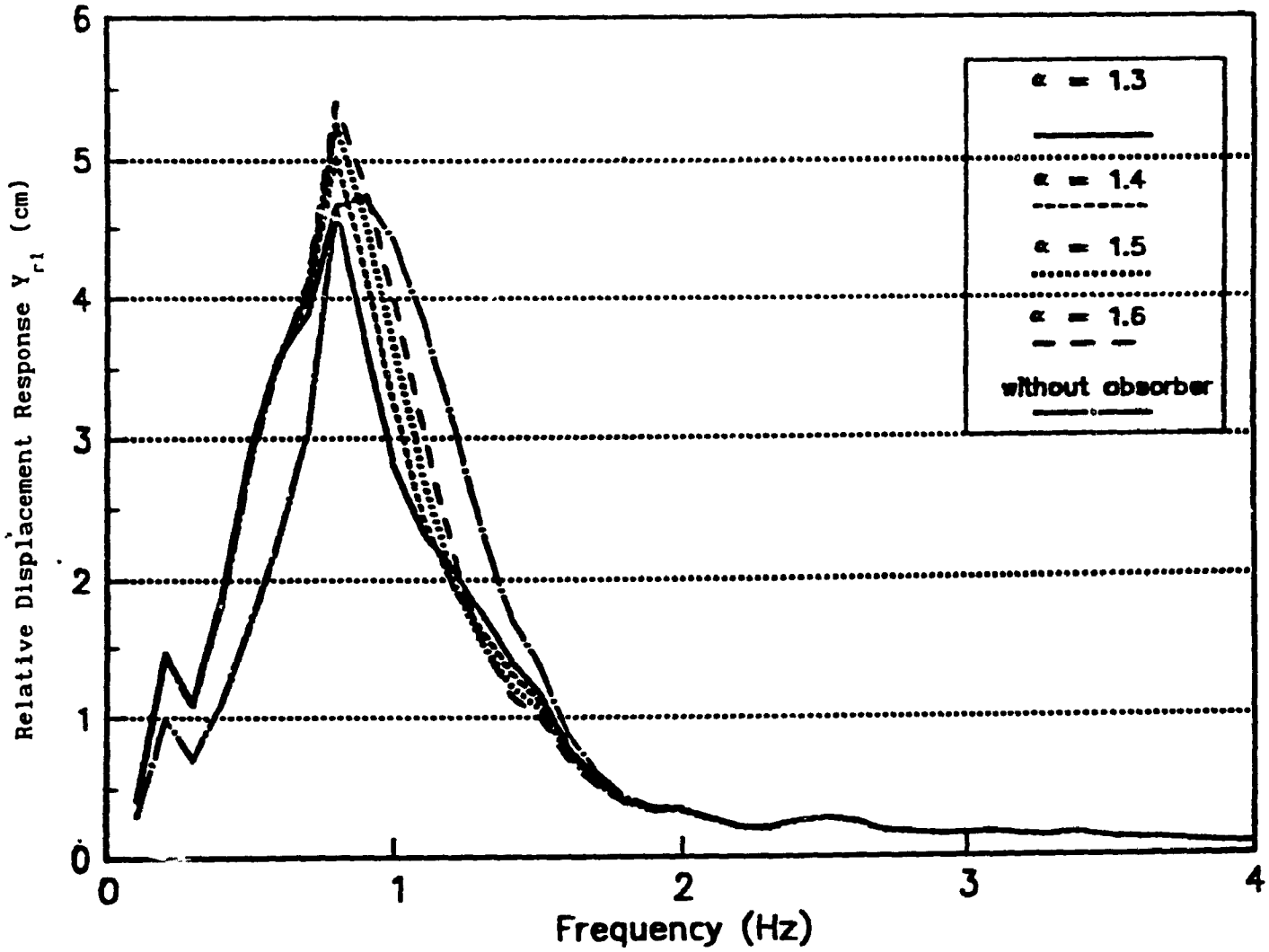

Fig.3.23 Influence of Absorber Tuning Ratio on the Relative Displacement Response of the Driver Mass

that, by carefully choosing absorber parameters, the acceleration and relative displacement response of the driver mass can be both reduced.

The relative displacement response of the driver mass with the variation in the main system damping ratio is plotted against frequency in Fig.3.24. For the entire frequency range of interest, higher main system damping produces lower relative displacement response.

The relative displacement response of the driver mass, as shown in Fig.3.25., indicates that the absorber mass ratio has little influence on the peak response. However, the peak relative displacement response is approximately 10% higher than that of system without absorber.

3.5.5 Influence of System Parameter Variations on the Relative Transmissibility of the Absorber Mass

Although a number of researchers have reported on the application of absorbers for vibration control[32-39], their study has been focused on the motion response of the primary system. Little work has been reported on the motion of the absorber. It should be argued that the response of the secondary mass is equally important. Excessively large vibration response of absorber has practical limitations if an absorber is to be added to a real system. In the present study, the relative displacement between the absorber mass and seat base can be used to indicate the severity of the motion of the absorber and thus the following is studied in this investigation.

The influence of the main system damping ratio on the relative transmissibility of the absorber mass is shown in Fig.3.26. The results reveal that high main system damping is needed to reduce the relative transmissibility for excitation frequencies below 0.9 Hz, but the

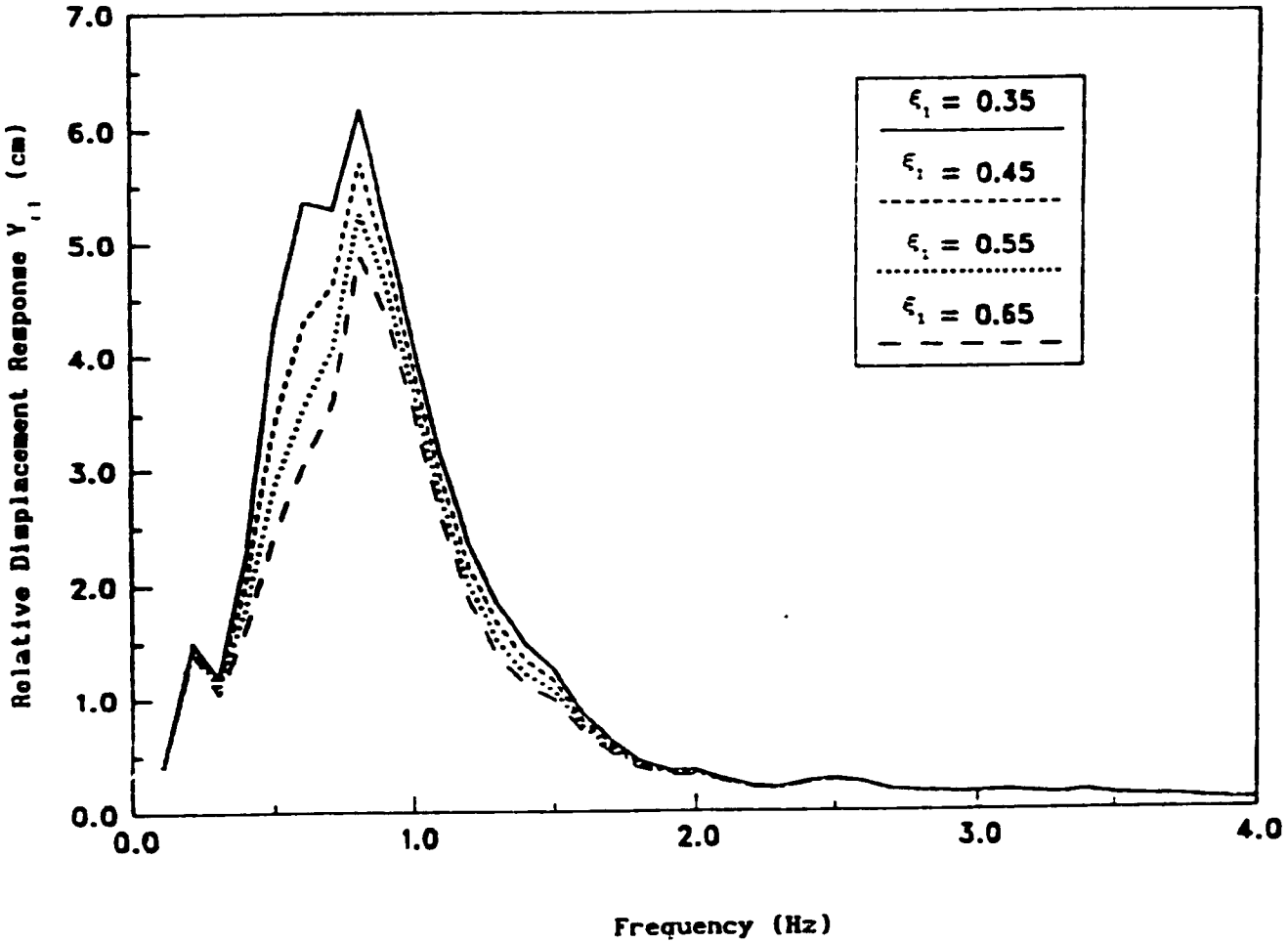

Fig.3.24 Influence of Main System Damping Ratio on the Relative Displacement Response of the Driver Mass

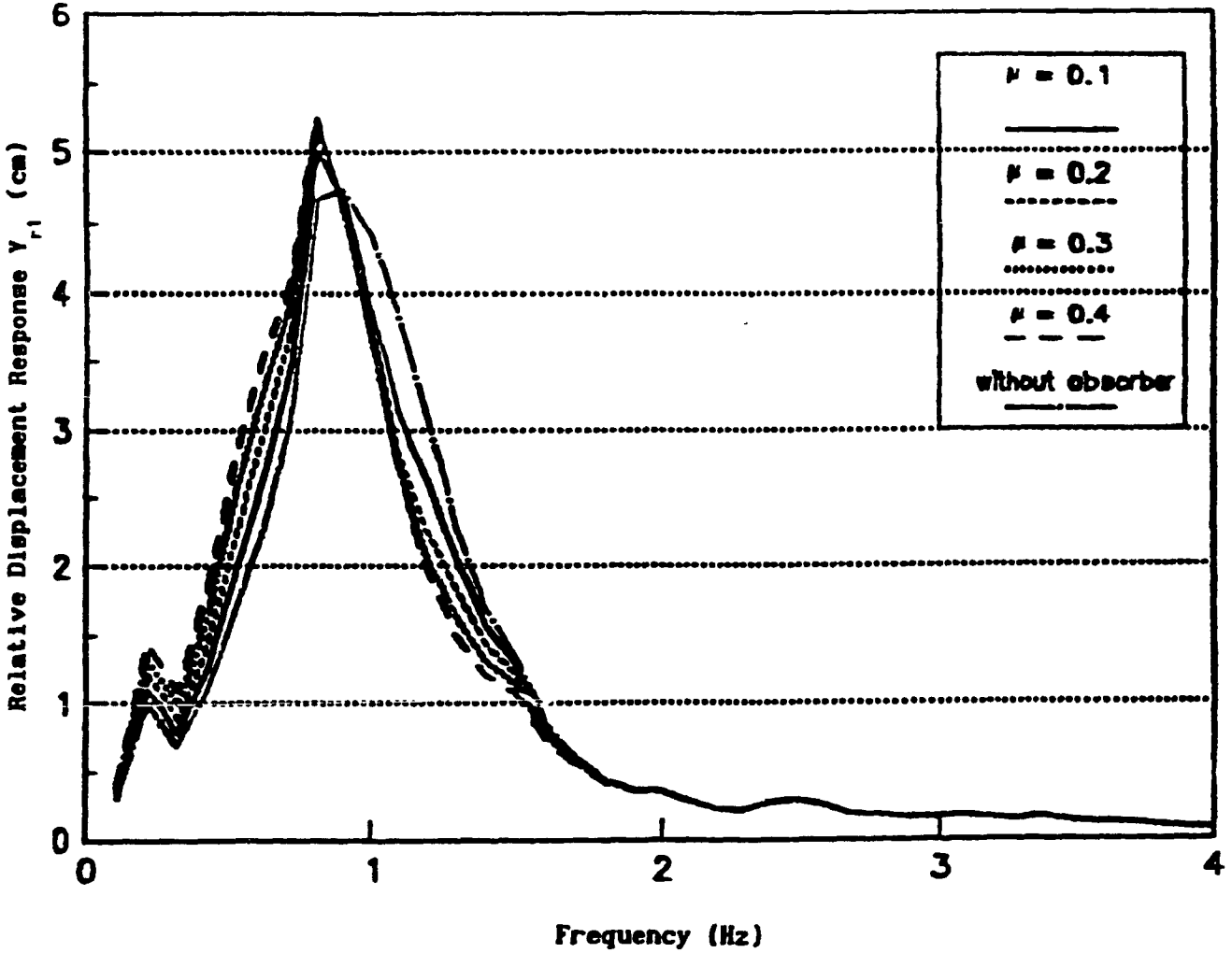

Fig.3.25 Influence of Absorber Mass Ratio on the Relative Displacement Response of the Driver Mass

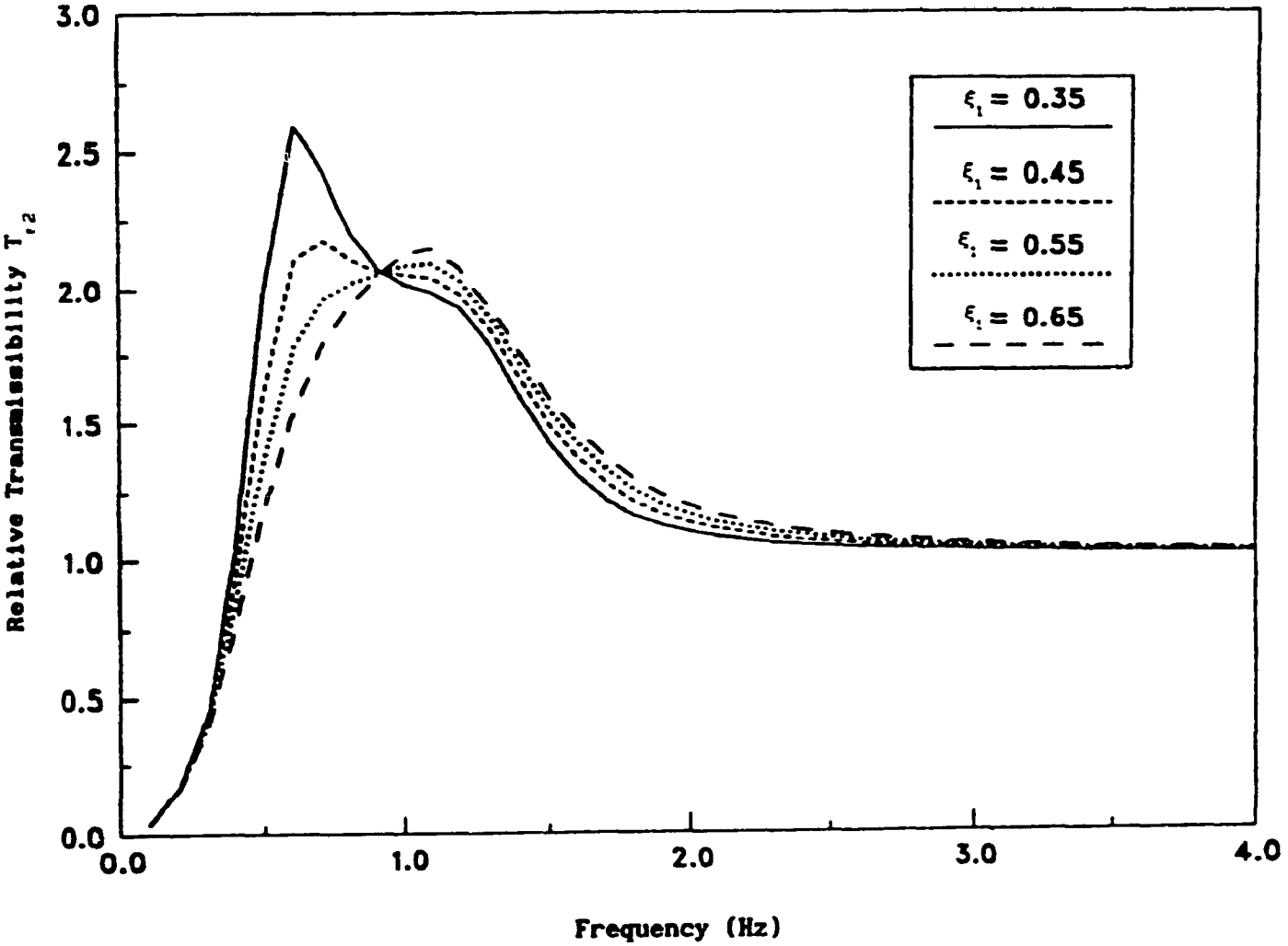

Fig.3.26 Influence of Main System Damping Ratio on the Relative Transmissibility of the Absorber Mass

relative transmissibility for excitation frequencies greater than 0.9 Hz increases with increasing ξ_1. The main system damping has little influence for excitation frequencies below 0.3 Hz or above 3 Hz.

The absorber mass ratio and the absorber damping ratio have considerable influence on the relative transmissibility of the absorber mass. From Figs.3.27 and 3.28, one can easily draw the conclusion that large values of absorber mass and absorber damping ratios will help in reducing the relative transmissibility.

The influence of the absorber tuning ratio on the relative transmissibility of the absorber mass is shown in Fig.3.29. It indicates that higher tuning ratio will produce lower peak for the relative transmissibility.

3.5.6 Influence of System Parameter Variations on the Relative Displacement Response of the absorber Mass

The influence of tuning factor on the relative displacement response of absorber mass is demonstrated in Fig.3.30. It indicates that higher tuning factor help in reducing the response. This is mainly because higher tuning factor means stiffer spring and hence absorber gives larger resistance to displacement response.

The relative displacement response of the absorber mass with variations in absorber damping in the range 0.05-0.35 is shown in Fig.3.31. The results show that higher absorber damping ratio is desirable for reducing the relative displacement response.

The influence of the main system damping ratio on the relative displacement response of the absorber mass is shown in Fig.3.32 which

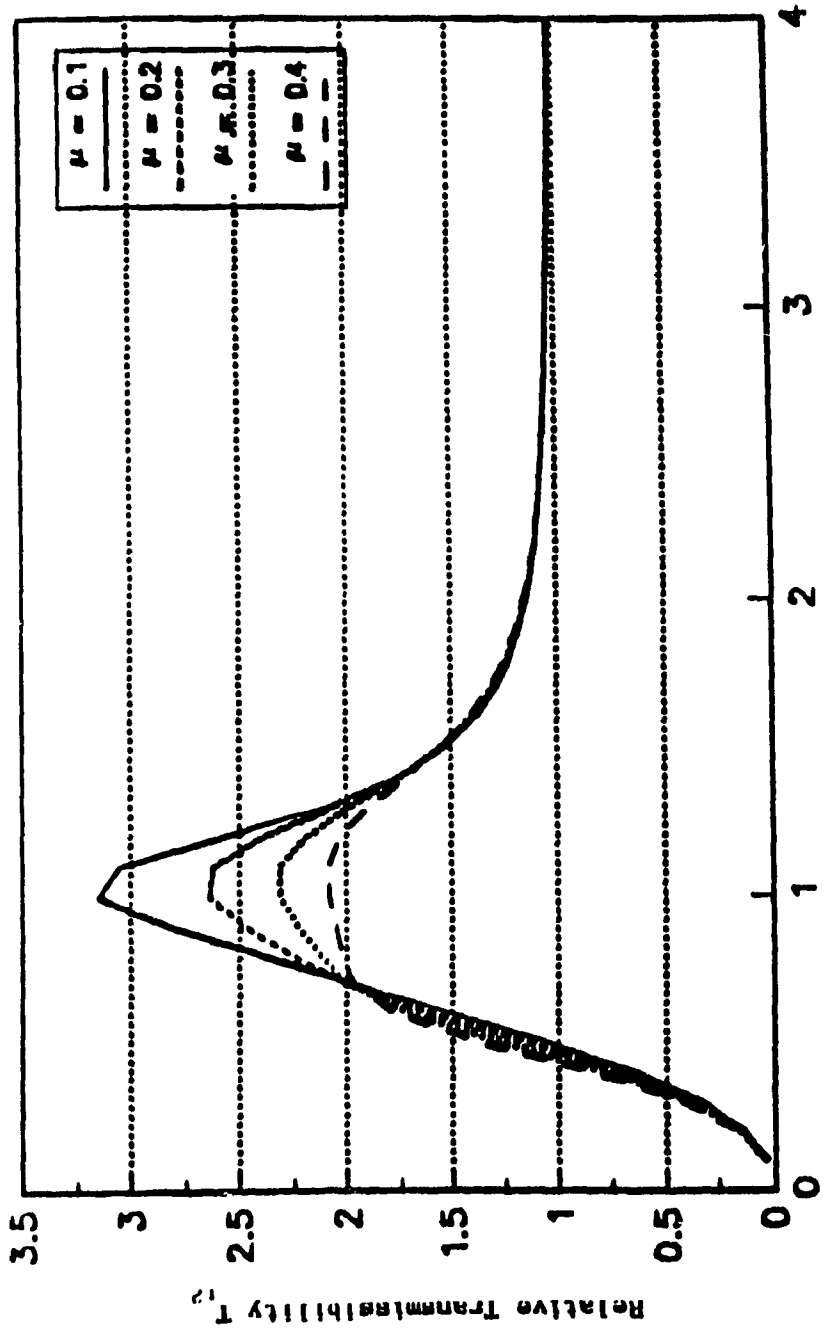

Fig.3.27 Influence of Absorber Mass on the Relative Transmissibility of the Absorber Mass

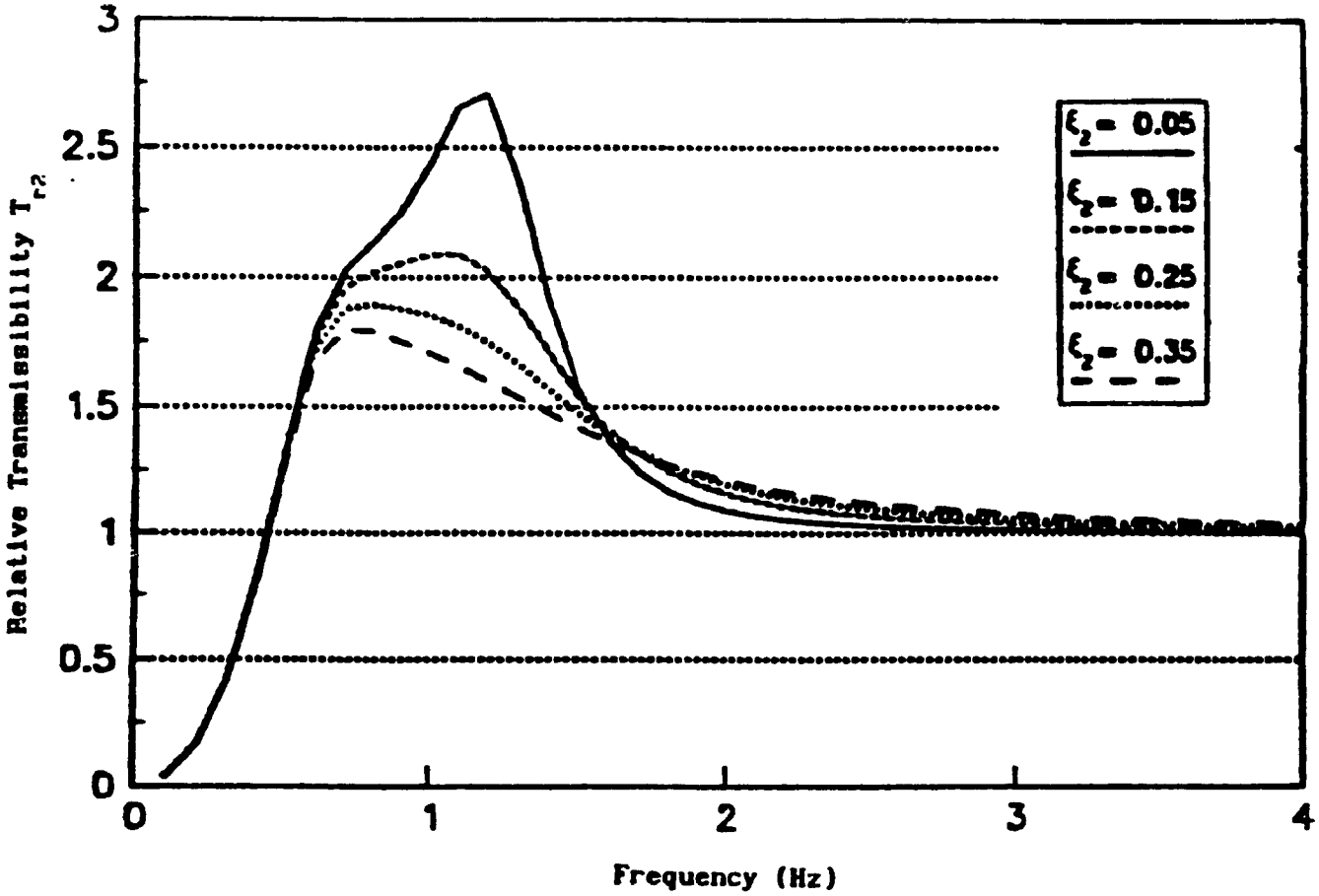

Fig.3.28 Influence of Absorber Damping Ratio on the Relative Transmissibility of the Absorber Mass

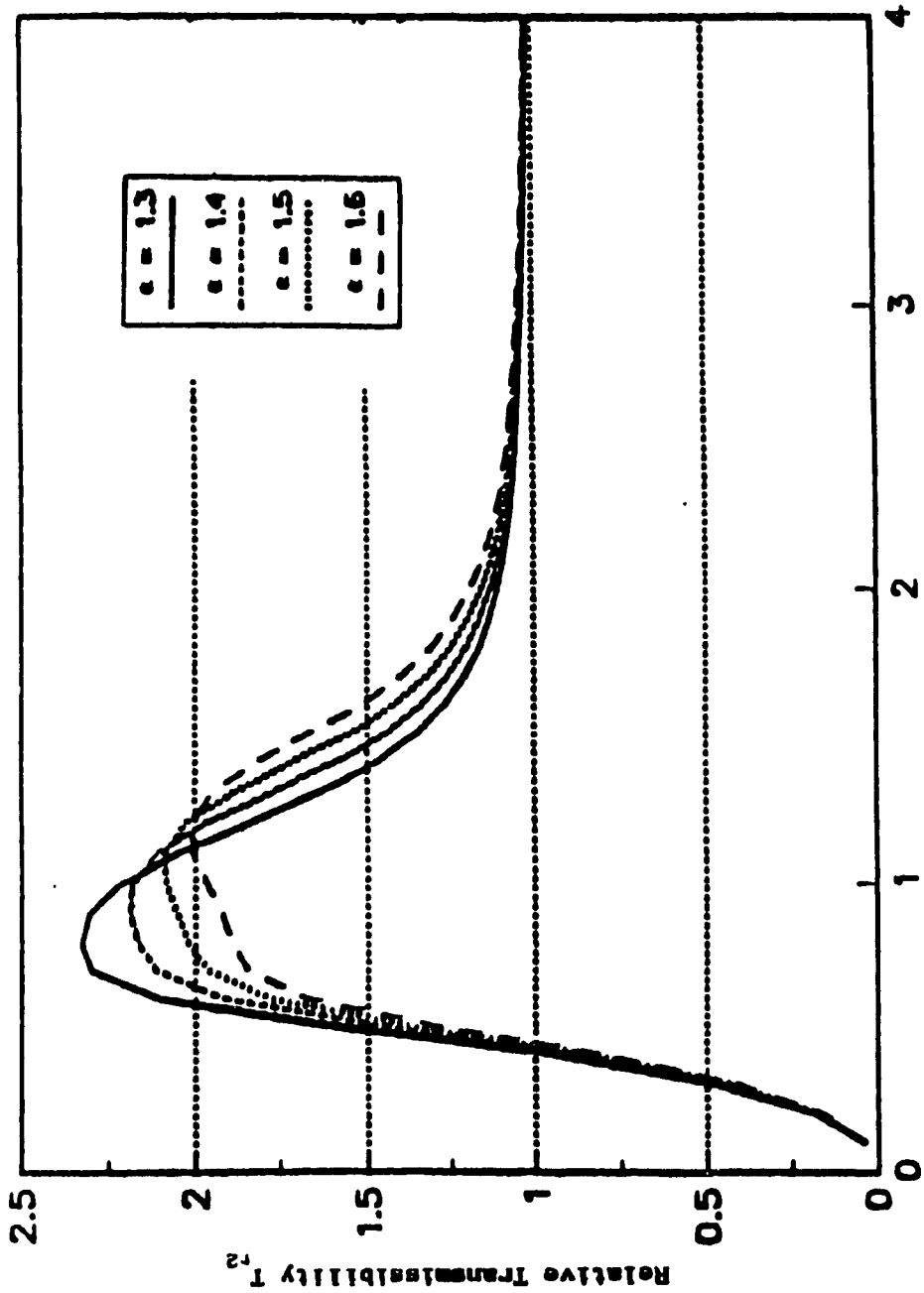

Fig.3.29 Influence of Absorber Tuning Ratio on the Relative Transmissibility of the Absorber Mass

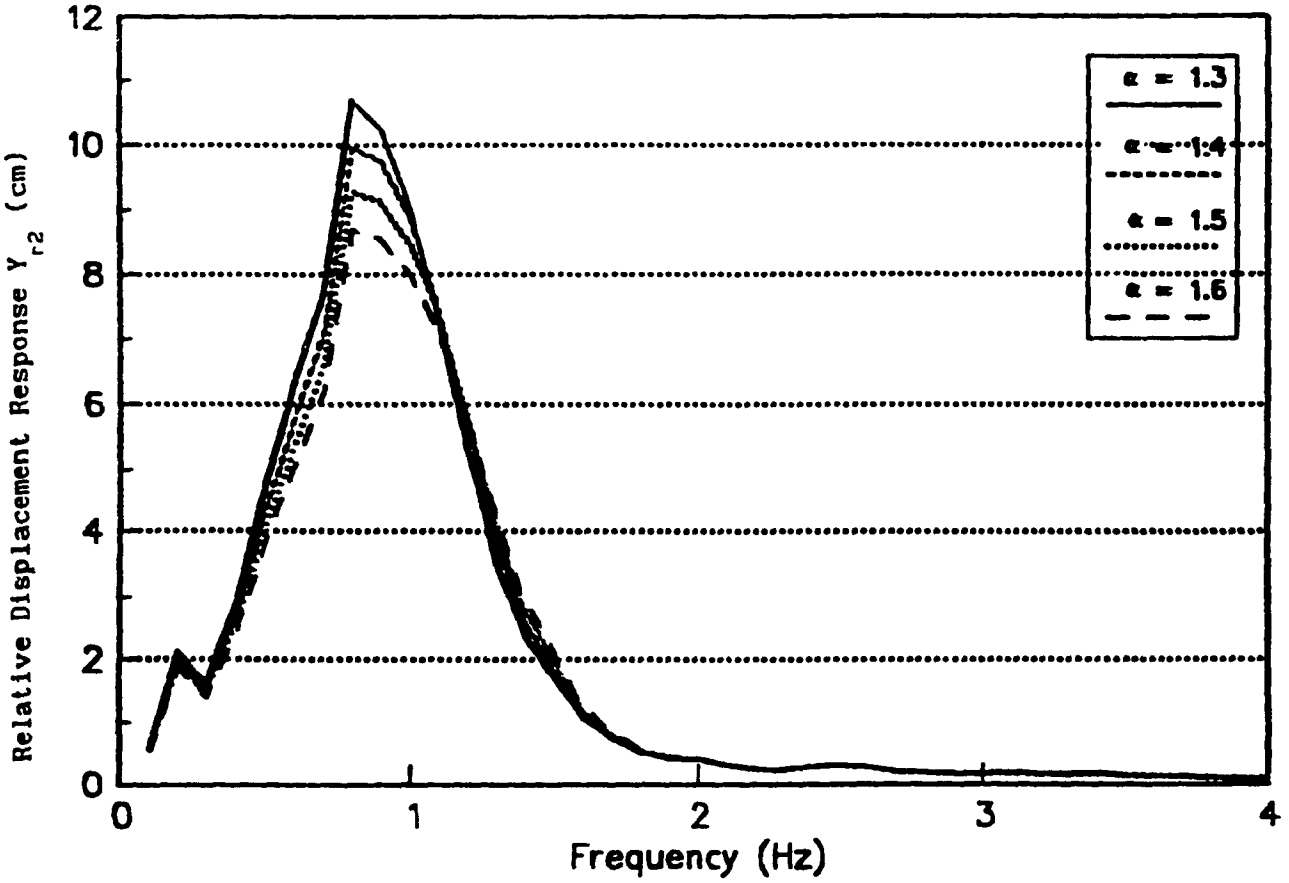

Fig.3.30 Influence of Absorber Tuning Ratio on the Relative Displacement Response of the Absorber Mass

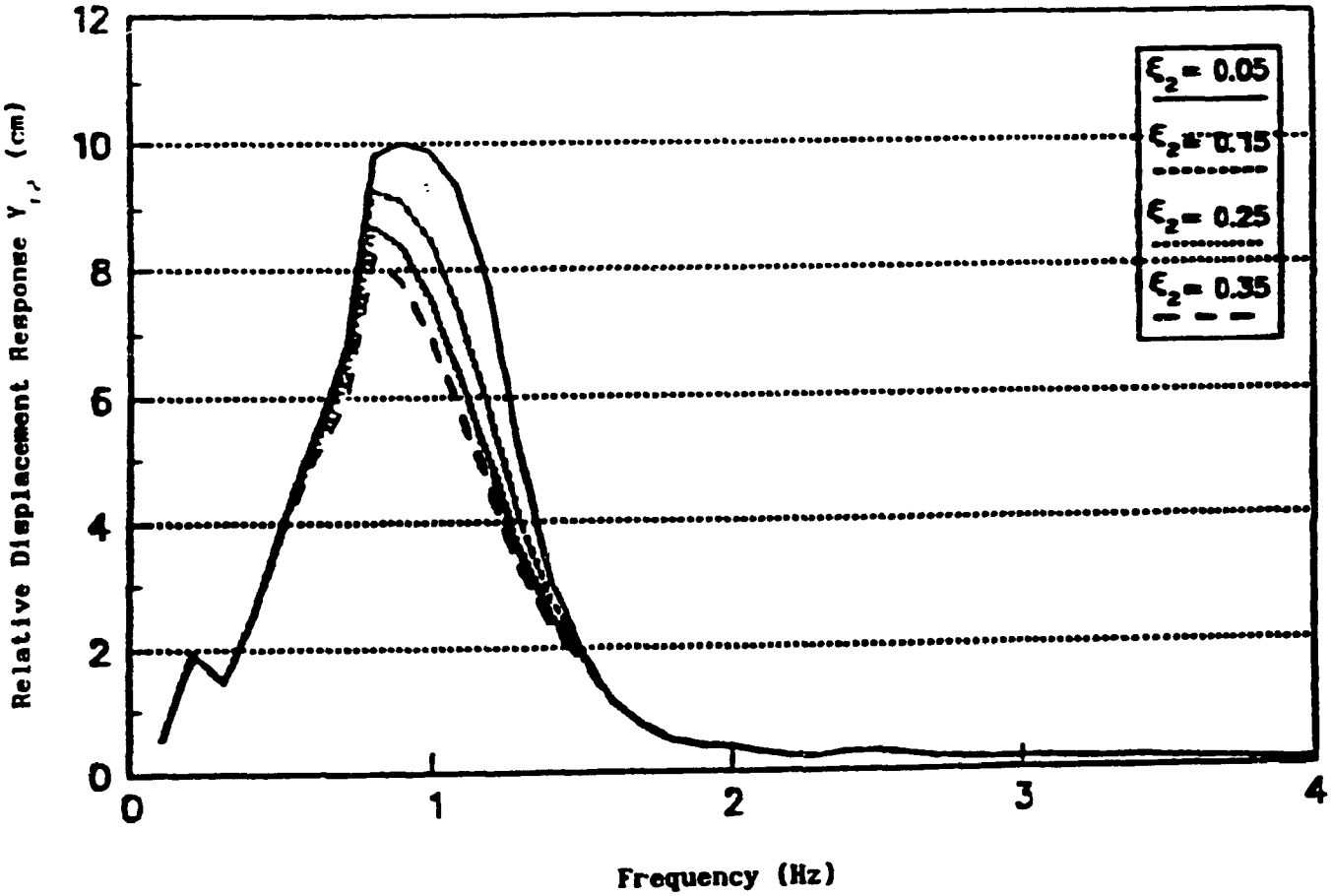

Fig.3.31 Influence of Absorber Damping Ratio on the Relative Displacement Response of the Absorber Mass

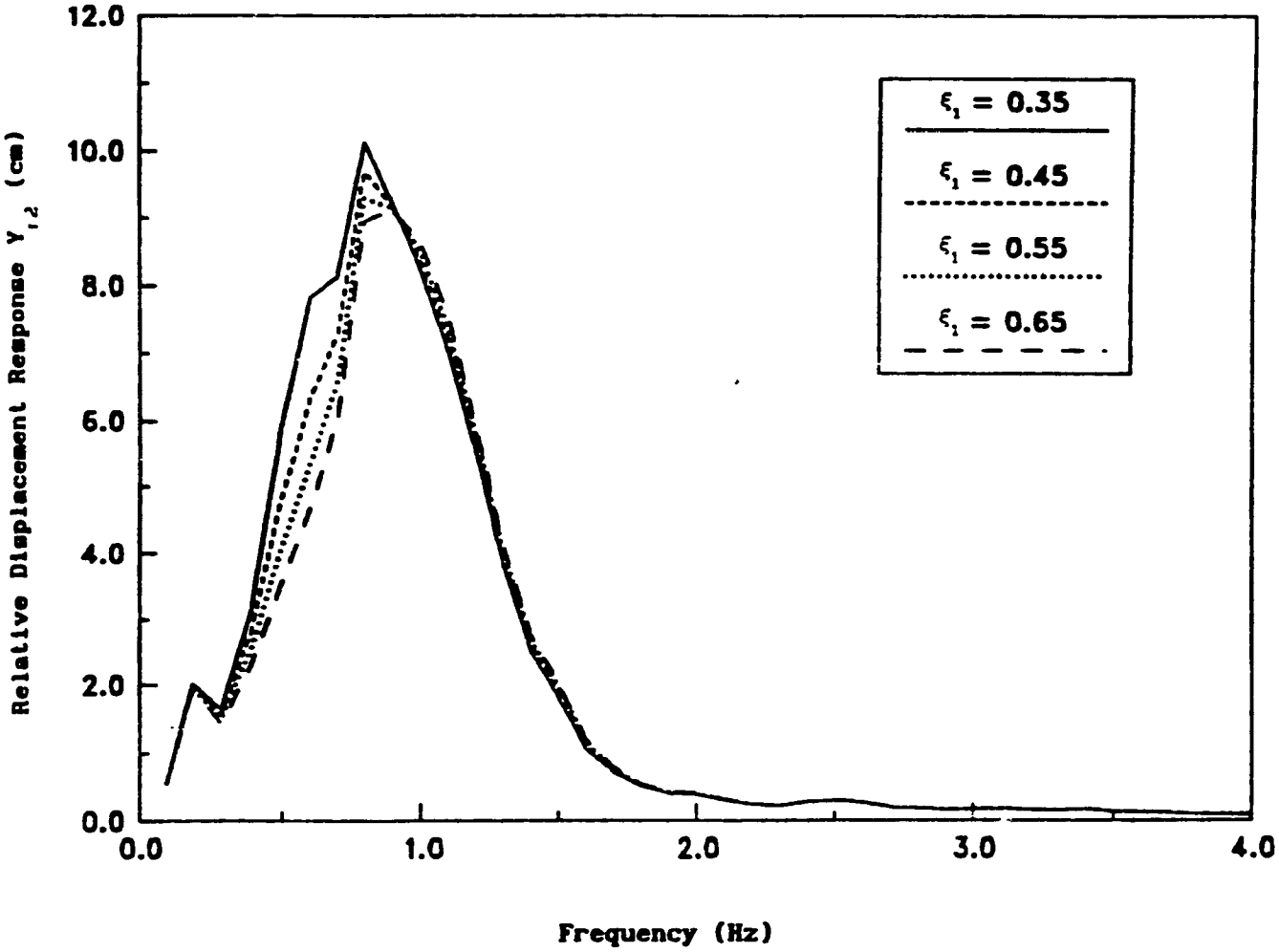

Fig.3.32 Influence of Main System Damping Ratio on the Relative Displacement Response of the Absorber Mass

demonstrates little influence of the main system damping ratio on the response. It is also shown that the peak relative displacement response of the absorber mass is approximately two times as large as that of the driver mass.

The relative displacement response of the absorber, as demonstrated in Fig.3.33 shows that larger absorber mass will produce smaller relative displacement response.

3.6 Lateral Seat Suspension with a Dynamic Absorber Employing Elastically Coupled Damper

3.6.1 Mathematical Model

The primary seat suspension with a three-element absorber is shown in Fig.3.34. The three-element absorber is composed of auxiliary mass M_a, viscous damper C_a, and two springs with stiffness values K_{a1} and K_{a2}, respectively. The absorber utilizes a so-called three-element combination of two springs and dashpot rather than the single spring and dashpot of the conventional dynamic absorber. The real part of the complex stiffness K_e of the three element combination and the effective resonant frequency of the absorber both varies with frequency. As a direct consequence, the absorber becomes active over greater frequency range and, at the center of this range (between the two resonant peaks), the absorber effectiveness is increased. The effectiveness of a three-element dynamic absorber in reducing the transmissibility across a simple spring-mass system at resonance has been investigated by Snowdom[40]. He concluded that the three-element absorber can be more effective than a conventional

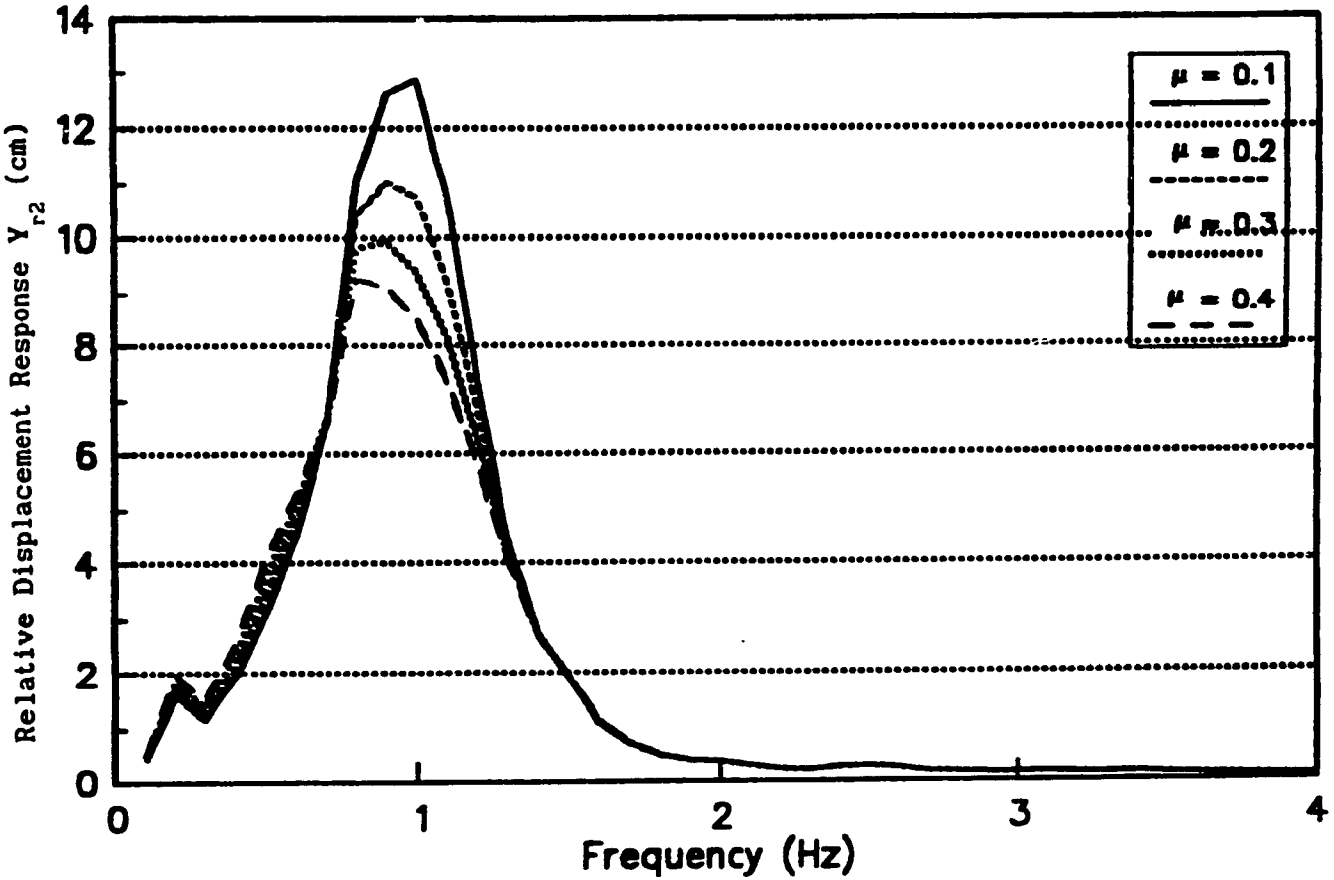

Fig.3.33 Influence of Absorber Mass on the Relative Displacement Response of the Absorber Mass

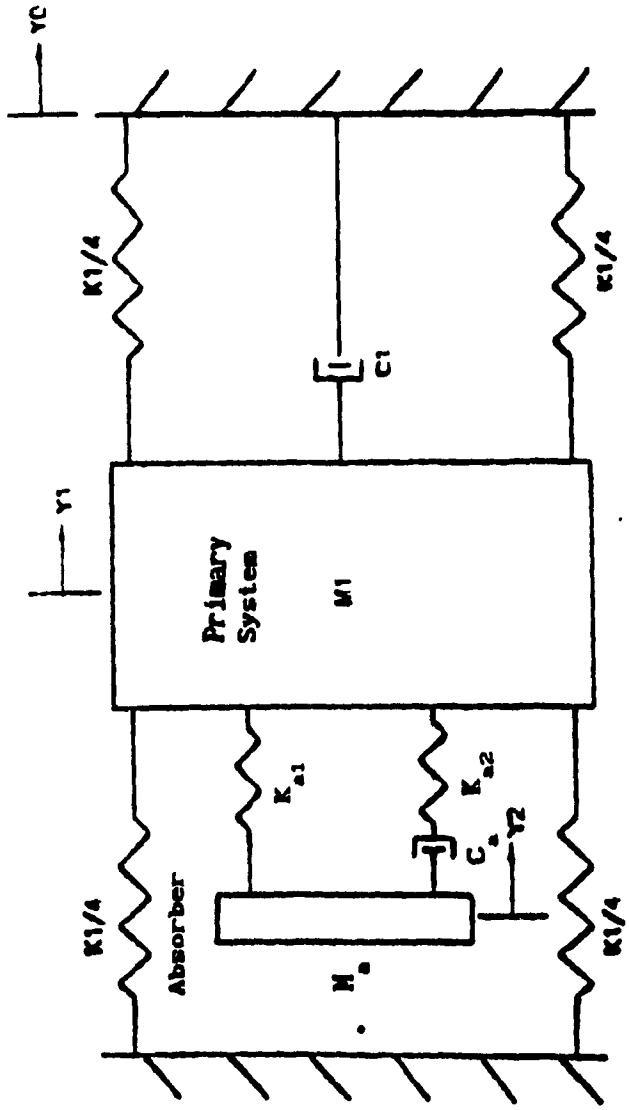

Fig.3.34 The Lateral Seat Suspension with Absorber Employing Elastically Coupled Damper

absorber of twice its mass. The application of the three-element absorber to the damped primary system with frequency dependent excitation input is not available and will be studied in this investigation. Since the influences of absorber mass and tuning ratios of a three-element absorber on the ride performance is similar to those with a conventional absorber, the present study will focus on the parametric study of the absorber stiffness ratio Q ($Q = K_{a2}/K_{a1}$) and absorber damping ratio ξ_2.

3.6.2 Equations of Motion

The mathematical model for the seat suspension with three-element absorber may be written as:

$$M_a \ddot{Y}_2 = -K_e (Y_2 - Y_1) \tag{3.16}$$

$$M_1 \ddot{Y}_1 = K_e (Y_2 - Y_1) - K_1 (Y_1 - Y_0) - C_1 (\dot{Y}_1 - \dot{Y}_0) \tag{3.17}$$

where K_e is the equivalent complex spring stiffness of the absorber and is given by

$$K_e = \frac{(Ca/Ka1)D + Q/(1+Q)}{Q + (Ca/Ka1)D} Ka1(1+Q) \tag{3.18}$$

where

M_a is the absorber mass

K_e is the equivalent complex stiffness of the absorber

Q is the stiffness ratio, equals to Ka2/Ka1

D is $\frac{d}{dt}$

Applying the Laplace transformation and introducing the following notations:

$$\omega_1^2 = K_1/M_1 \qquad \omega_2^2 = K_{a1}/M_a$$

$$C_a/K_{a1}=2\xi_2/\omega_2 \qquad C_1/M_1=2\xi_1\omega_1$$

$$\omega_e^2 = \frac{(2\xi_2/\omega_2)(j\omega) + Q/(1+Q)}{Q + (2\xi_2/\omega_2)(j\omega)}(1+Q)\omega_2^2 \tag{3.19}$$

Eqns.3.16 and 3.17 can be rewritten as:

$$-\omega^2 Y_2(j\omega) = -\omega_e^2(Y_2(j\omega)-Y_1(j\omega)) \tag{3.20}$$

$$-\omega^2 Y_1(j\omega) = \mu\omega_e^2(Y_2(j\omega)-Y_1(j\omega))-\omega_1^2(Y_1(j\omega)-Y_0(j\omega))-$$
$$-j2\xi_1\omega_1\omega(Y_1(j\omega)-Y_0(j\omega)) \tag{3.21}$$

The frequency response functions of absolute acceleration $\ddot{Y}_1$, and relative displacements Y_{r1} ($Y_{r1}=Y_1-Y_0$) and Y_{r2} ($Y_{r2}=Y_2-Y_o$) with respect to Y_o can be found as:

$$H''_{y_1}(j\omega) = \frac{(\omega_e^2-\omega^2)(\omega_1^2+j2\xi_1\omega\omega_1)}{\Delta} \tag{3.22}$$

$$H_{r_1} = \frac{(1+\mu)\omega_e^2-\omega^2}{\Delta} \tag{3.23}$$

$$H_{r_2} = \frac{(1+\mu)\omega_e^2-\omega_1^2-\omega^2-j2\xi_1\omega\omega_1}{\Delta} \qquad (3.24)$$

where

$$\Delta = \omega^4+\omega_1^2\omega_e^2-\omega^2\omega_e^2-\mu\omega^2\omega_e^2-\omega^2\omega_1^2+j2\xi_1\omega\omega_1(\omega_e^2-\omega^2) \qquad (3.25)$$

3.6.3 Influence of Absorber Spring Stiffness Ratio and the Damping Ratio on the Motion Response of the Driver Mass

In the three-element absorber, the damping element is elastically coupled. The result of the coupling can be represented by the equivalent spring stiffness K_e. The effectiveness of the absorber depends on the proper parameter combination. There are two phases of study in this investigation. Firstly, the absorber damping ratio is assumed to be a constant ($\xi_2 = 0.25$), and the simulation is carried out for variation in absorber stiffness. Secondly, the absorber stiffness is kept as a constant ($Q = 3.0$), and the influence of absorber damping ratio is studied.

3.6.3.1 The Absolute Transmissibility of the Driver Mass

The influence of the absorber stiffness ratio and the damping ratio on the absolute transmissibility of the driver mass are shown in Fig.3.35 and Fig.3.36 respectively. It can be seen that absorber stiffness ratio Q and the absorber damping ratio ξ_2 have similar effect on the absolute transmissibility. Smaller stiffness ratio and absorber damping ratio produce better isolation performance at the neighborhood of the tuned frequency and poorer vibration attenuation around the system's second

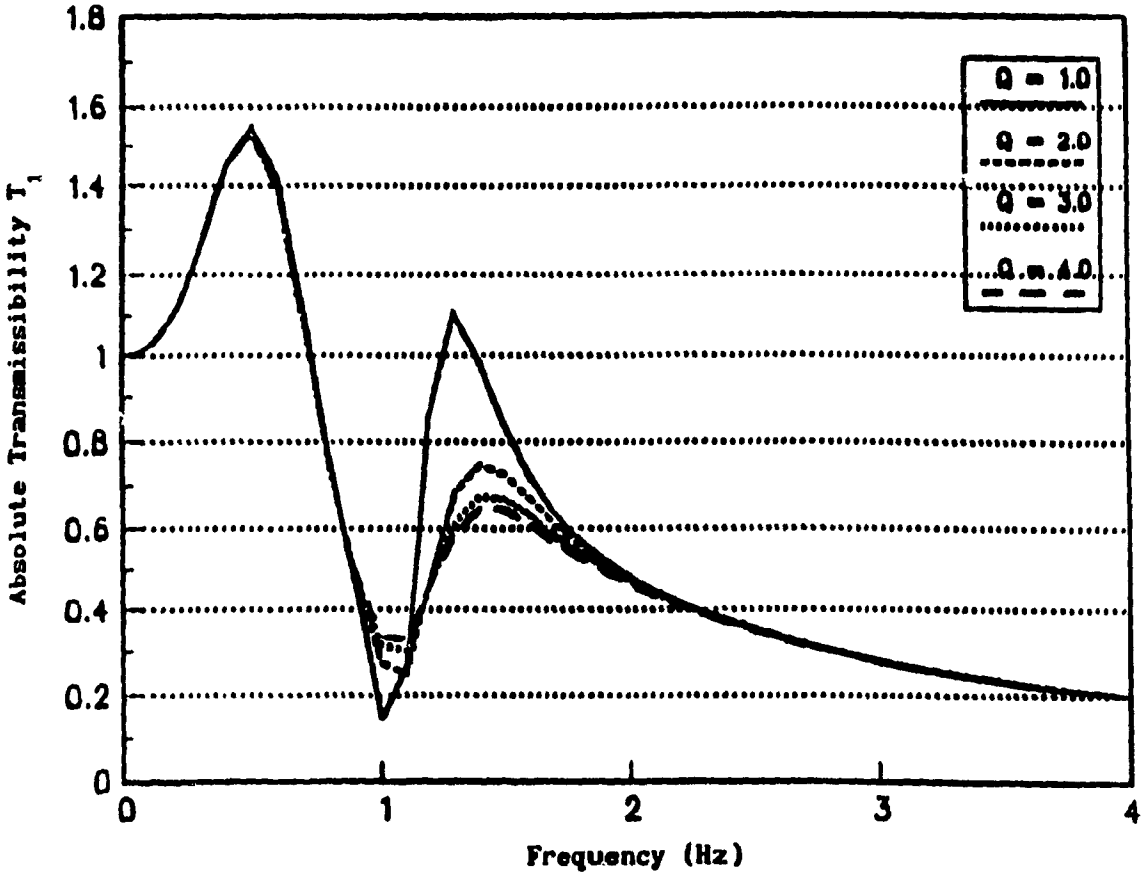

Fig.3.35 Influence of the Absorber Stiffness Ratio on the Absolute Transmissibility of the Driver Mass

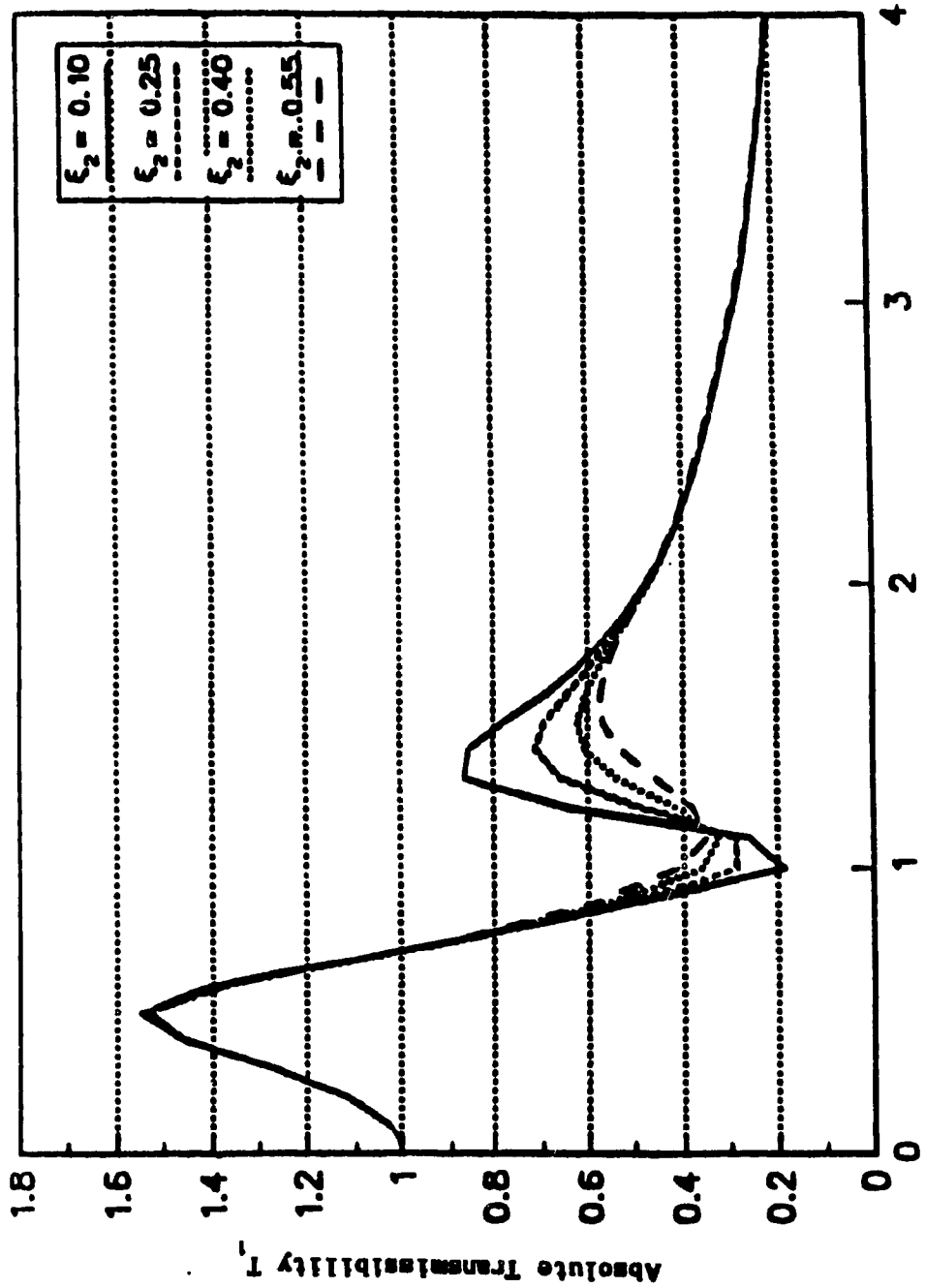

Fig.3.36 Influence of Absorber Damping Ratio on the Absolute Transmissibility of the Driver Mass

resonant frequency. The absolute transmissibility plot has very little change for Q greater than 3. Comparing with the conventional absorber, it can be seen that higher damping is needed for the three-element absorber.

3.6.3.2 The Acceleration Response of the Driver Mass

The acceleration response of the driver mass with variations of absorber stiffness ratio and damping ratio are plotted in Fig.3.37 and Fig.3.38. It can be observed that smaller stiffness ratio produces good isolation performance at the neighborhood of the tuned frequency. However, the isolation performance for excitation away from that frequency is poor. Small absorber damping ratio will also produce good isolation performance at the neighborhood of the tuned frequency. However, high resonant response occurs at the second natural frequency of the combined system.

3.6.3.3 The Relative Transmissibility of the Driver Mass

The Influence of the absorber stiffness ratio and damping ratio on the relative transmissibility of the driver mass are plotted in Fig.3.39 and Fig.3.40. It is shown that the absorber stiffness ratio Q and damping ratio ξ_2 have similar influence on the relative transmissibility T_{r1}. Small absorber stiffness ratio and damping ratio both produce good isolation performance at the tuned excitation frequency and poor isolation performance at other frequencies, especially at the system's

3.6.3.4 The Relative Displacement Response of the Driver Mass

The influence of absorber stiffness ratio and damping ratio on the relative displacement response of the driver mass are shown in Fig.3.41

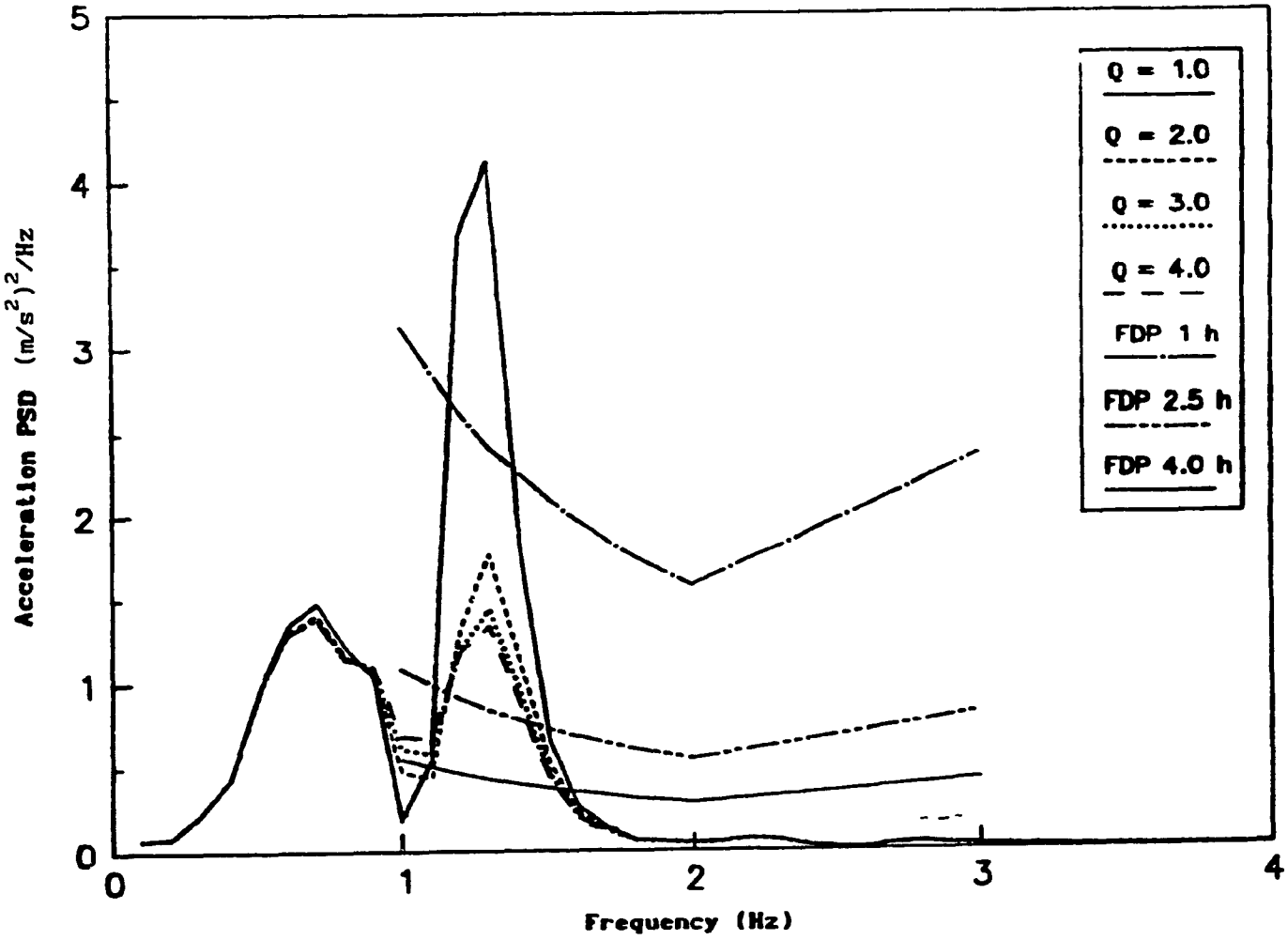

Fig.3.37 Influence of Absorber Stiffness Ratio on the Acceleration Response of the Driver Mass

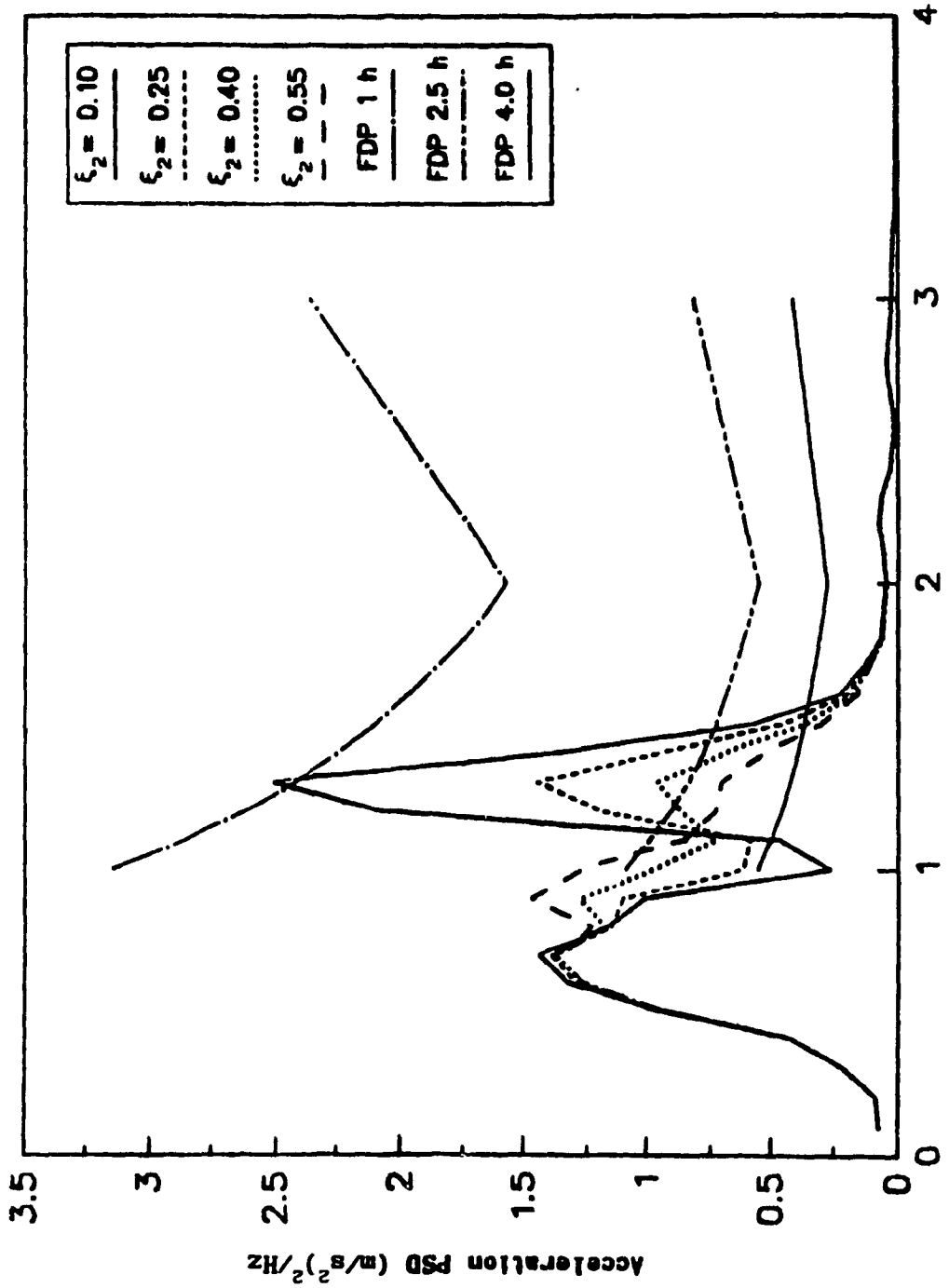

Fig.3.38 Influence of Absorber Damping Ratio on the Acceleration Response of the Driver Mass

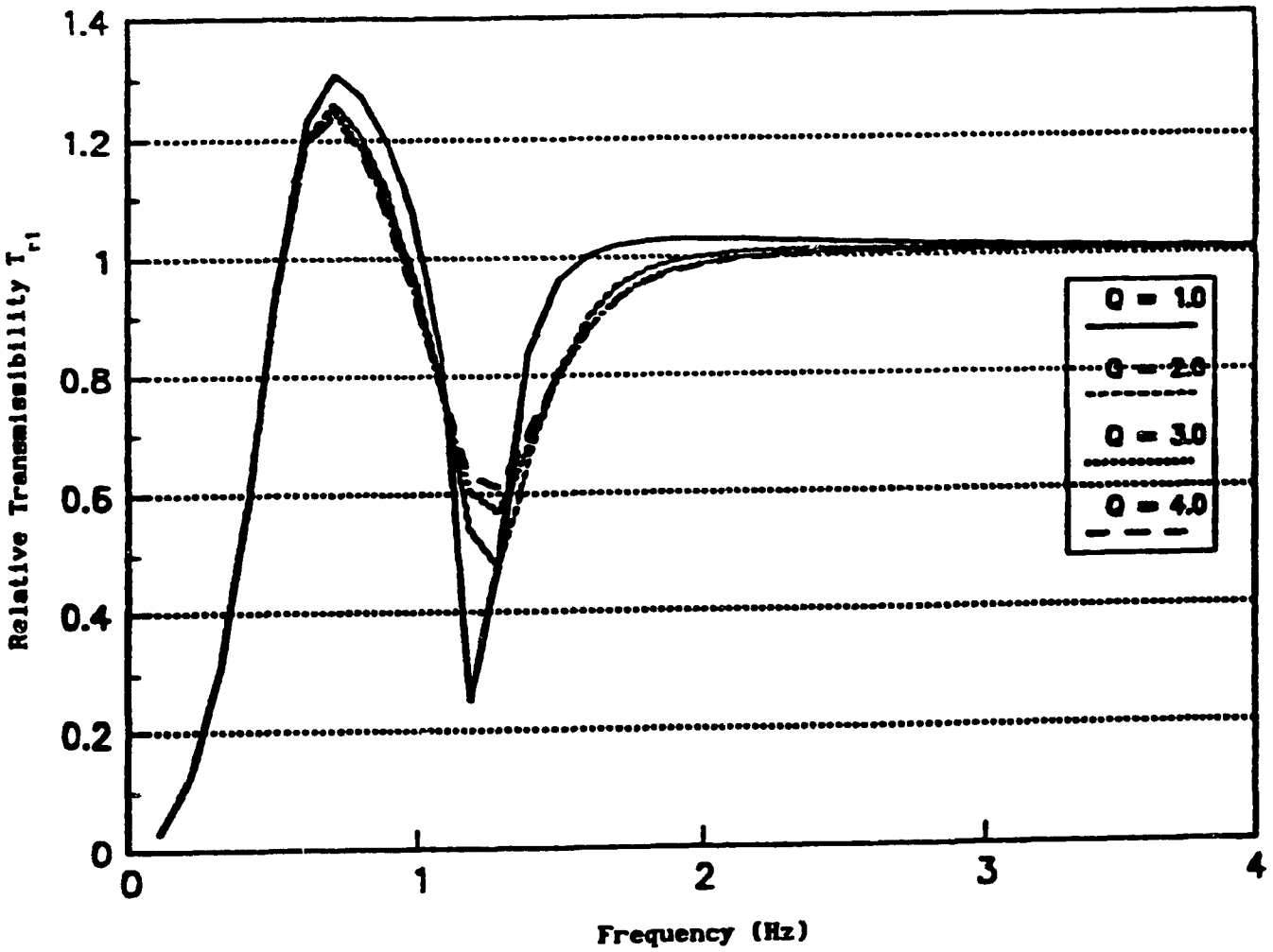

Fig.3.39 Influence of Absorber Stiffness Ratio on the Relative Transmissibility of the Driver Mass

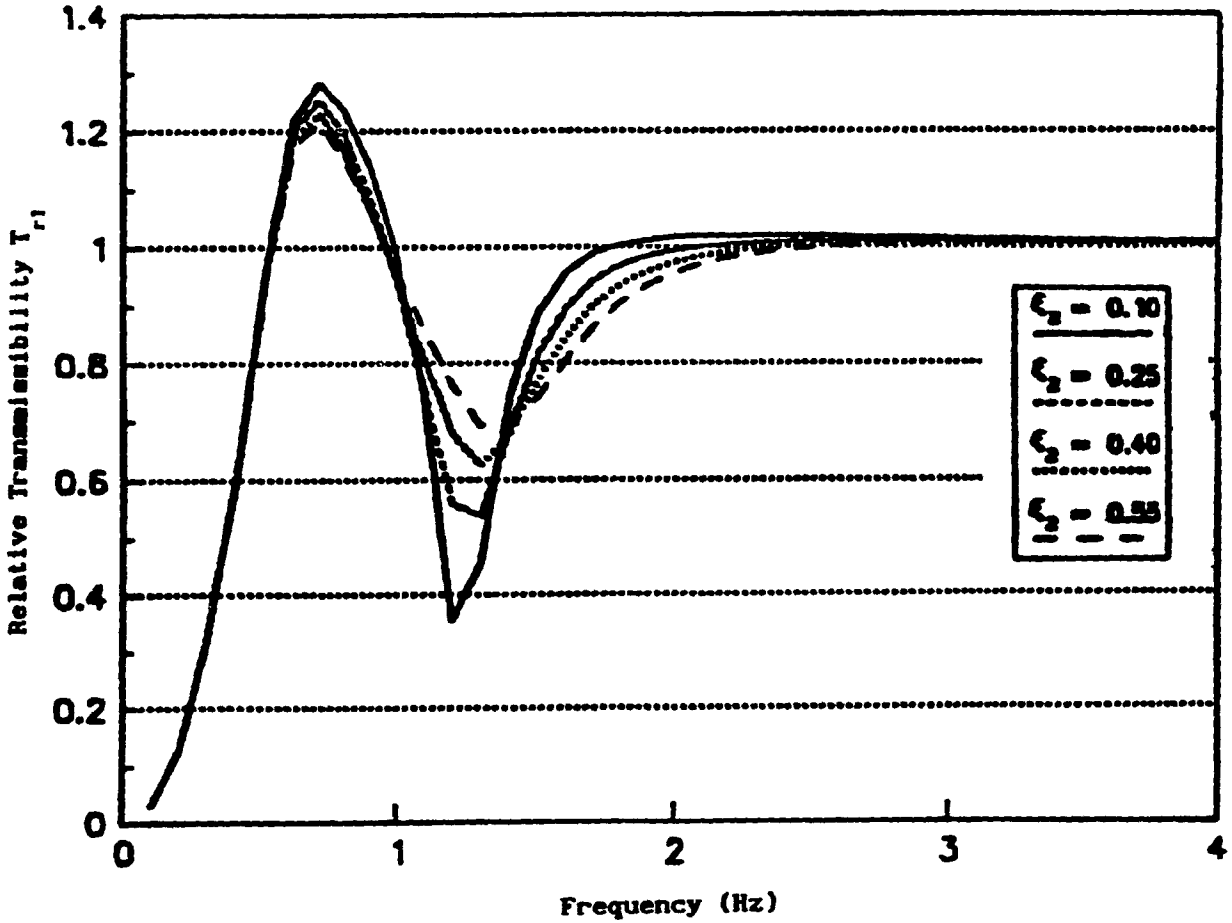

Fig.3.40 Influence of Absorber Damping Ratio on the Relative Transmissibility of the Driver Mass

and Fig.3.42. It can be seen that variation of absorber stiffness ratio or absorber damping has little influence on the relative displacement response. However, smaller absorber stiffness ratio will have larger relative displacement response occurring at the system's second natural frequency. Generally speaking, the adoption of the three-element absorber shows little advantage for reducing the relative displacement response of the driver mass.

3.6.3.5 The Relative Motion Response of the absorber Mass

The relative transmissibility and the relative displacement displacement responses of absorber mass are plotted in Figs.3.43-3.46. They indicate that higher absorber damping ratio and stiffness ratio are both desirable for reducing the relative motion.

3.7 Conclusions

In this chapter, the influence of absorber parameters as well as the main system damping ratio on the lateral dynamic performance is fully investigated. From the simulation results, the following conclusions can be drawn:

1. The selection of absorber damping can greatly influence the vibration isolation performance. Generally speaking, light damping in absorber provides good acceleration isolation at the neighborhood of the tuned frequency and poor isolation performance for other frequencies. The influence of absorber damping on the relative displacement response of driver mass is not significant. However, choosing light absorber damping results in large relative displacement response of absorber mass. From simulation results, the absorber damping ratio of 0.15 provides good

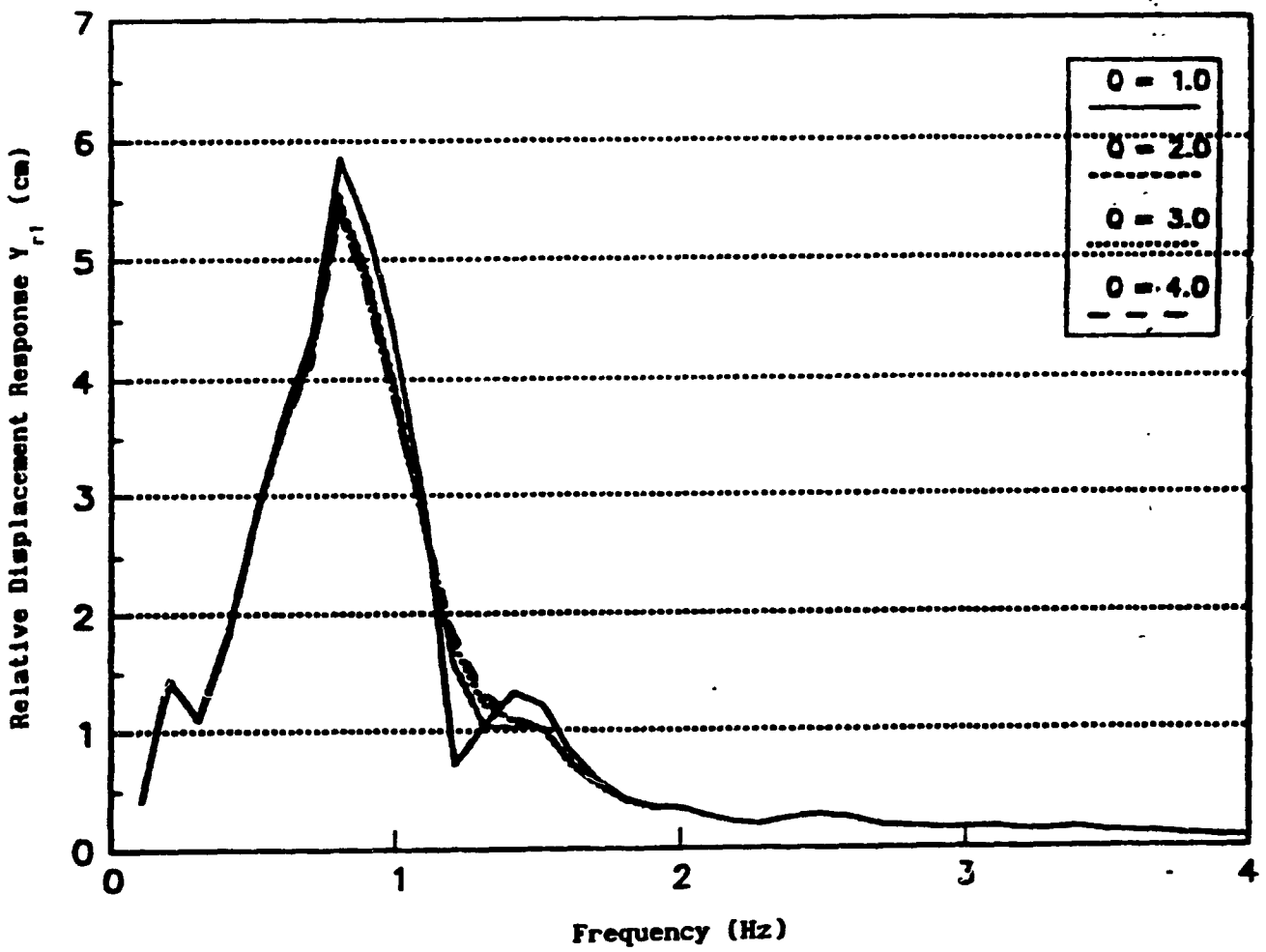

Fig.3.41 Influence of Absorber Stiffness Ratio on the Relative Displacement Response of the Driver Mass

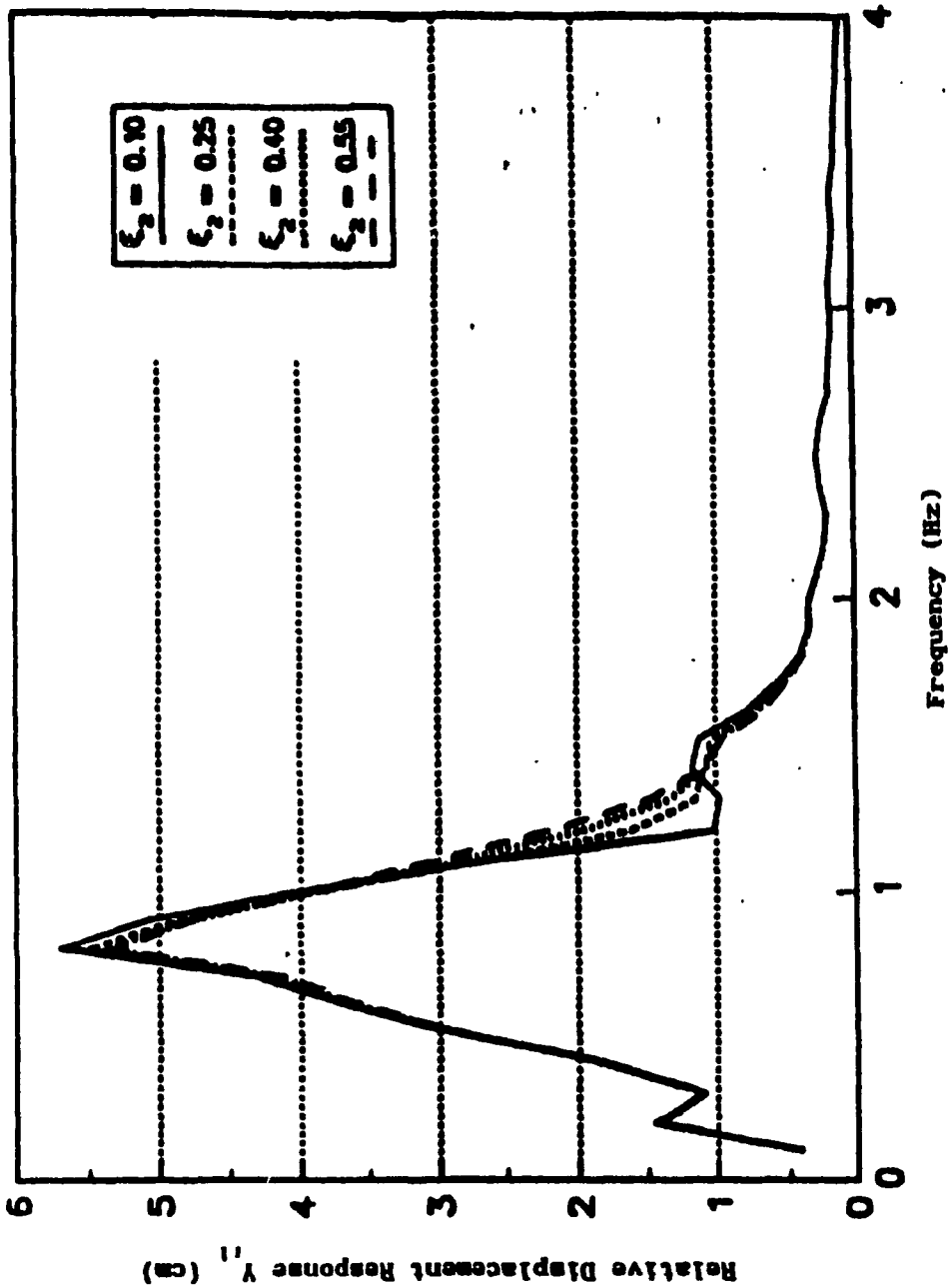

Fig.3.42 Influence of Absorber Damping Ratio on the Relative Displacement Response of the Driver Mass

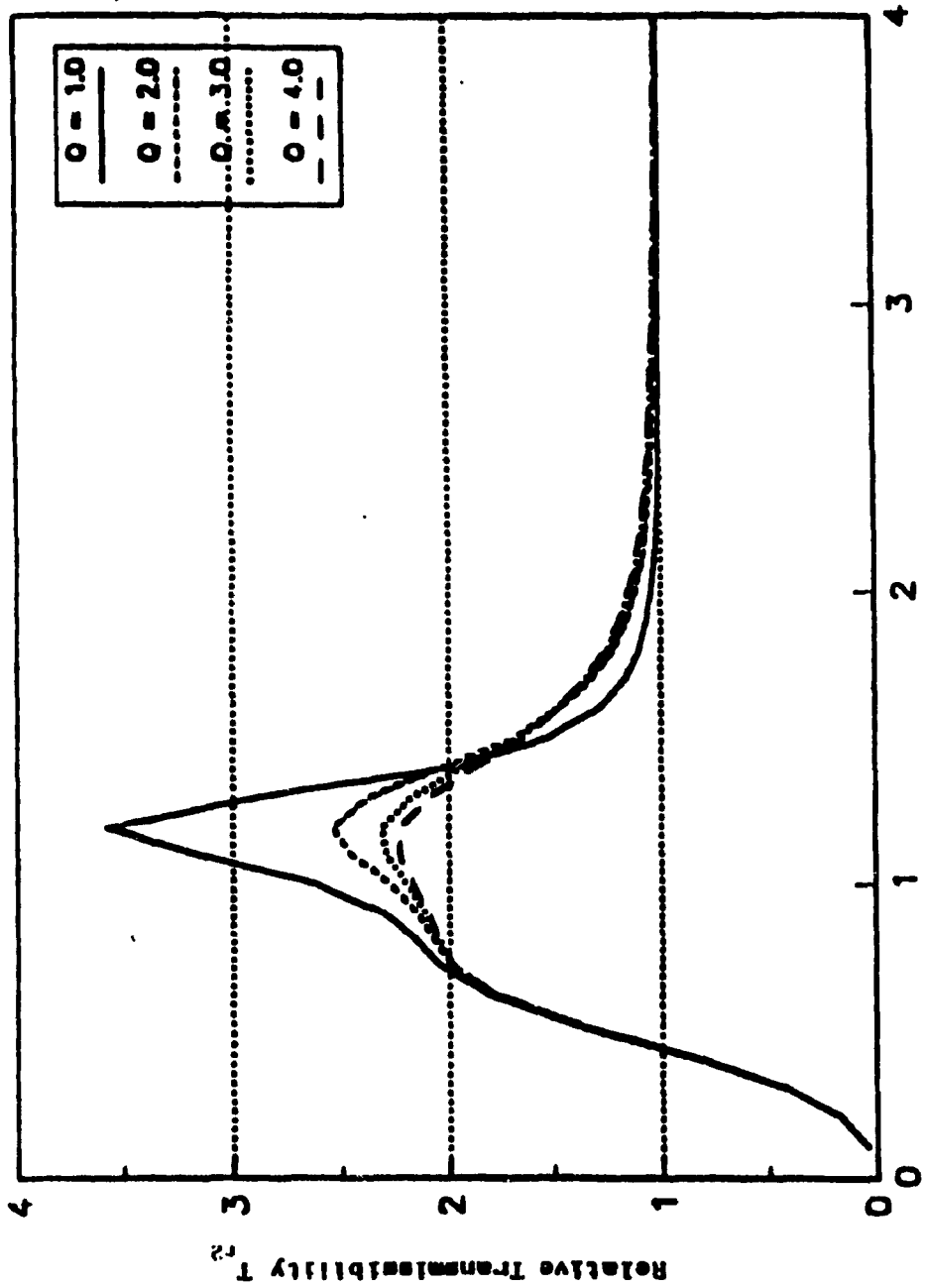

Fig.3.43 Influence of Absorber Stiffness Ratio on the Relative Transmissibility of the Absorber Mass

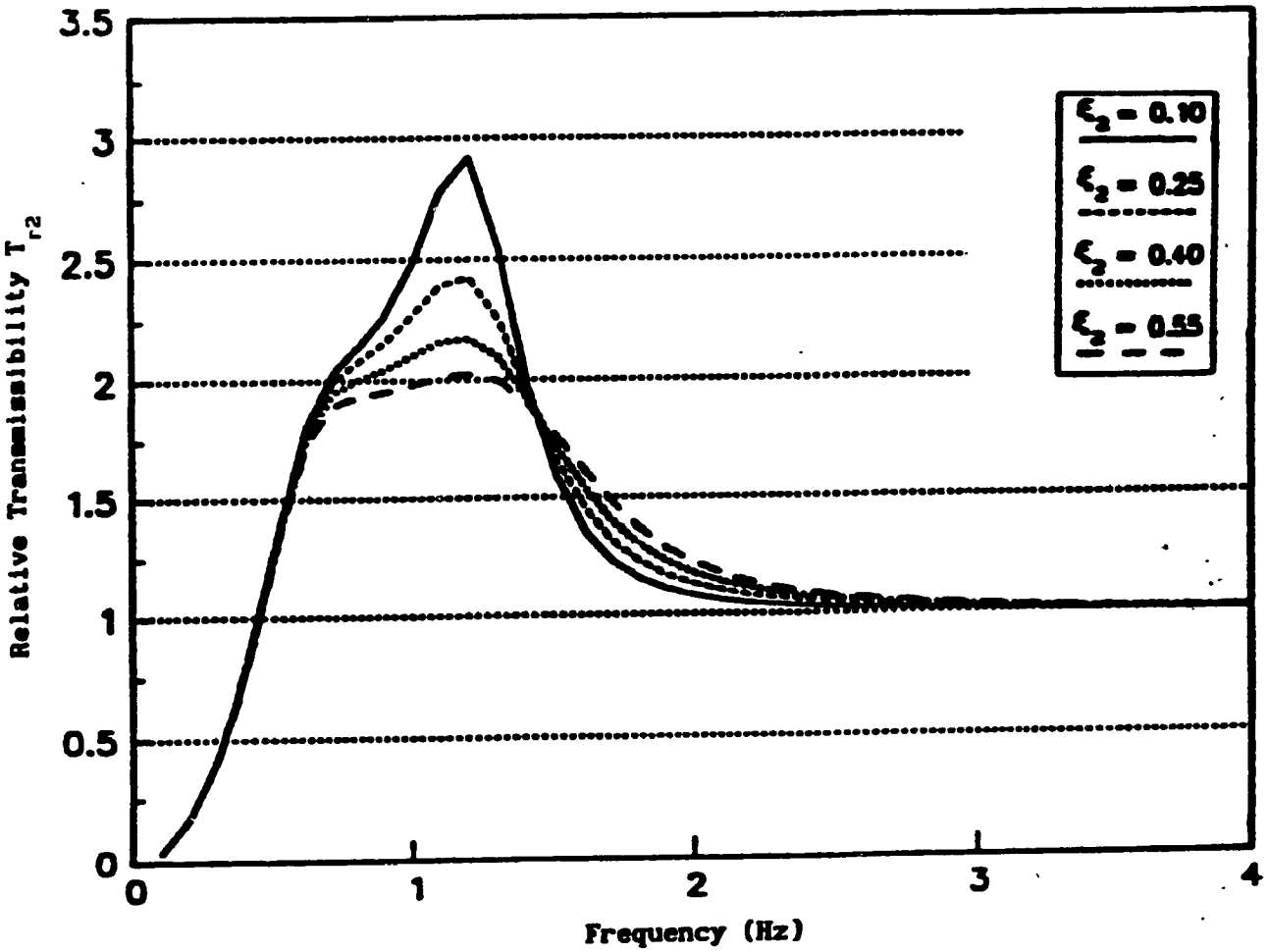

Fig.3.44 Influence of Absorber Damping Ratio on the Relative Transmissibility of the Absorber Mass

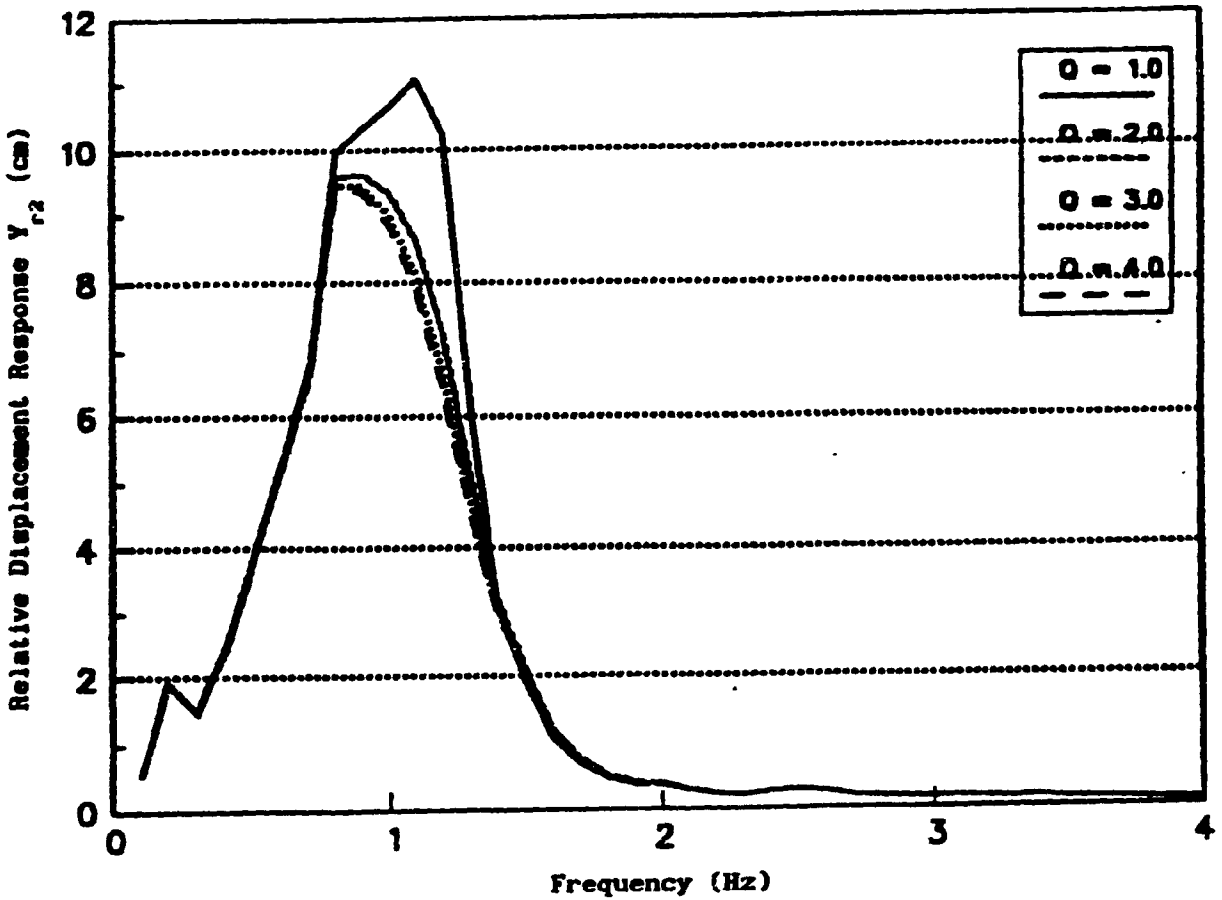

Fig.3.45 Influence of Absorber Stiffness Ratio on the Relative Displacement Response of the Absorber Mass

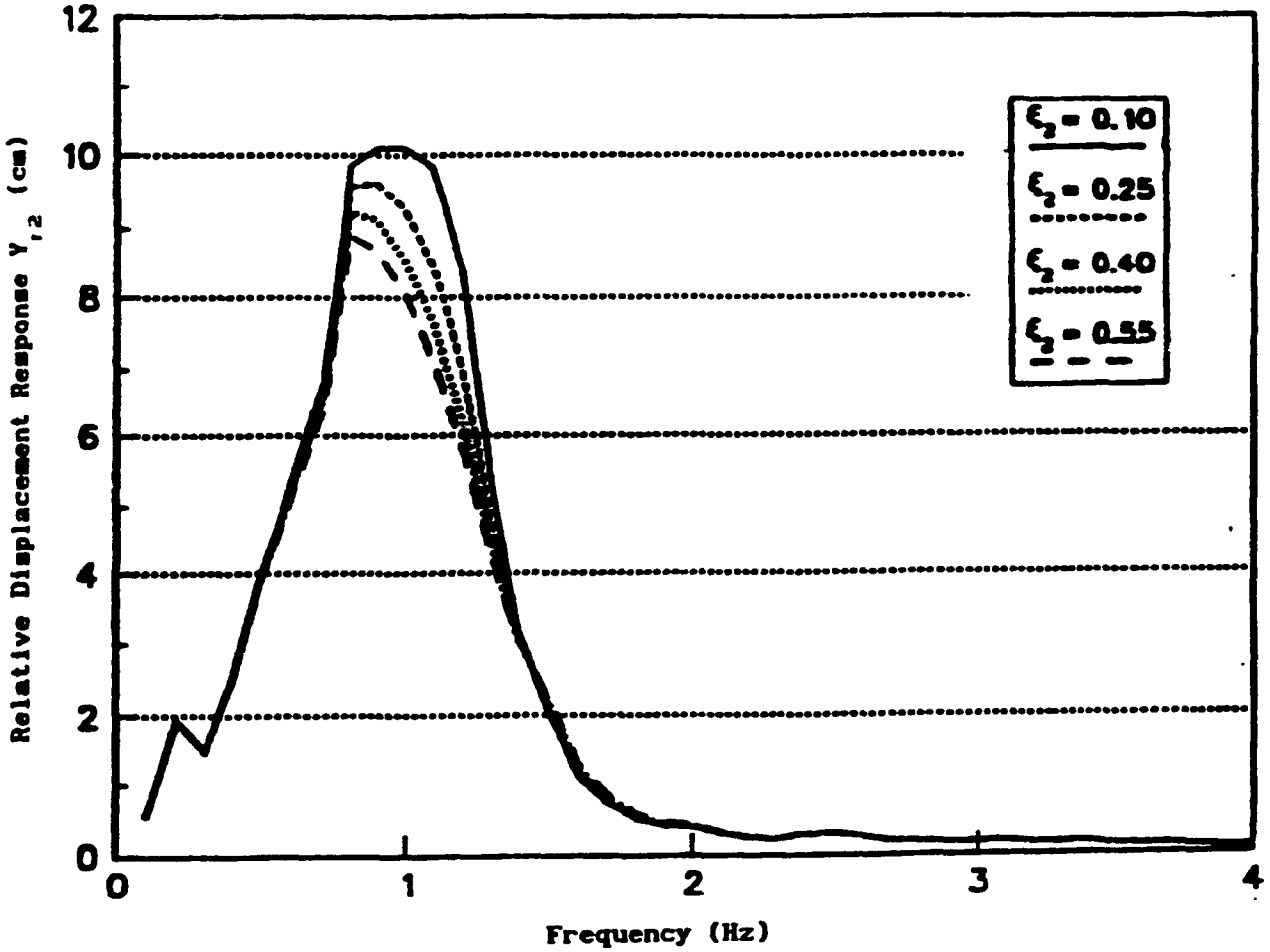

Fig.3.46 Influence of Absorber Damping Ratio on the Relative Displacement Response of the Absorber Mass

vibration isolation performance.

2. Larger absorber mass provides better ride performance and also reduces the peak relative displacement response of the absorber mass. However, it will increase the weight of the resultant system. The selection of absorber weight is compromised between the effectiveness of vibration attenuation and the weight of the resultant system.

3. Tuning factor has great influence on the acceleration isolation. In order to obtain good acceleration isolation performance, the natural frequency of absorber must be tuned around the excitation frequency at which peak acceleration amplitude occurs. Smaller tuning ratio reduces the relative displacement response of the driver mass, but increases the relative displacement of the absorber mass. It is also found that, by carefully choosing the tuning ratio, the acceleration and relative displacement response of driver mass can be both reduced.

4. From the simulation results, it can be easily seen that, with vibration absorber and assumed absorber mass ratio (μ = 0.4), the peak level of lateral acceleration response PSD of the driver mass is reduced to approximately 1.37 m^2/s^4Hz, about 80% vibration reduction in comparison to lateral seat suspension without absorber. However, the lateral relative displacement response of the driver mass is approximately 0.5 cm greater than seat suspension without absorber.

5. The implementation of three-element absorber can slightly increase the effectiveness of the acceleration performance at the vicinity of the tuned frequency.

6. The attachment of vibration absorber to the primary seat suspension can significantly reduce the lateral vibration response. However, the vibration response of the seat and driver mass is still much

higher than the ISO recommended 8 hour fatigue decreased proficiency limit.

CHAPTER 4

Lateral Seat Suspension With Dual Absorbers

4.1 Introduction

In the preceding chapter, the ride performance of lateral seat suspension with a conventional absorber and a three-element absorber is presented. The addition of vibration absorber to the primary lateral seat suspension has shown to have significant improvement in the lateral ride performance. However, the drawback of the conventional vibration absorber and the three-element absorber has always been the compromise between vibration attenuation performance at the tuned frequency and at the two natural frequencies of the resultant system. When an undamped absorber is applied to the lateral seat suspension, excellent vibration attenuation can be achieved at the tuned frequency while large vibration response occurs at the natural frequencies of the resultant system. Although the addition of the primary damping and absorber damping can successfully suppress these two resonances, this is accomplished at the cost of deteriorating the vibration attenuation performance at the tuned frequency. In this chapter, the lateral seat suspension with dual absorbers will be investigated[40]. It will be shown that, through the use of dual absorbers, it is possible to achieve good vibration attenuation at the system's natural frequencies as well as at the tuned frequency. Such results can be obtained through appropriate selection of the damping, tuning and mass ratios of dual absorbers.

4.2 Equations of Motion

The lateral seat suspension with dual absorbers is shown schematically in Fig.4.1, where a conventional viscously damped absorber (M_2, K_2) is attached to M_1 in parallel with an absorber of mass M_3, which is suspended from M_1 by a spring of stiffness rate K_3 and a small damping C_3. The mass M_3 is assumed to be small in comparison to M_2. The equations of motion of the system can be written as follows:

$$M_1\ddot{Y}_1+K_1(Y_1-Y_0)+C_1(\dot{Y}_1-\dot{Y}_0)+K_2(Y_1-Y_2)+C_2(\dot{Y}_1-\dot{Y}_2)+K_3(Y_1-Y_3)+C_3(\dot{Y}_1-\dot{Y}_3)=0 \quad (4.1)$$

$$M_2\ddot{Y}_2+K_2(Y_2-Y_1)+C_2(\dot{Y}_2-\dot{Y}_1)=0 \quad (4.2)$$

$$M_3\ddot{Y}_3+K_3(Y_3-Y_1)+C_3(\dot{Y}_3-\dot{Y}_1)=0 \quad (4.3)$$

Introducing the following notation :

$$K_1/M_1=\omega_1^2 \qquad K_2/M_2=\omega_2^2 \qquad K_3/M_3=\omega_3^2$$

$$C_1/2\sqrt{K_1M_1}=\xi_1 \qquad C_2/2\sqrt{K_2M_2}=\xi_2 \qquad C_3/2\sqrt{K_3M_3}=\xi_3$$

$$M_2/M_1=\mu_1 \qquad M_3/M_1=\mu_2 \quad (4.4)$$

Eqns.(4.1)-(4.3) can be rewritten as follows:

$$\ddot{Y}_1+\omega_1^2(Y_1-Y_0)+2\xi_1\omega_1(\dot{Y}_1-\dot{Y}_0)+\mu_1\omega_2^2(Y_1-Y_2)+2\xi_2\mu_1\omega_2(\dot{Y}_1-\dot{Y}_2)+\mu_2\omega_3^2(Y_1-Y_3)+$$
$$+2\xi_3\mu_2\omega_3(\dot{Y}_1-\dot{Y}_3)=0 \quad (4.5)$$

$$\ddot{Y}_2+\omega_2^2(Y_2-Y_1)+2\xi_2\omega_2(\dot{Y}_2-\dot{Y}_1)=0 \quad (4.6)$$

$$\ddot{Y}_3+\omega_3^2(Y_3-Y_1)+2\xi_3\omega_3(\dot{Y}_3-\dot{Y}_1)=0 \quad (4.7)$$

Taking Laplace transformation and reorganizing the above equations in

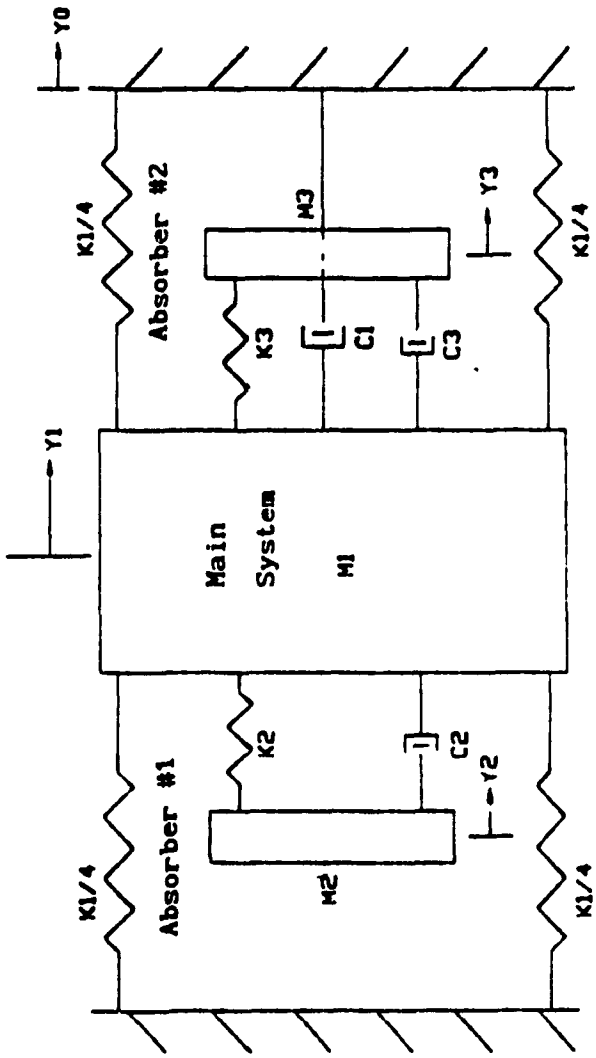

Fig.4.1 The Lateral Seat Suspension with Dual Absorbers

matrix form , the steady state response of the vibratory system is given by the following governing equation:

$$\begin{bmatrix} a_{11} & a_{12} & a_{13} \\ a_{21} & a_{22} & a_{23} \\ a_{31} & a_{32} & a_{33} \end{bmatrix} \begin{bmatrix} Y_1(j\omega) \\ Y_2(j\omega) \\ Y_3(j\omega) \end{bmatrix} = \begin{bmatrix} b_1 \\ b_2 \\ b_3 \end{bmatrix} Y_0 \qquad (4.8)$$

In which:

$$a_{11} = -\omega^2 + \omega_1^2 + \mu_1\omega_2^2 + \mu_2\omega_3^2 + j2\omega(\xi_1\omega_1 + \mu_1\xi_2\omega_2 + \mu_2\xi_3\omega_3)$$

$$a_{12} = -\mu_1\omega_2^2 - j2\xi_2\mu_1\omega\omega_2$$

$$a_{13} = -\mu_2\omega_3^2 - j2\xi_3\mu_2\omega\omega_3$$

$$a_{21} = -\omega_2^2 - j2\xi_2\omega_2\omega$$

$$a_{22} = -\omega^2 + \omega_2^2 + j2\xi_2\omega\omega_2$$

$$a_{23} = 0$$

$$a_{31} = -\omega_3^2 - j2\xi_3\omega_3\omega$$

$$a_{32} = 0$$

$$a_{33} = -\omega^2 + \omega_3^2 + j2\xi_3\omega\omega_3$$

$$b_1 = \omega_1^2 + j2\xi_1\omega\omega_1$$

$$b_2 = 0$$

$$b_3 = 0$$

applying the following notation

$$T = \frac{1}{Y_0(j\omega)} \begin{bmatrix} Y_1(j\omega) \\ Y_2(j\omega) \\ Y_3(j\omega) \end{bmatrix}$$

$$M = \begin{bmatrix} a_{11} & a_{12} & a_{13} \\ a_{21} & a_{22} & 0 \\ a_{31} & 0 & a_{33} \end{bmatrix} \qquad B = \begin{bmatrix} b_1 \\ 0 \\ 0 \end{bmatrix}$$

The transmissibility vector T can be written as :

$$T = M^{-1}B \tag{4.9}$$

M^{-1} is the inverse matrix of M and is given in the following

$$M^{-1} = \frac{1}{\Delta}\begin{bmatrix} A_{11} & A_{12} & A_{13} \\ A_{21} & A_{22} & A_{23} \\ A_{31} & A_{32} & A_{33} \end{bmatrix} \tag{4.10}$$

where

$A_{11}=a_{22}a_{33}$ $\quad A_{12}=-a_{12}a_{33}$ $\quad A_{13}=-a_{22}a_{13}$

$A_{21}=a_{21}a_{33}$ $\quad A_{22}=a_{11}a_{33}-a_{13}a_{31}$ $\quad A_{23}=a_{12}a_{31}$

$A_{31}=-a_{22}a_{13}$ $\quad A_{32}=a_{21}a_{13}$ $\quad A_{33}=a_{11}a_{22}-a_{12}a_{21}$

$\Delta=a_{11}a_{22}a_{33}-a_{12}a_{21}a_{33}-a_{22}a_{13}a_{31}$

The acceleration transmissibility of the driver mass is found to be:

$$T_{\ddot{y}_1}(j\omega) = \frac{A_{11}b_1}{\Delta} \tag{4.11}$$

The transmissibility of the relative displacement of driver mass with respect to the seat base is:

$$T_{y_{r1}}(j\omega) = \frac{A_{11}b_1-\Delta}{\Delta} \tag{4.12}$$

The acceleration PSD response $S_o(\omega)$ and the relative displacement response $Y_r(\omega)$ of the driver mass are found to be:

$$S_o(\omega) = T_{\ddot{y}_1}(j\omega)T^*_{\ddot{y}_1}(j\omega)S_i(\omega) \tag{4.13}$$

$$Y_r(\omega) = T_{y_{r1}}(j\omega)Y_o \tag{4.14}$$

Where $T^*_{\ddot{y}_1}(j\omega)$ is the conjugate function of $T_{\ddot{y}_1}(j\omega)$.

4.3 Parametric Study of Absorber parameters

It is known from the previous study that the primary lateral seat suspension should be heavily damped because of the excitation input at the low frequency. For the heavily damped primary system, the first transmissibility peak is greatly reduced. The main problem is the second transmissibility peak, which is usually large because of the demand of effective vibration attenuation at the tuned frequency. For a single vibration absorber, the reduction of the second transmissibility peak is usually achieved at the cost of deteriorating the effectiveness of vibration reduction at the tuned frequency.

The advantage of applying dual absorbers is to achieve good vibration attenuation at the tuned frequency while constraining the second transmissibility peak to a minimum possible. The appropriate absorber damping value and the tuning ratio of the two absorbers are the key factors in determining the effectiveness of dual absorber. In this chapter, parametric study on the damping, tuning and mass ratios of the

dual absorbers will be conducted to study their influences on the ride performance. For this simulation study, the damping ratio of the primary system is kept a constant at 0.55.

4.3.1 Variation of Tuning Factor for First Absorber

In the dual absorber system, the absorber with small mass and damping is usually tuned to the frequency where peak input occurs. The tuning factor of the second absorber is determined by the characteristics of the vibration input. Because of the complexity of vehicle vibration input, the appropriate tuning factor can only be determined through parametric study. In the simulation, the following values are assumed for the design variables:

$$\mu_1 = 0.30$$

$$\xi_2 = 0.15$$

$$\mu_2 = 0.10$$

$$\xi_3 = 0.005$$

$$\alpha_2 = 1.586$$

The simulation results for variation in tuning factor of the first absorber are plotted in Figs.4.2-4.5. The results are similar to those with a single absorber. Increasing the absorber tuning factor will increase the first peak and reduce the second peak of the acceleration PSD response. It can be seen that the absorber tuning factor of $\alpha_1 = 1.5$ gives the best vibration attenuation performance by bringing the two peaks of the acceleration PSD response to the same level. It is also demonstrated that small absorber tuning factor is preferred for reducing

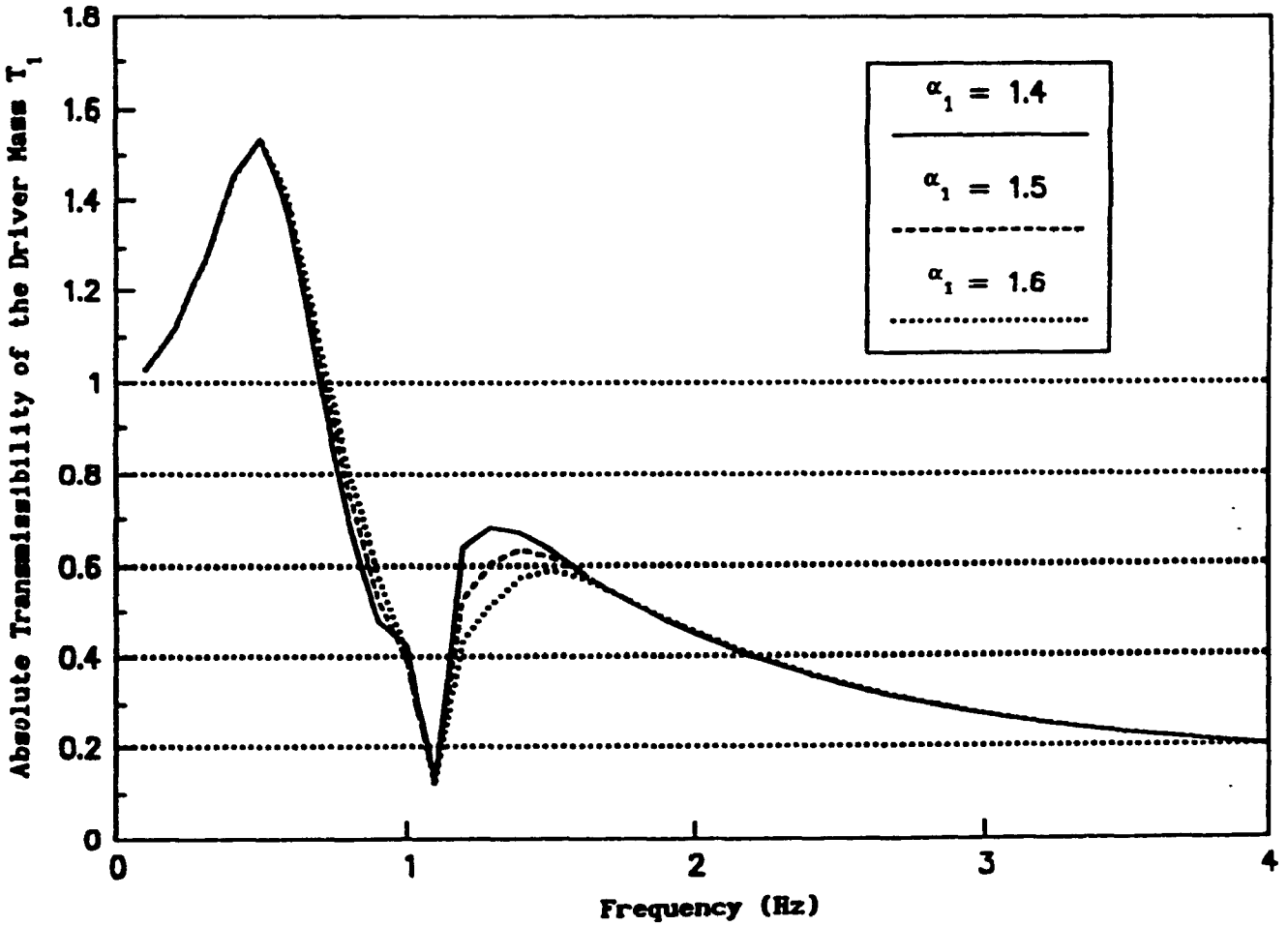

Fig.4.2 The Influence of the first Absorber Tuning Factor On the Absolute Transmissibility of the Driver Mass

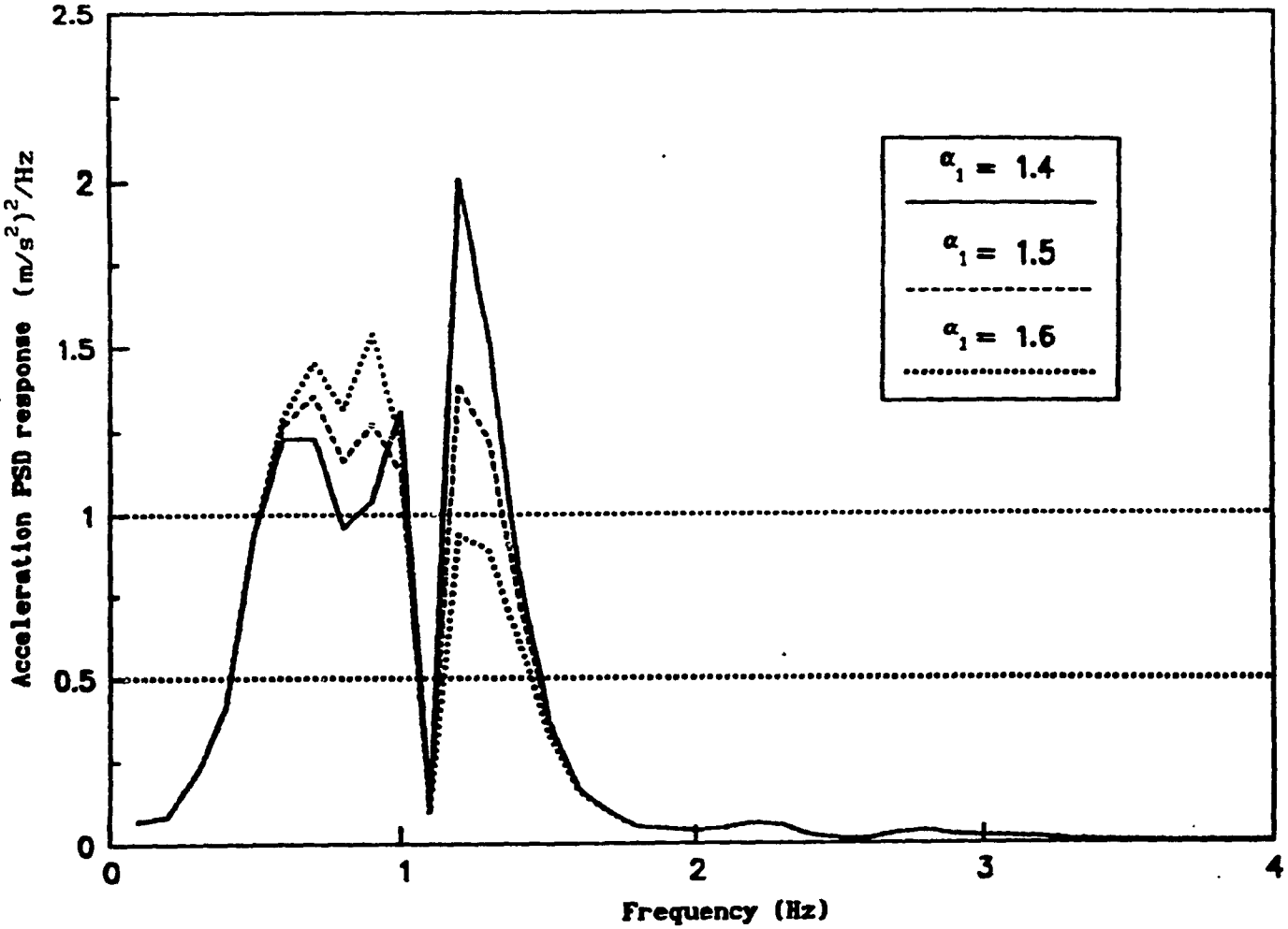

Fig.4.3 The Influence of the first Absorber Tuning Factor On the Acceleration PSD Response of the Driver Mass

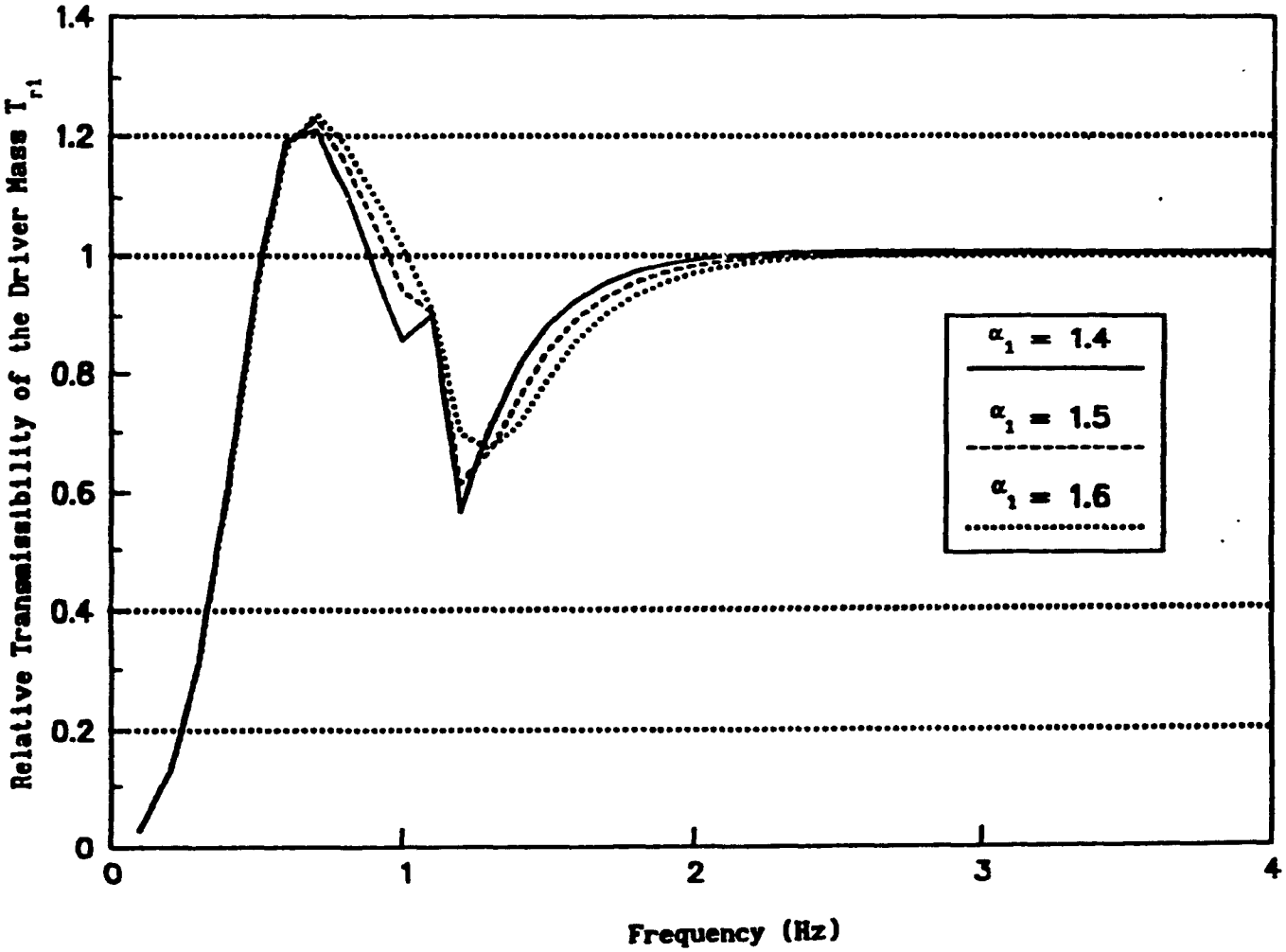

Fig.4.4 The Influence of the first Absorber Tuning Factor On the Relative Transmissibility of the Driver Mass

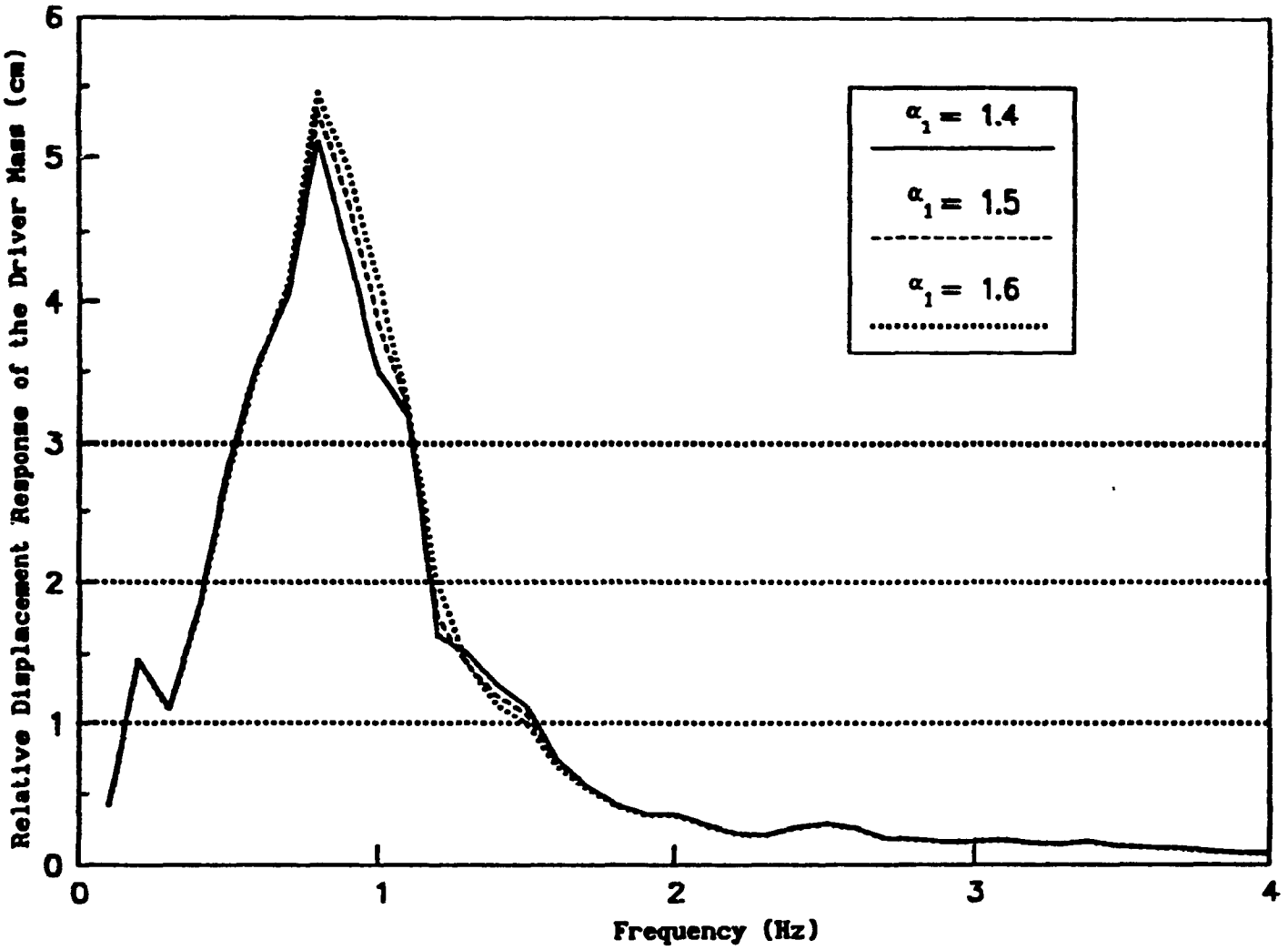

Fig.4.5 The Influence of the first Absorber Tuning Factor On the Relative Displacement Response of the Driver Mass

the peak of the relative displacement response of the driver mass.

4.3.2 Variation in Absorber Damping Ratio

As it has been shown before, the selection of absorber damping value is a trade-off between the effectiveness of vibration control around the tuned frequency and at other frequencies. For a single vibration absorber, it is impossible to avoid this compromise. It is shown by Snowdon[40] that with dual absorbers, it is possible to obtain a significant trough in transmissibility while avoiding the two resonant peaks of large magnitude that are normally introduced at neighboring frequencies. In the dual absorber system incorporated in a lateral seat suspension as shown in Fig.4.1, the absorber mass M_2 is assumed to be of greater mass with some damping (denoted by the damping ratio ξ_2). The second absorber is chosen to be of smaller mass M_3 than M_2 and has very little damping. For the purpose of comparison, the sum of absorber mass (M_2 and M_3) is kept equal to that of a single absorber, i.e. $\mu_1+\mu_2 = 0.4$. In this study, the tuning factor α_1 is assumed to be 1.5. The second absorber is tuned to the peak input ($\alpha_2 = 1.586$). The numerical values for the other parameters are given as follows:

$\xi_1 = 0.55$

$\mu_1 = 0.3$

$\xi_2 = 0.15$

$\mu_2 = 0.1$

The simulation results are plotted in Figs.4.6-4.9. The absolute transmissibility plot shows that the second absorber damping ratio ξ_3

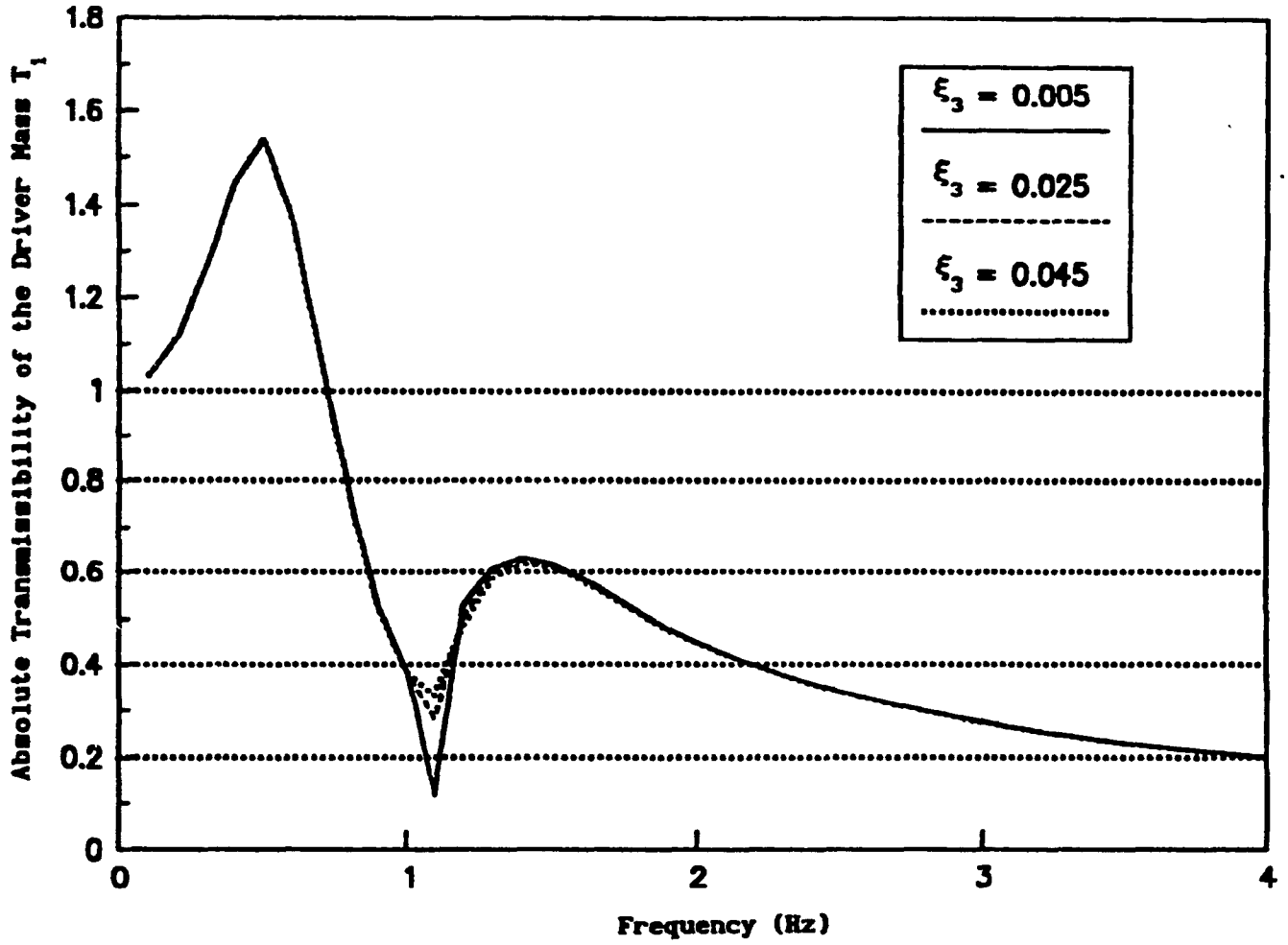

Fig.4.6 The Influence of the Second Absorber Damping Factor On the Absolute Transmissibility of the Driver Mass

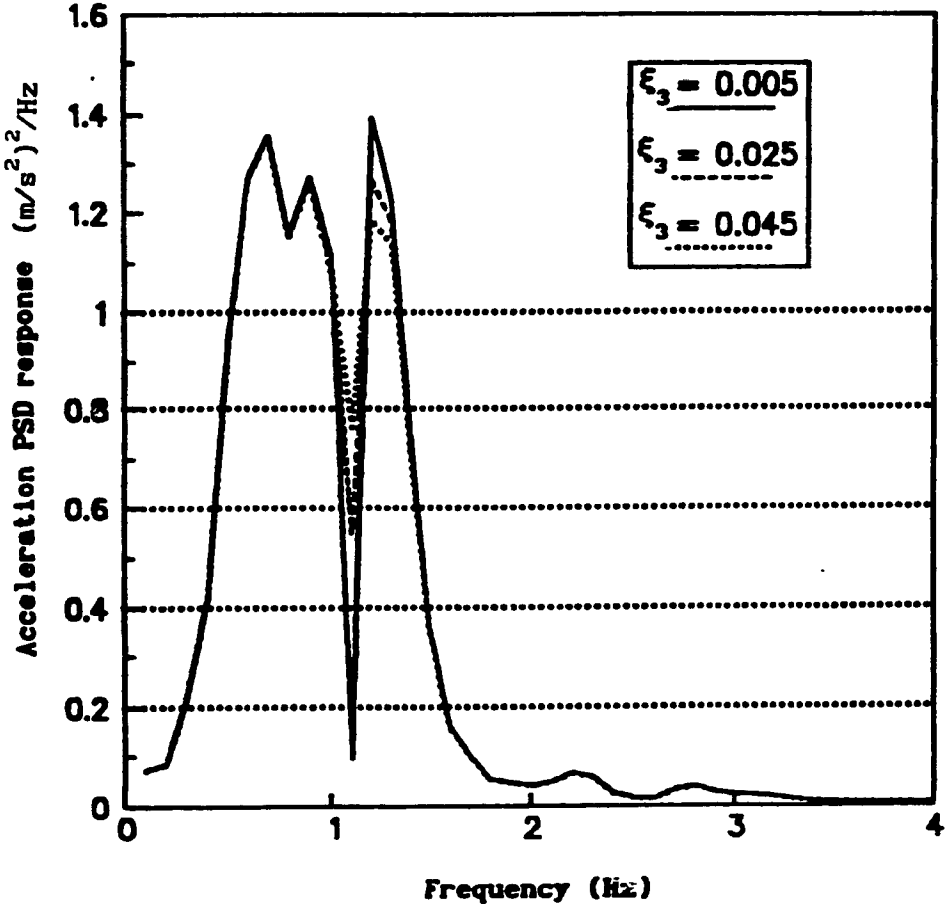

Fig.4.7 The Influence of the Second Absorber Damping Factor On the Acceleration PSD Response of the Driver Mass

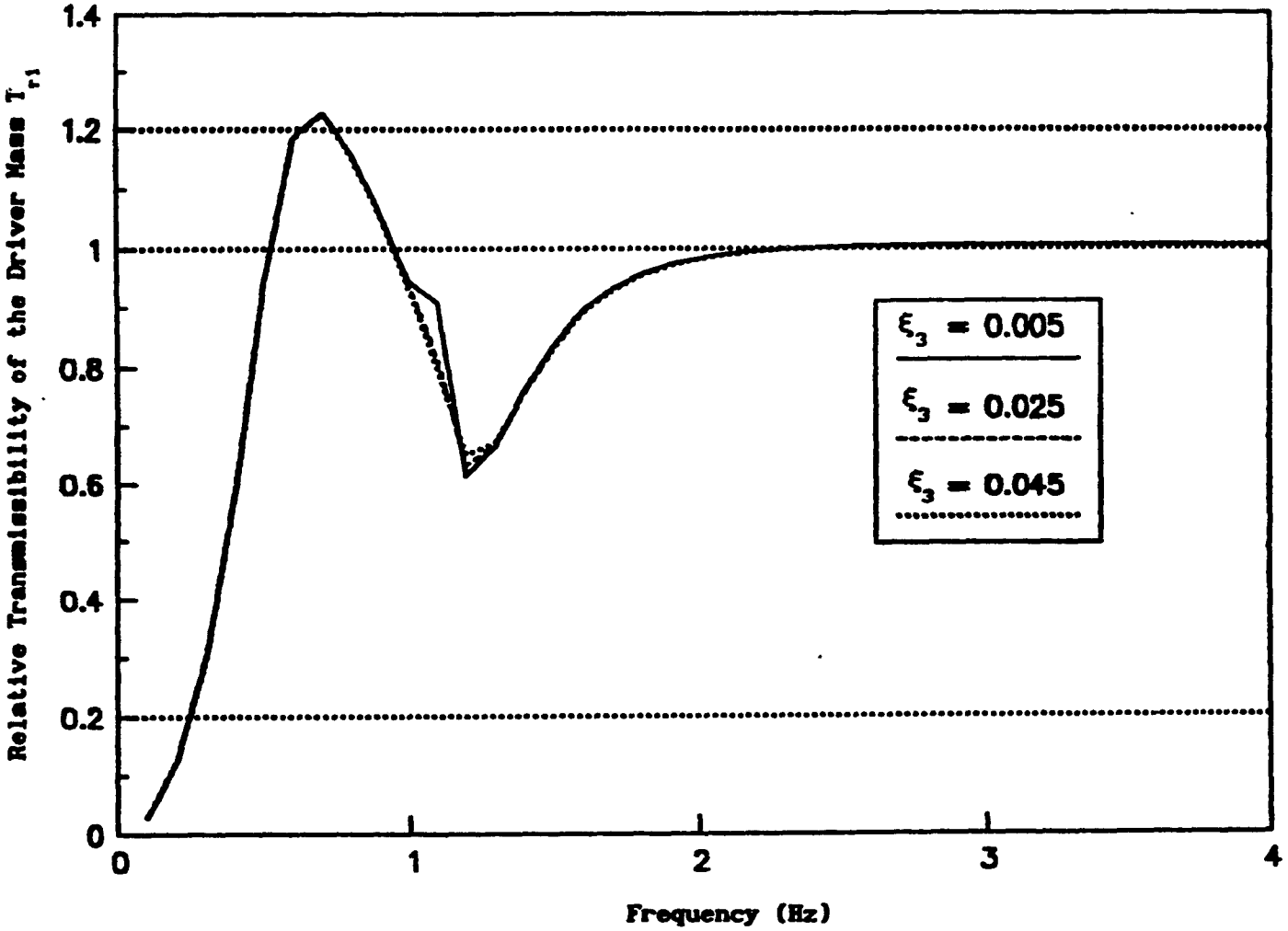

Fig.4.8 The Influence of the Second Absorber Damping Factor On the Relative Transmissibility of the Driver Mass

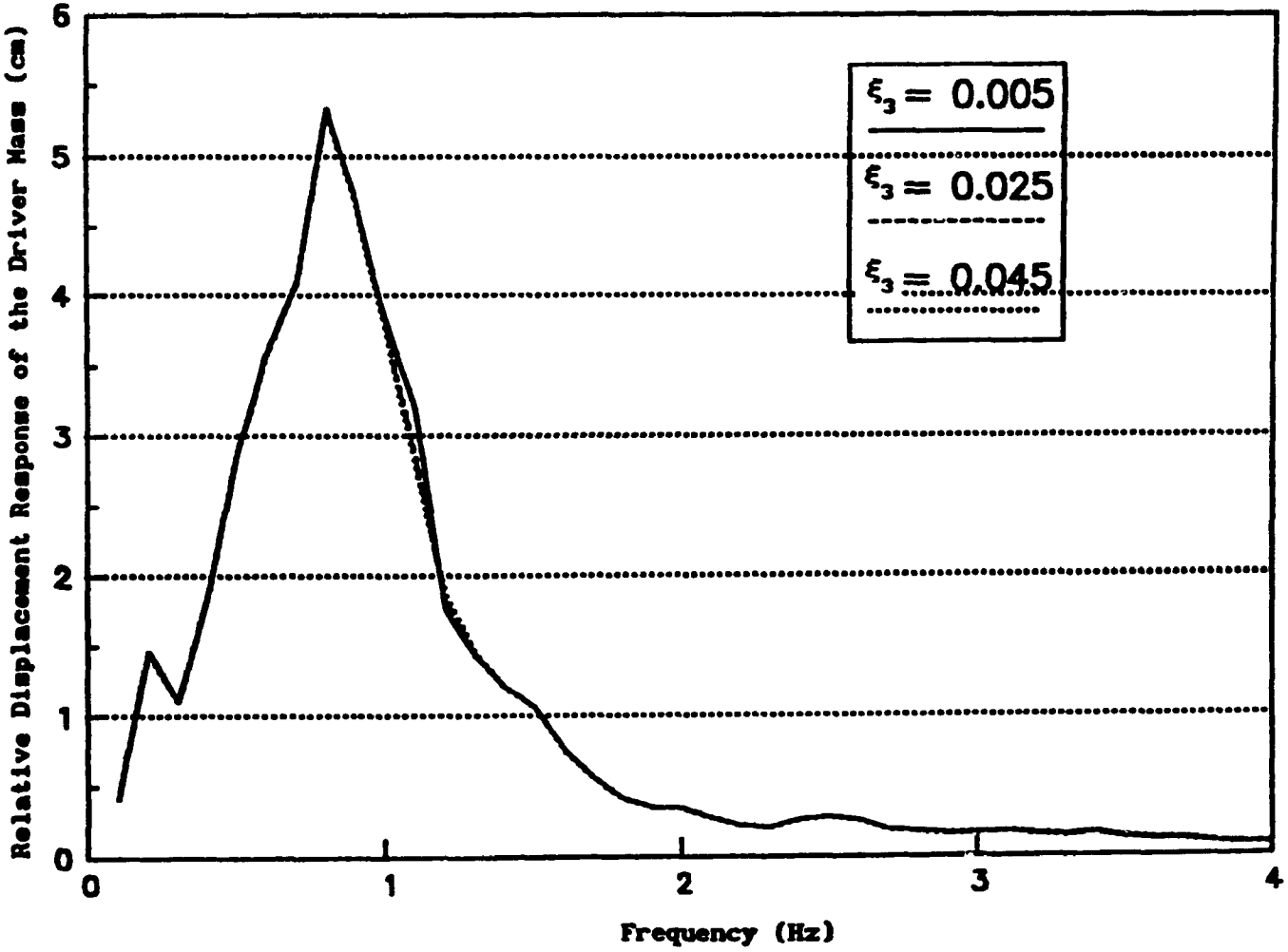

Fig.4.9 The Influence of the Second Absorber Damping Factor On the Relative Displacement Response of the Driver Mass

will greatly influence the effectiveness of vibration attenuation around the tuned frequency and the system's second resonant frequency. The influence of the second absorber damping ratio on the transmissibility at other frequencies is negligible. Comparing the results with that of lateral seat suspension with a single vibration absorber, the major difference is that, with dual absorbers, the acceleration PSD response at the tuned frequency can be significantly reduced without the cost of poor vibration attenuation at the system's second natural frequency.

The relative transmissibility plot, as shown in Fig.4.8, indicates that the second absorber damping ratio has visible influence only at the tuned frequency (because of the small mass of the second absorber). Since the displacement input at the tuned frequency is very small, the influence of the second absorber damping ratio on the relative displacement response can be neglected.

4.3.3 Variation in Absorber Mass Ratio

In the preceding simulation, the ratio of the two absorber mass ratio β ($\beta = M_3/M_2$), is assumed to be small. The influence of varying the absorber mass ratio on the vibration attenuation performance will be studied in this section. For the investigation, the total mass of the dual absorbers is kept unchanged. i.e. $\mu_1 + \mu_2 = 0.4$. The tuning factors and damping ratio of the two absorbers are given as follows:

$\alpha_1 = 1.5$

$\xi_2 = 0.15$

$\alpha_2 = 1.586$

$\xi_3 = 0.005$

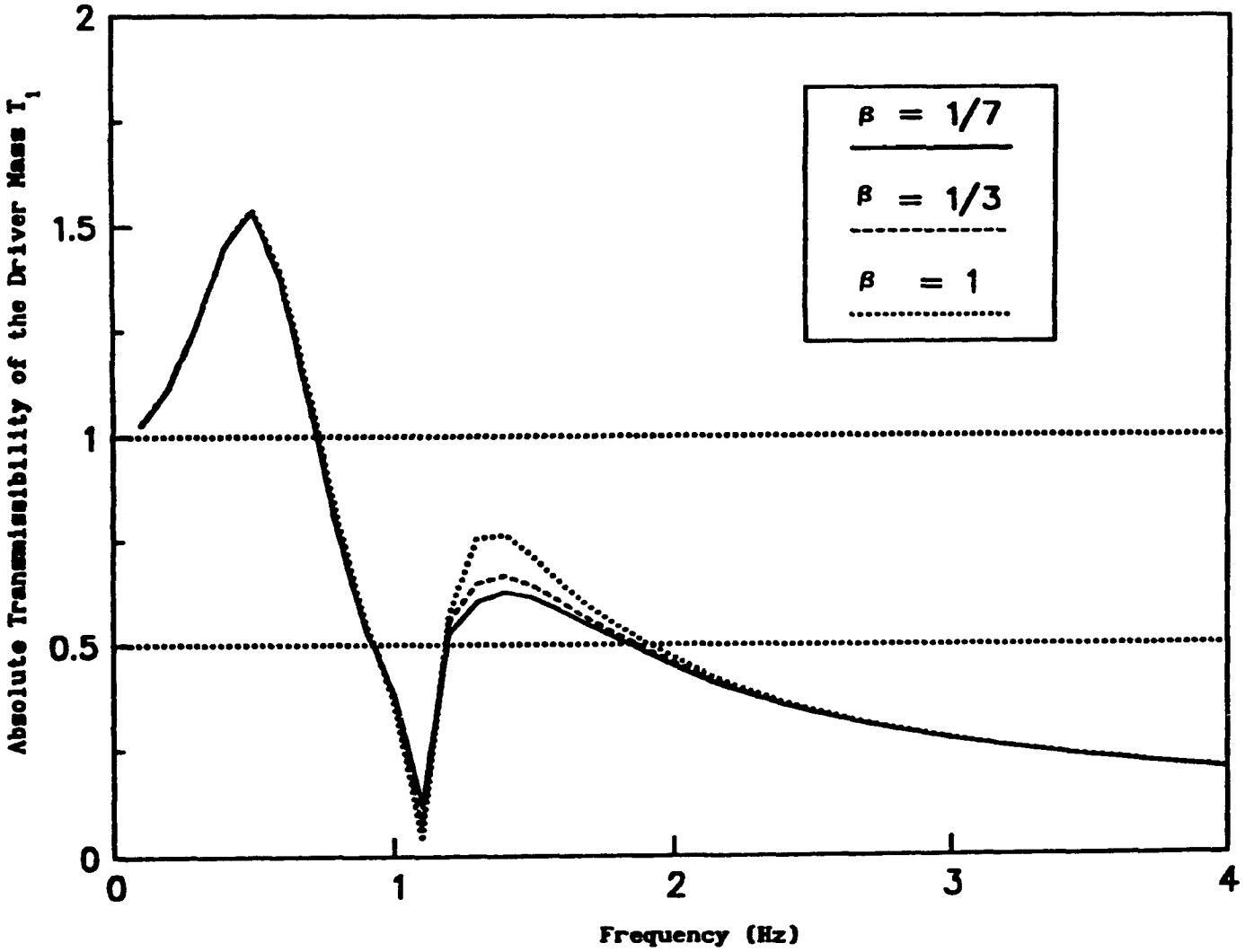

Fig.4.10 The Influence of the Two Absorber Mass Ratio β On the Absolute Transmissibility of the Driver Mass

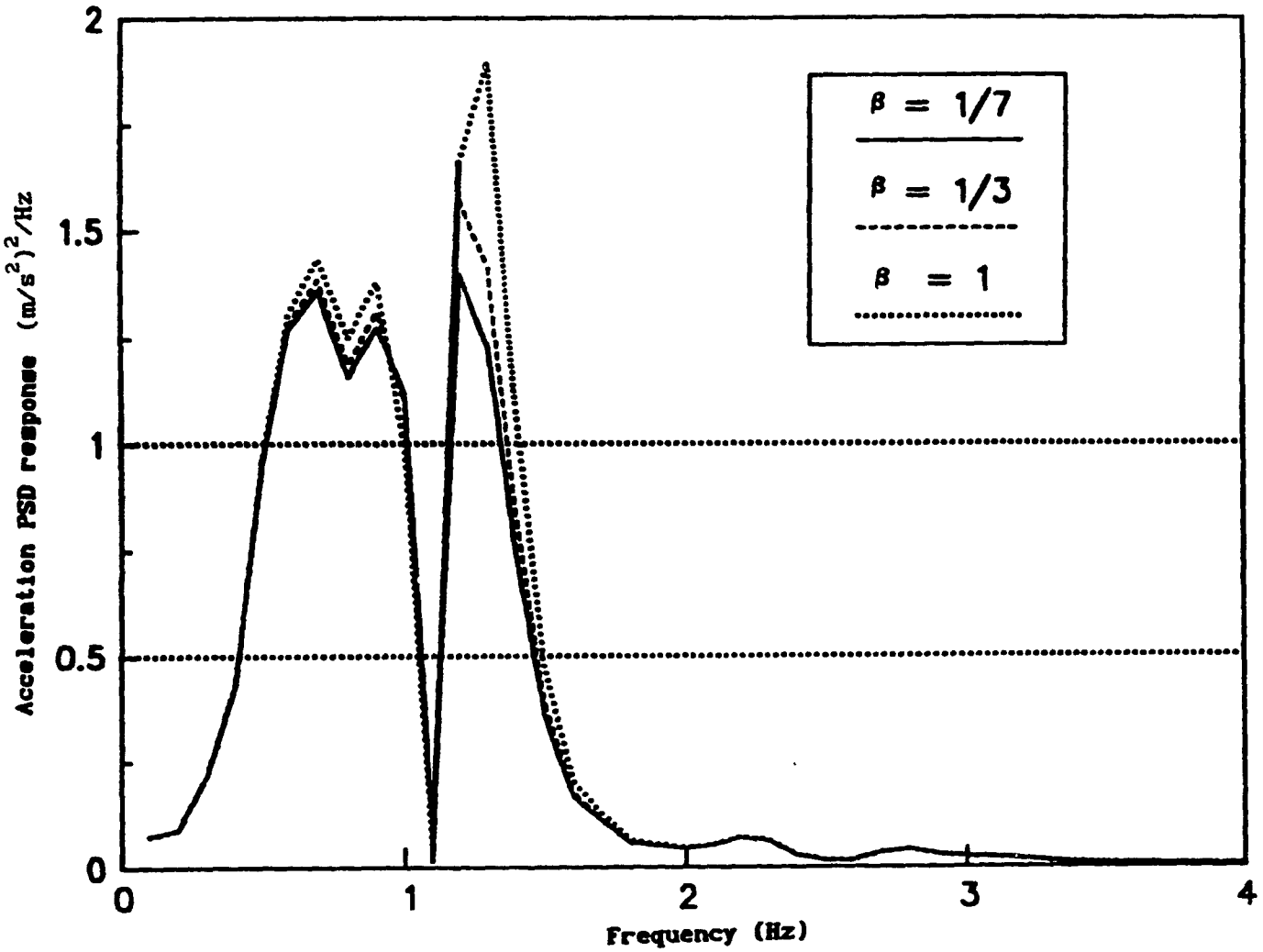

Fig.4.11 The Influence of the Two Absorber Mass Ratio β On the Acceleration PSD Response of the Driver Mass

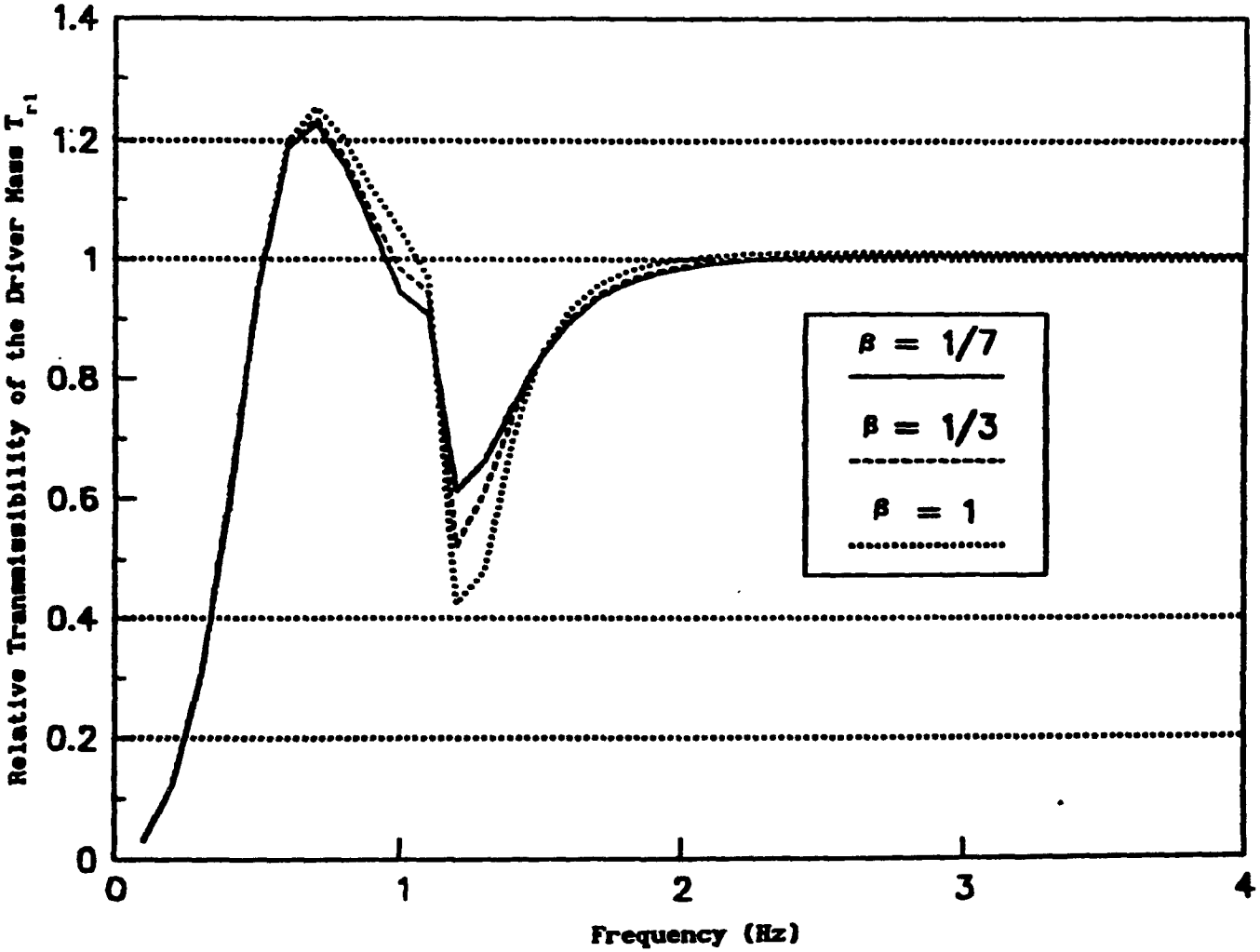

Fig.4.12 The Influence of the Two Absorber Mass Ratio β On the Relative Transmissibility of the Driver Mass

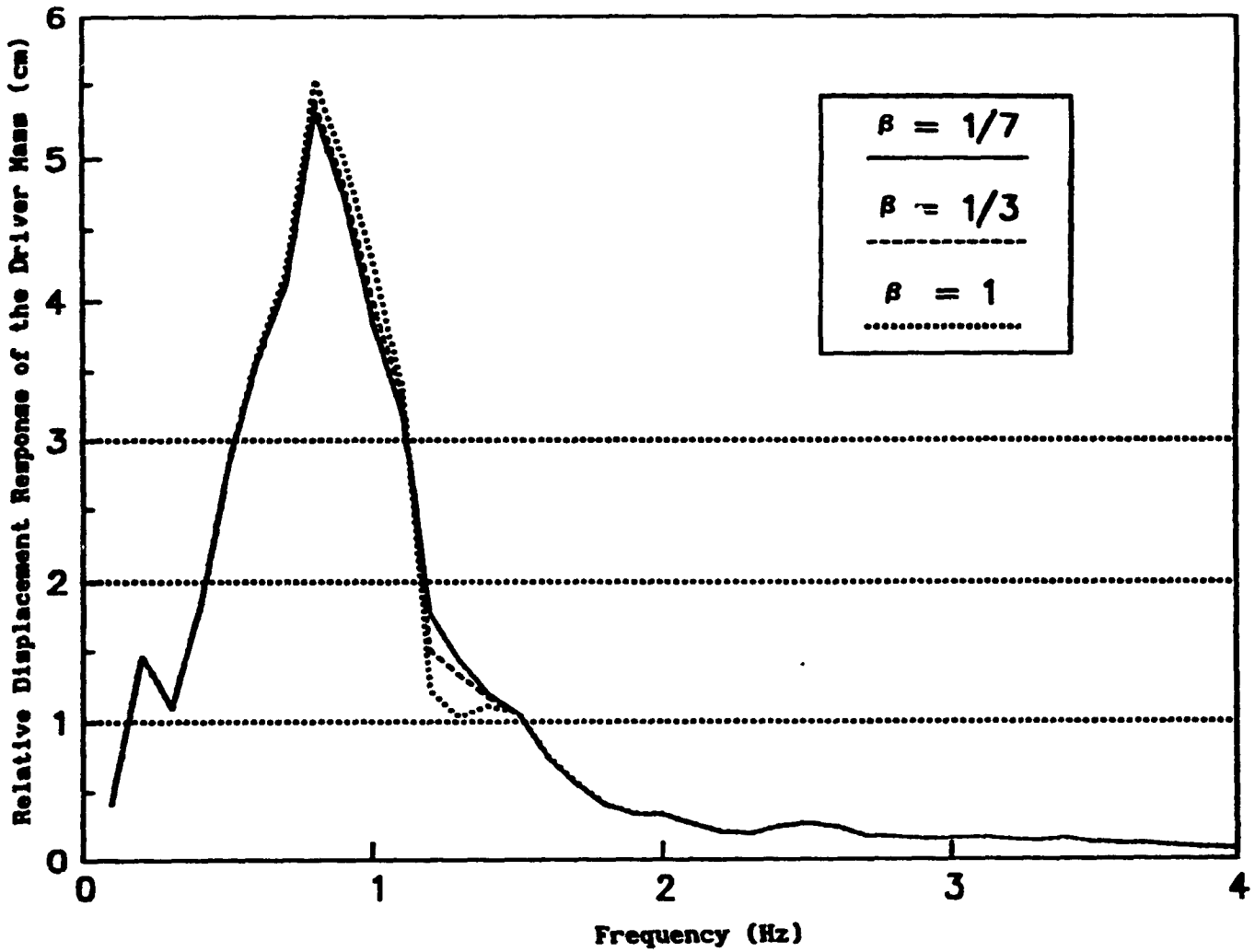

Fig.4.13 The Influence of the Two Absorber Mass Ratio β On the Relative Displacement Response of the Driver Mass

The simulation results are shown in Figs.4.10-4.13. It can be seen that increasing the absorber mass ratio β will have great influence on the second transmissibility peak and have little effect on the transmissibility at the tuned frequency. Increasing absorber mass ratio will introduce larger peaks in the acceleration PSD response at the system's resonant frequency. The relative displacement response of the driver mass also shows that small absorber mass ratio β has the advantage in suppressing the peak relative displacement response.

4.4 Conclusions

In this chapter, parametric study of dual absorbers is carried out. From the simulation results, the following conclusions can be made:

1. Dual absorbers can be used to reduce the vibration response at the tuned frequency without the drawback of introducing large motion response at the system's natural frequencies. The performance is very sensitive to the damping ratio of the second absorber ξ_3. In order to have effective vibration attenuation performance at the tuned frequency, the absorber damping ratio ξ_3 should be small.
2. The ratio of the two absorber mass β should be small so as not to introduce large vibration response at the system's natural frequencies.

CHAPTER 5

Parametric Optimization of Lateral Seat Suspensions

5.1 Introduction

In the previous chapters, the influence of varying a single parameter on the ride performance has been investigated when all other parameters are kept as constant. The parametric study reveals only the trend of the influence of each single parameter on the ride performance. In this chapter, the optimal suspension parameters will be sought by performing a constraint multi-parameter optimization. The influence of absorber mass on the ride performance will also be investigated to probe the trade-off between ride performance and the resultant system weight.

5.2 Formulation of the Optimization Problem

The objective in the design of a seat suspension is to achieve minimum acceleration level and smaller relative displacement response of the driver with respect to the cab floor. In addition to the ride requirement, the mass of the absorber should be as small as possible to achieve a lighter resultant suspension. The solution of such system can be viewed as a multi-objective, multi-parameter optimization problem. One simple way to address this issue is to assign some subjective weighting factors to each independent objective and create a new single objective by summing up all the objectives multiplied by their corresponding weighting factors. One difficulty associated with such an approach is the determination of the weighting factors for each objective. An alternate approach is to select from the objectives one that can be considered the most important criterion and the others are treated as constraints by

restricting the functions to be within some prescribed acceptable limits. In this study, the peak lateral acceleration response PSD in the frequency range 0-4 Hz is taken as the objective and the maximum amplitude of relative displacement of the driver mass is imposed as a constraint. The mathematical form for the optimization problem in its generic form is:

Minimize $F(\underline{X})$ with respect to $\underline{X}$,

Subjected to:

$$C_i(\underline{X}) \leq 0, \qquad i = 1,2,\ldots,m$$
$$E_j(\underline{X}) = 0, \qquad j = 1,2,\ldots,k \tag{5.1}$$

The vector $\underline{X}$ contains n unknown design variables which are to be calculated by minimizing the objective function $F(\underline{X})$. Any solution must also satisfy m inequality constraints $C_i(\underline{X}) \leq 0$ and k equality constraints $E_j(\underline{X}) = 0$. For this study, the constraint imposed on the design variables(absorber damping ratio, absorber tuning factor, absorber mass and main system damping ratio) is that they all possess positive values.

5.3 The Optimization Package PAROPT[41]

The optimization package used in this work is called PAROPT. It is an interactive, multiple choice optimization package. It can be used to solve unconstrained as well as constrained optimization problems.

The minimization algorithms in PAROPT basically solve the problem of finding the unconstrained minimum of a function of n variables:

$F(\underline{X})$, where $\underline{X}$ represents the vector $(x_1,x_2,\ldots,x_n)$ (5.2)

In order to find the optimum of a function which is subjected to inequality and/or equality constraints of the form:

$$C_i(\underline{X}) \leq 0, \qquad i = 1,2,---,m$$

$$E_j(\underline{X}) = 0, \qquad j = 1,2,---,k$$

a weighted penalty function is constructed to account for the constraints. A subroutine CONPEN is created to calculate the quantities

$$CN = \sum_{i=1}^{m} a_i C_i^2(\underline{X}) \qquad \text{and} \qquad EQ = \sum_{j=1}^{k} E_j^2(\underline{X}) \tag{5.3}$$

where

$$a_i = \begin{cases} 1 & \text{for } C_i(\underline{X})>0 \\ 0 & \text{otherwise} \end{cases}$$

The original constrained optimization problem is converted into an unconstrained optimization of the augmented objective function

$$f(\underline{X},W) = F(\underline{X}) + W*(CN + EQ) \tag{5.4}$$

where W is the weight of the penalty function.

The original constrained optimization problem is thus solved from the unconstrained augmented objective function $f(\underline{X},W)$.

To use the PAROPT optimization package, one has to provide a function subroutine which includes the objective function and constraints, as well as to define the design variables. Programs OPTIM1, OPTIM2 and OPTIM3 are developed for this purpose. Generally, no constraints have been imposed on the design variables other than that

they are of positive values.

5.3.1 Weighting Factor for the Penalty Function

From the augmented objective function $f(\underline{X},W)$, one can conclude that the value of $f(\underline{X},W)$ depends on the penalty weight if the inequality and/or equality constraints are violated. The selected value for the weight W should be large enough relative to the unconstrained function value to force the optimization process to move out of the constrained area, but not too large to cause difficulties such as floating point overflow. The weight for the calculation is chosen as 10^{25} for this investigation.

PAROPT optimization package provides nine unconstrained optimization algorithms for users. Algorithms can be classified under two categories: gradient-dependent optimal search and direct optimal search. The gradient-dependent optimal search requires that the derivative or differential of the objective function be available. Since the objective function in this investigation is the peak acceleration response PSD in the frequency range of interest, the derivative of the objective function is not readily available. Because of this, the gradient-dependent optimization methods are not suitable for the present study. In this investigation, a direct search technique, the SIMPLEX optimization algorithm is selected.

5.3.2 Evaluation of the Augmented Objective Function $f(\underline{X},W)$

The evaluation of the augmented objective function and the relative displacement constraint are carried out in the following way:

1. For an initial set of system parameter values, calculate the motion responses (acceleration and relative displacement responses) in the given

frequency range (0 - 4 Hz);

2 Find the maximum motion responses by comparing the responses at each excitation frequency;

3 Calculate the augmented objective function $f(\underline{X},W)$ according to Eqns. (5.3) and (5.4).

5.4 Sensitivity of Relative Displacement Constraint on the Peak Acceleration Response PSD

Studies in the optimal design of seat suspension systems have emphasized the trade off between the acceleration level transmitted and the relative displacement occurring between driver and control panels. The objective of optimal design of seat suspension is to achieve best ride comfort within the control safety limit. The optimization should then be formulated with the peak relative displacement constrained to be below the safety limit. Unfortunately, the safety limit for the lateral control has not been available. The upper bound of the relative displacement constraint is usually determined by the designer. The optimal results are based on this assumed constraint. The drawback of arbitrary selection of relative displacement constraint is that the designer has no knowledge of the severity of the influence of the relative displacement constraint imposed on the optimal results. In this study, sensitivity of relative displacement on the optimal acceleration response PSD is presented.

5.4.1 Optimization Results of a Lateral Seat Suspension with a Single Conventional Absorber

For the optimization of a lateral seat suspension, the main system damping ratio ξ_1, absorber damping ratio ξ_2 and absorber tuning ratio α are taken as design variables. The absorber mass ratio is taken as a

constant (μ=0.4).

The optimization results with a single conventional absorber are tabulated in Table 5.1. The influence of the variation in relative displacement constraint on the peak acceleration response, the optimal main system damping ξ_{1opt}, the optimal absorber tuning ratio α_{opt} and the optimal absorber damping ratio ξ_{2opt} are plotted in Fig.5.1. It can be seen that smaller peak acceleration response will result as larger relative displacement response is allowed. Variation in the optimal design variables and the objective function has its greater influence if small relative displacement is permitted. The variations decrease as larger displacement is allowed. For relative displacement greater than 5.1 cm, the influence of relative displacement constraint has negligible effect on the acceleration response. In such cases, the lowest minimum peak acceleration response is obtained.

The relative displacement constraint has strong influence on the optimal main system damping ratio. Larger main system damping is required for smaller relative displacement response. The relative displacement constraint has little influence on the optimal tuning ratio.

The optimal absorber damping ratio with variation in relative displacement constraint demonstrates that as the peak relative displacement constraint is increased, the ξ_2 initially decreases, then increases, and finally reaches a constant value.

5.4.2 Optimization Results With an Absorber Employing Elastically Coupled Damper

The optimization results with a single absorber employing elastically coupled damper are listed in Table 5.2 and plotted in Fig.5.2.

The effect of relative displacement constraint on the selection of

Table 5.1 Optimization Results with Variations in the Relative Displacement Constraint for a Single Conventional Absorber

Constraint	Optimal Design Parameters			Objective Function
$(Y_{r1})_{max}$ m	ξ_1	ξ_2	α	Peak Acc. PSD (m^2/s^4Hz)
0.015	3.055	0.193	1.391	4.744
0.020	2.787	0.095	1.506	3.353
0.025	1.979	0.114	1.498	2.846
0.030	1.446	0.130	1.495	2.397
0.035	1.139	0.132	1.498	2.056
0.040	0.931	0.136	1.498	1.784
0.045	0.766	0.136	1.500	1.543
0.050	0.636	0.128	1.506	1.325
0.051	0.570	0.166	1.481	1.293
0.055	0.570	0.166	1.481	1.293
0.060	0.567	0.166	1.481	1.293

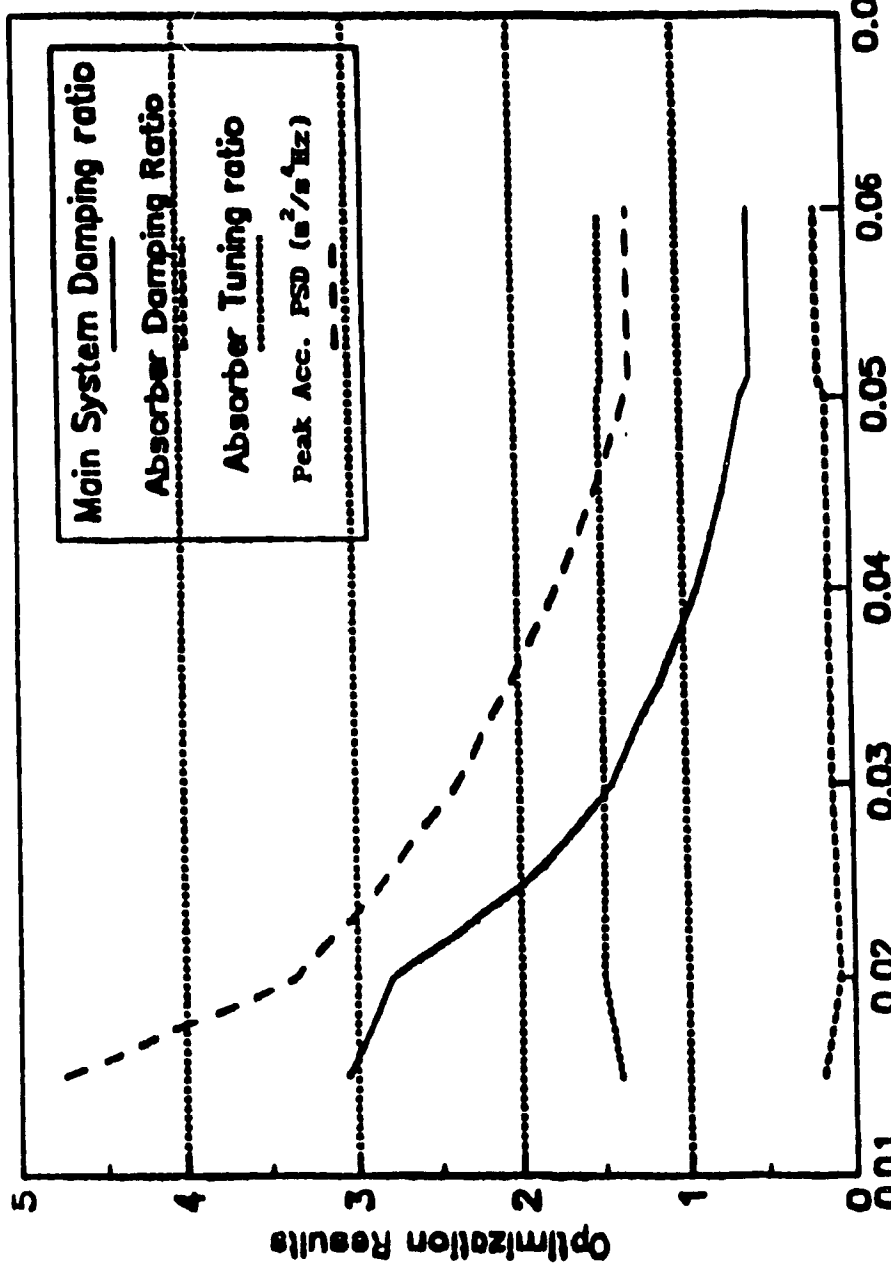

Fig.5.1 Influence of Relative Displacement Constraint on Optimization Results for a Conventional Absorber

Table 5.2 Optimization Results for Variations in the Relative Displacement Constraint in a Single Absorber with Elastically Coupled Damper

Constraint	Optimal Design Parameters				Objective Function
$(Y_{r1})_{max}$ m	ξ_1	ξ_2	α	Q	Peak Acc. PSD (m^2/s^4Hz)
0.015	3.152	0.491	1.344	4.589	4.613
0.020	2.806	0.278	1.477	3.330	3.295
0.025	1.979	0.451	1.431	2.403	2.758
0.030	1.415	0.605	1.384	2.347	2.265
0.035	1.115	0.623	1.378	2.451	1.920
0.040	0.899	0.750	1.348	2.350	1.637
0.045	0.732	0.521	1.404	3.089	1.435
0.050	0.561	0.800	1.313	3.641	1.188
0.055	0.561	0.800	1.313	3.641	1.188
0.060	0.561	0.800	1.313	3.641	1.188

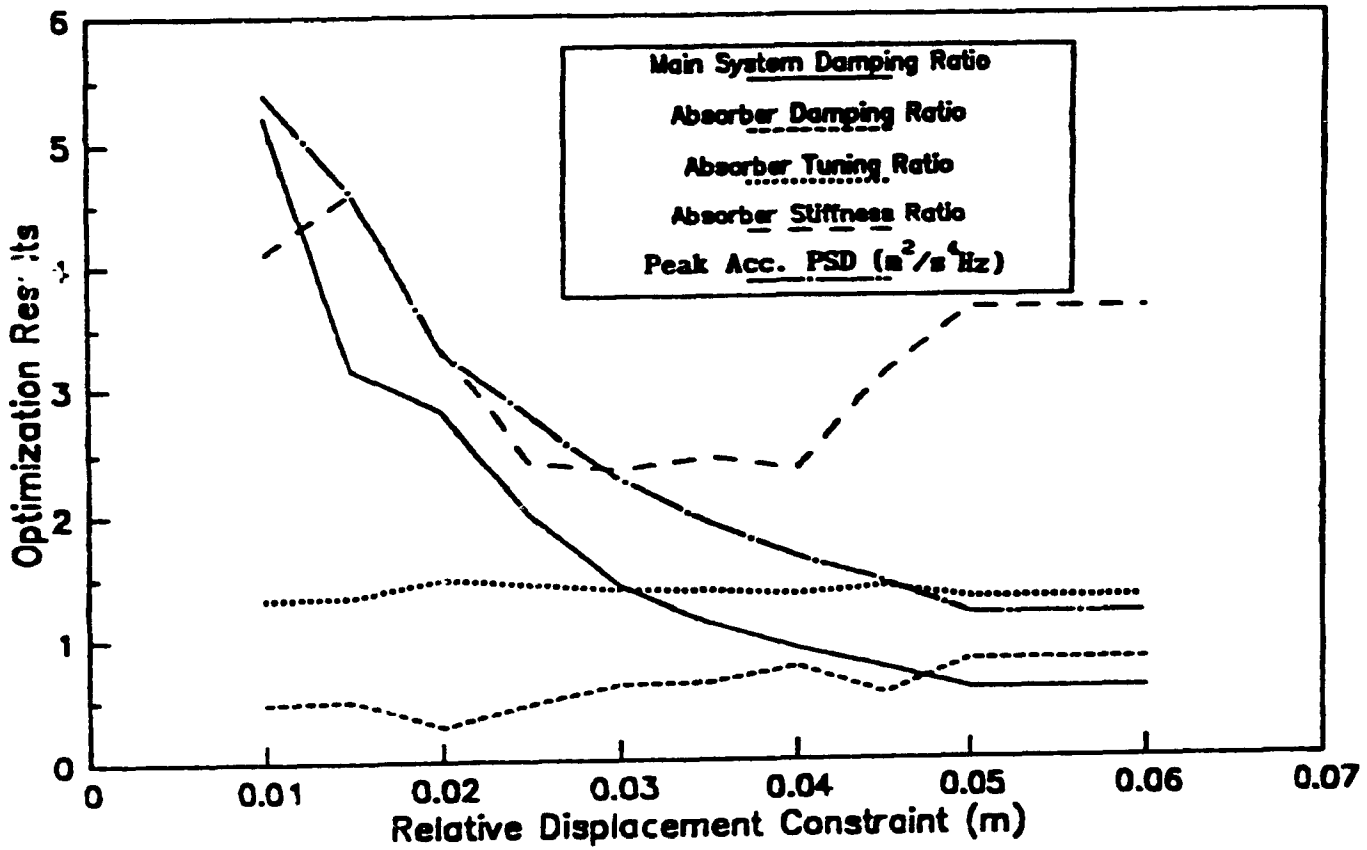

Fig.5.2 Influence of the Relative Displacement Constraint on Optimization Results for a Single Absorber with Elastically Coupled Damper

the optimal main system damping ratio, absorber damping ratio and the optimal tuning is similar to those with conventional absorber. The difference, however, is in the optimal absorber damping ratio of the three-element absorber, which is generally larger than that of conventional absorber.

The influence of the relative displacement constraint on the optimal absorber stiffness ratio is that as the peak relative displacement constraint is increased, the absorber stiffness ratio Q initially decreases, then increases, and finally reaches a constant value.

Comparing the acceleration results with those with conventional absorber, it can be concluded that the three-element absorber can provide marginaly improved ride performance.

5.4.3 Optimization Results With Two Conventional Absorbers

In the preceding sections, the parameter optimization of lateral seat suspension with single vibration absorber is presented. In this section, optimization algorithm will be applied to optimize the lateral seat suspension with two conventional absorbers. The mathematical equations for the motion transmissibility can be found in previous chapter.

The optimization results with two conventional absorbers are listed in Table 5.3. The sum of the two absorber mass is kept equal to the single absorber's mass for the purpose of comparison. The results show that two conventional absorbers behave slightly better than single conventional absorber for the relative displacement constraint below 2.5 cm or above 5 cm. For the relative displacement constraint between 3 cm and 4.5 cm, the optimal results indicate that two conventional absorbers are combined into one and thus behave basically the same as that of single conventional absorber.

Table 5.3 Optimization Results for Variations in the Relative Displacement Constraint Using Two Conventional Absorbers

Constraint	Optimal Design Parameters						Objective Function
$(Y_{r1})_{max}$ m	ϵ_1	ϵ_2	ϵ_3	μ_1	α_1	α_2	Peak Acc. PSD, m^2/s^4Hz
0.015	3.479	0.119	0.065	0.169	1.297	1.507	4.036
0.020	2.747	0.086	0.209	0.338	1.505	1.467	3.344
0.025	1.800	0.176	0.080	0.162	1.340	1.530	2.896
0.030	1.446	0.130		0.400	2.397		2.397
0.035	1.139	0.132		0.400	2.056		2.056
0.040	0.931	0.136		0.400	1.784		1.784
0.045	0.766	0.136		0.400	1.543		1.543
0.050	0.599	0.112	0.141	0.279	1.552	1.318	1.260
0.052	0.545	0.099	0.128	0.112	1.629	1.384	1.250

5.5 Sensitivity of Absorber Mass Ratio on the Lateral Ride Performance

The parametric study of the absorber mass ratio reveals that greater absorber mass ratio will give better ride performance, however, greater absorber mass will have the problem of heavier resultant system. The choice of the absorber mass is thus compromised between the ride performance and the system weight. In order to choose proper mass ratio, a sensitivity study is necessary. In this study, optimization algorithm is used to investigate the variation in absorber mass on the maximum acceleration response. Other parameters of the absorber and the main system damping ratio are also studied to investigate the influence of absorber mass on the selection of optimal values for these parameters.

The optimization results for a conventional absorber with mass ratio varying from 0.1 to 0.6 are listed in Table 5.4, The results are also plotted in Fig.5.3 and Fig.5.4.

The optimization results shows that the peak acceleration PSD response of driver mass decreases with the increasing absorber mass. The absorber mass ratio shows greater influence on the peak acceleration PSD response when μ is below 0.4. The variation in absorber mass has little influence on the absorber tuning ratio. Greater absorber mass requires higher main system damping to achieve optimization ride performance. Increasing absorber mass has the advantage of reducing the relative displacement response of the driver mass, but the improvement is very small for absorber mass ratio greater than 0.4.

The optimization results for an absorber employing elastically coupled damper are listed in Table 5.5 and presented in Fig.5.5 and Fig.5.6. Results show slightly better improvement in both acceleration response and relative displacement response over the suspension with a conventional absorber for all μ values. Since the damper is elastically

Table 5.4 Optimization Results for Variations in the Absorber Mass Ratio with a Single Conventional Absorber

Constraint	Optimal Design Parameters				Objective Function
μ	γ_{r1}	ξ_1	ξ_2	α	Peak Acc. PSD, m^2/s^4Hz
0.10	0.0673	0.376	0.078	1.486	2.945
0.15	0.0610	0.429	0.106	1.482	2.348
0.20	0.0575	0.464	0.129	1.481	2.000
0.25	0.0550	0.495	0.144	1.482	1.752
0.30	0.0530	0.524	0.154	1.483	1.568
0.35	0.0520	0.552	0.161	1.483	1.416
0.40	0.0510	0.576	0.166	1.483	1.293
0.45	0.0510	0.556	0.172	1.469	1.182
0.50	0.0500	0.588	0.175	1.474	1.091
0.55	0.0490	0.619	0.177	1.477	1.016
0.60	0.0490	0.649	0.178	1.480	0.952
0.70	0.0470	0.705	0.178	1.483	0.850

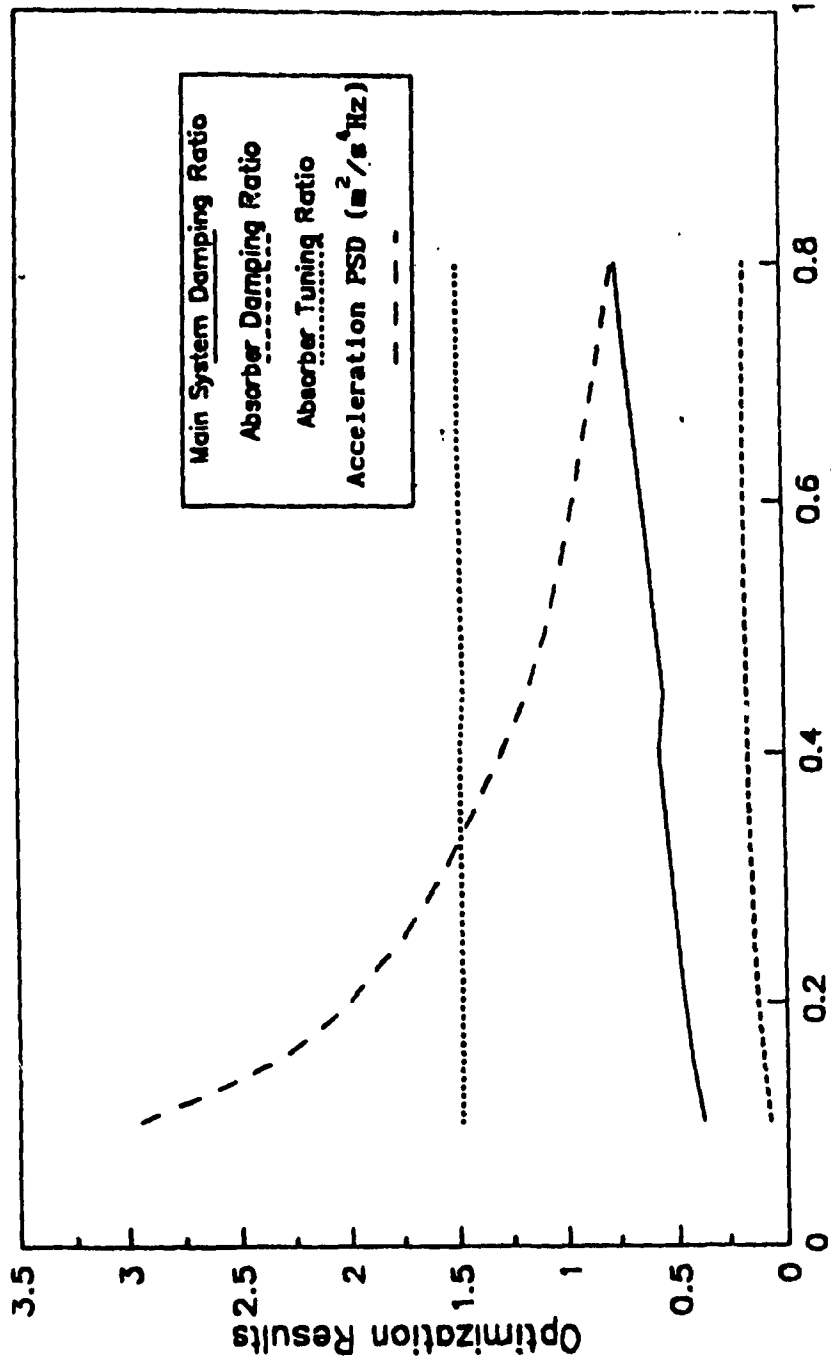

Fig.5.3 Optimization Results for Variations in the Absorber Mass Ratio for a Single Conventional Absorber

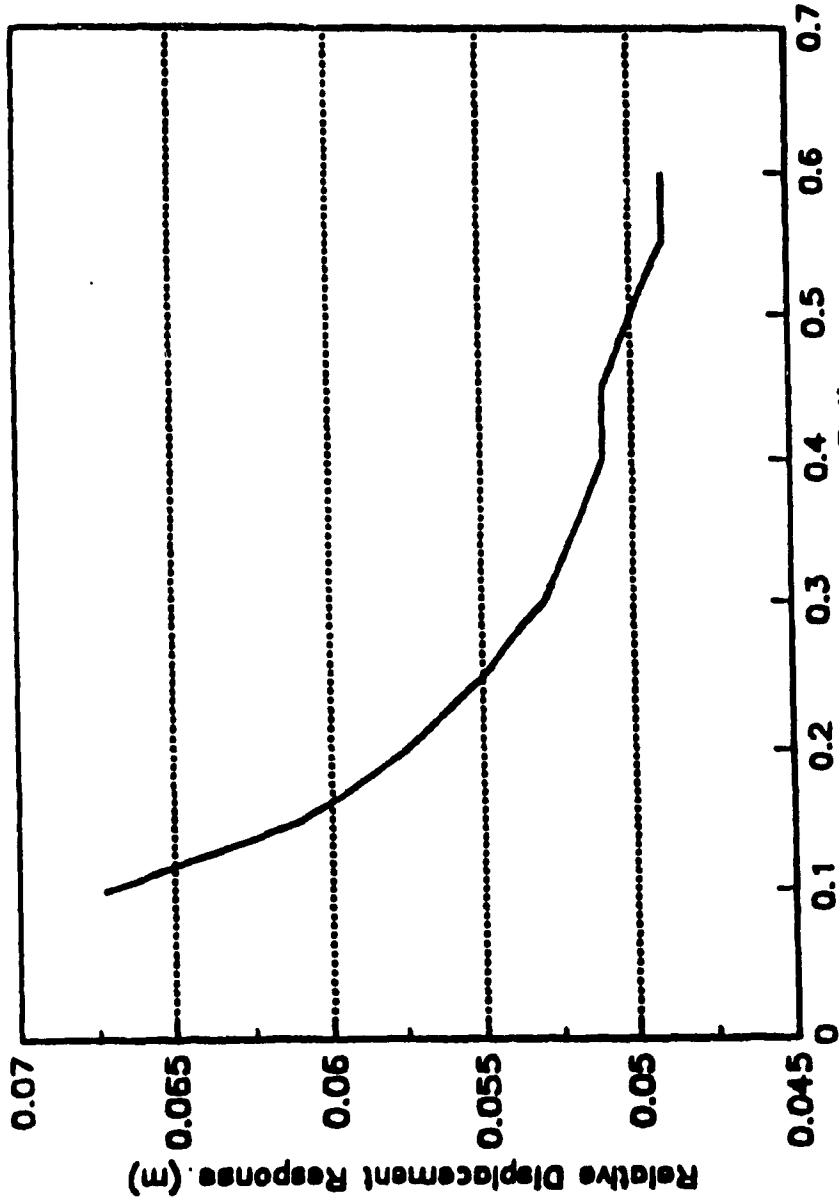

Fig.5.4 Influence of the Absorber Mass Ratio on the Peak Relative Displacement Response for a Single Conventional Absorber

Table 5.5 Optimization Results for Variation in the Absorber Mass Ratio for a Single Absorber with Elastically Coupled Damper

Constraint	Optimal Design Parameters					Objective Function
μ	γ_{r1}	ξ_1	ξ_2	a	Q	Peak Acc. PSD, a^2/a^4Hz
0.10	0.067	0.376	0.245	1.465	3.509	2.917
0.15	0.061	0.431	0.317	1.451	3.458	2.314
0.20	0.057	0.464	0.490	1.403	2.731	1.943
0.25	0.054	0.497	0.485	1.407	3.080	1.697
0.30	0.053	0.510	0.727	1.333	2.626	1.473
0.35	0.051	0.554	0.482	1.413	3.603	1.362
0.40	0.050	0.545	0.800	1.307	2.718	1.184
0.45	0.049	0.588	0.786	1.316	2.690	1.085
0.50	0.049	0.610	0.577	1.377	3.215	1.026
0.55	0.048	0.642	0.570	1.380	3.229	0.958
0.60	0.047	0.677	0.800	1.313	2.700	0.869

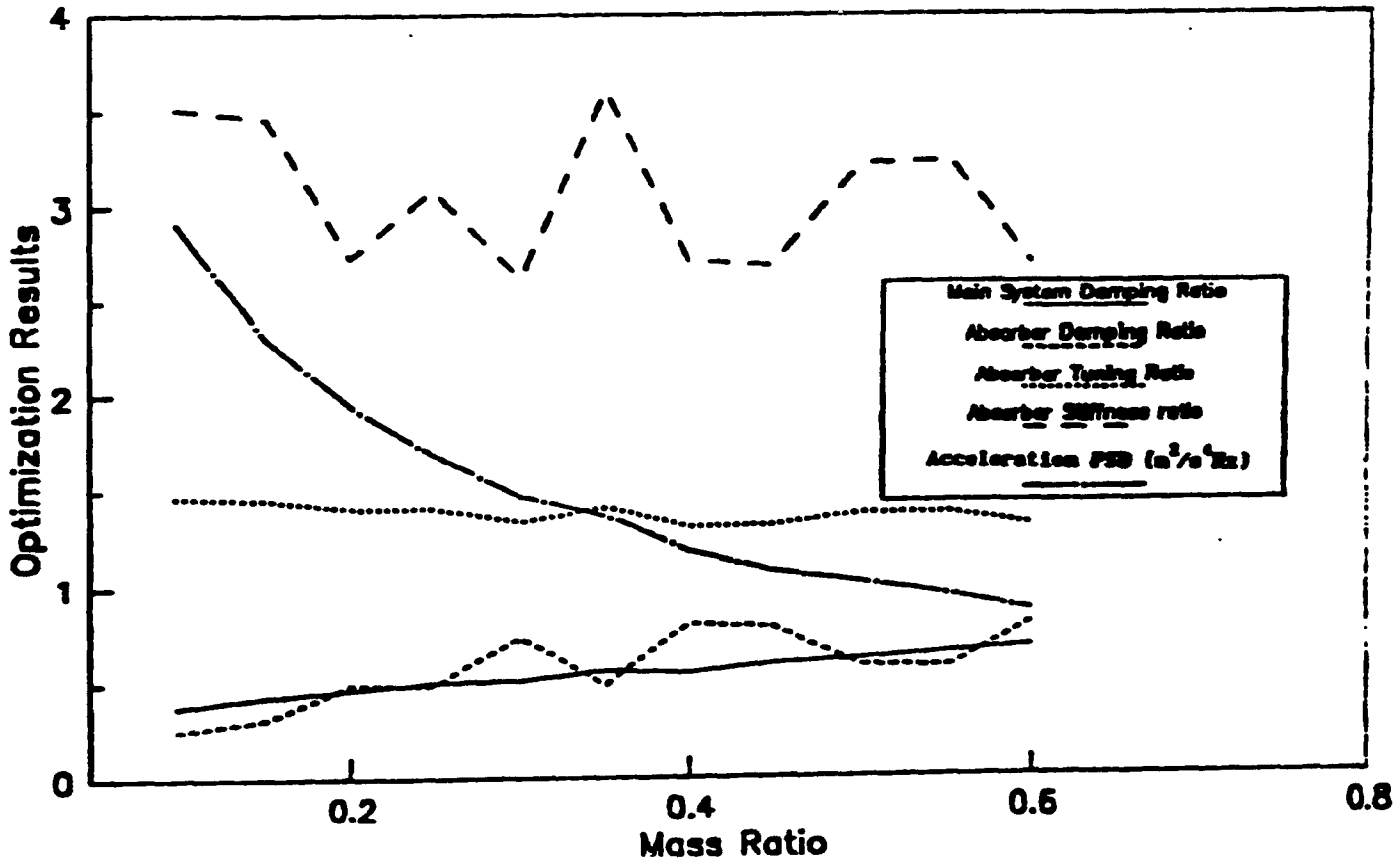

Fig.5.5 Optimization Results for Variations in the Absorber Mass Ratio for a Single Absorber with Elastically Coupled Damper

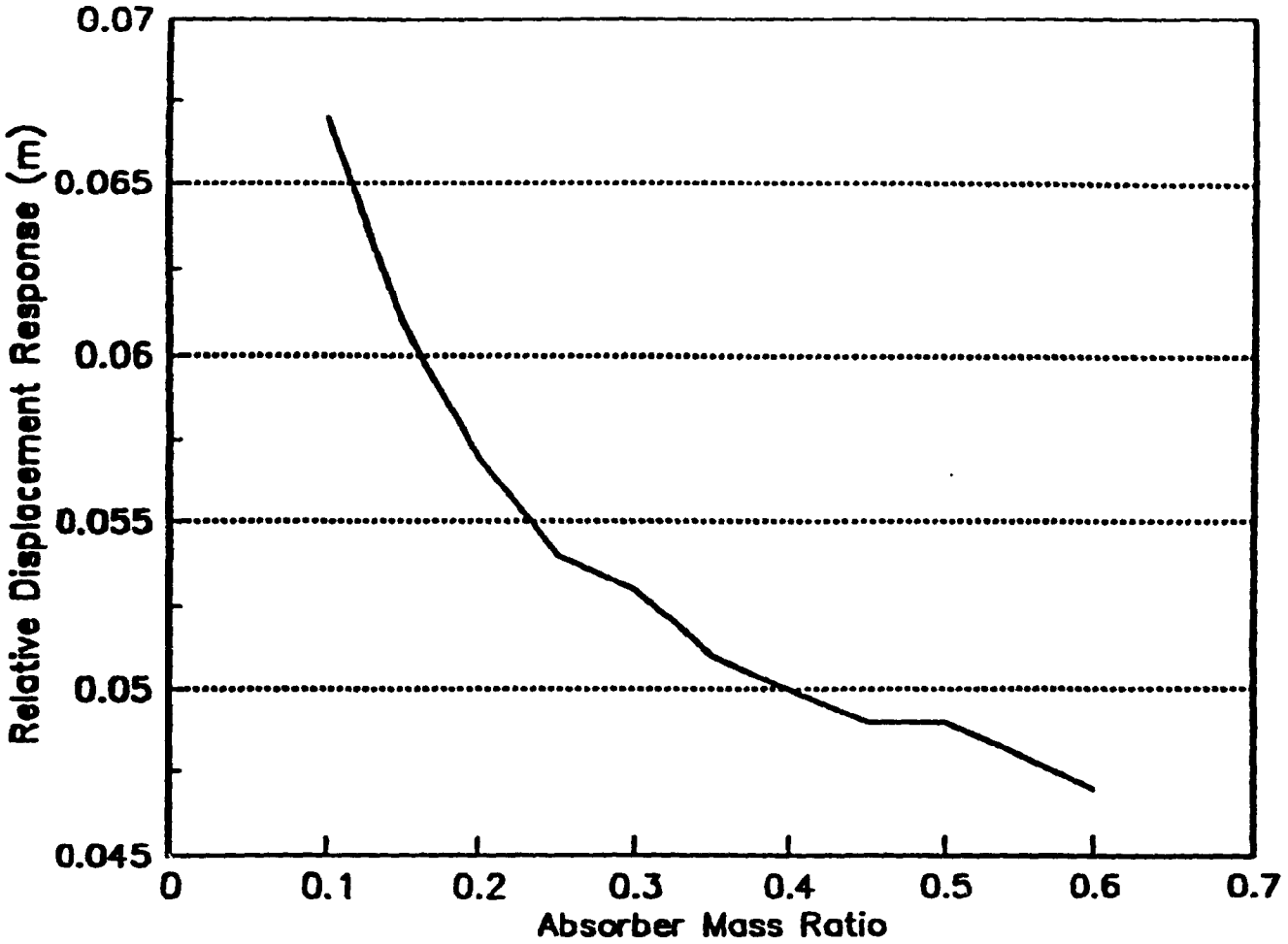

Fig.5.6 Influence of Absorber Mass Ratio on the Peak Relative Displacement Response in a Single Absorber with Elastically Coupled Damper

coupled, the absorber damping ratio corresponding to the optimal design is higher than the values required for conventional absorber. The main system damping ratios required for the optimal conditions also increase as greater absorber mass is used.

5.6 Comparison of Vibration Isolation Performance of Different Seat and Cab Suspensions

The parameter optimization of lateral seat suspensions with absorber has been presented in the previous sections. In this section, the effectiveness of vibration isolation performance of different lateral seat suspensions with absorber will be compared with the motion response level of the driver mass with seat suspension without absorber and seat/cab suspension systems. The acceleration and relative displacement response of the driver mass for different optimal suspension systems[4] are presented in Figs.5.7 and 5.8. It can be seen that seat suspensions with vibration absorber can provide much better vibration isolation for off-road vehicle operator than seat suspension only. All of the three types of seat suspension with dynamic absorber provide approximately 80% vibration attenuation in acceleration PSD response for the driver without lowering the spring stiffness rate of the primary system. The vibration isolation performance of seat suspensions with absorber is comparable or even slightly better than a system with optimal cab and seat of suspensions. Among the three types of lateral seat suspensions with absorber, the suspension with three-element absorber has the best acceleration isolation performance. The simulation results also indicate that the optimal seat suspension with absorber produces approximately cm greater relative displacement response for the vehicle operator. The peak relative displacement response of three kinds of lateral seat suspension systems with absorber is almost identical.

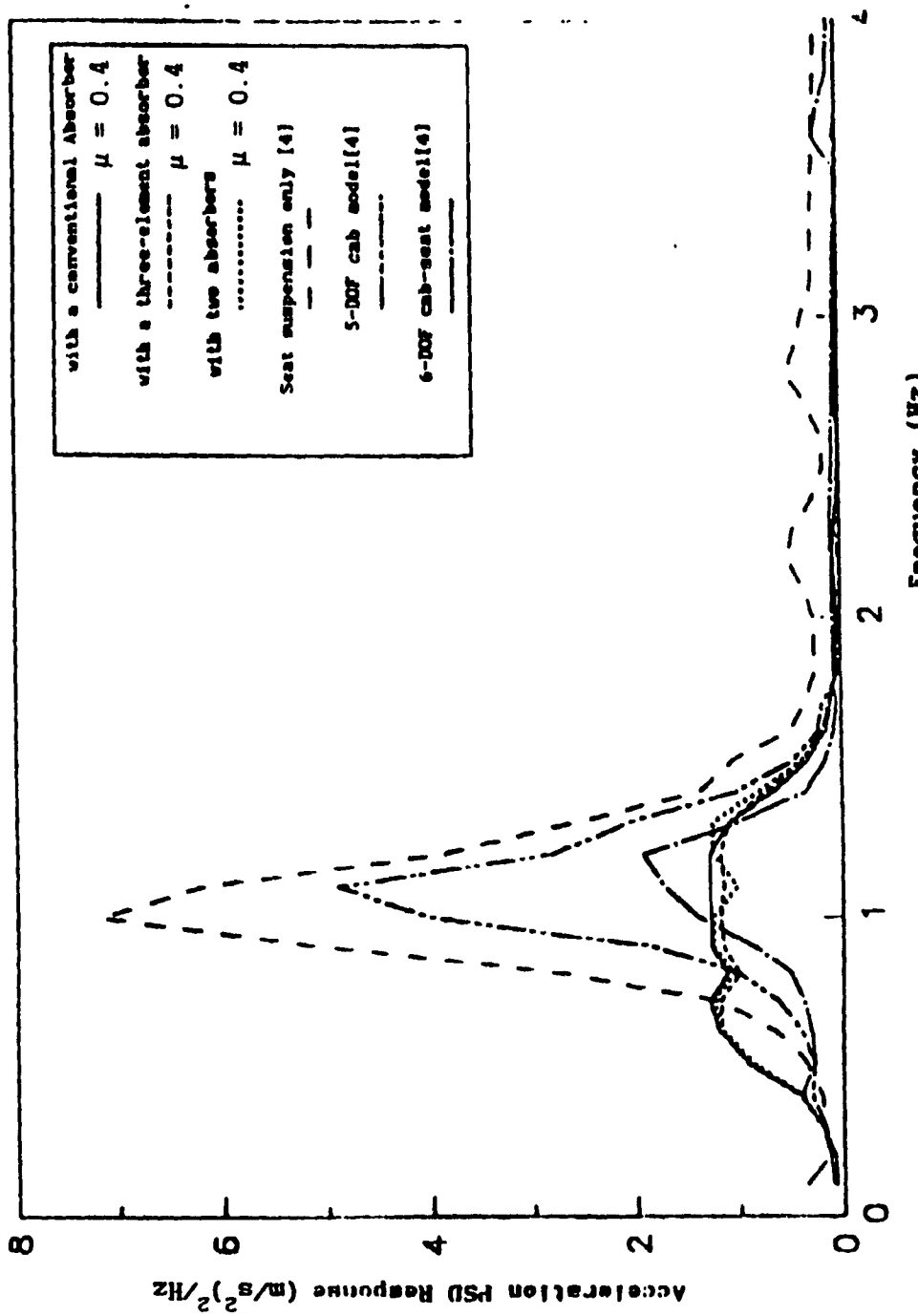

Fig.5.7 Acceleration PSD Response of The Driver Mass with Different Cab and Seat Suspensions

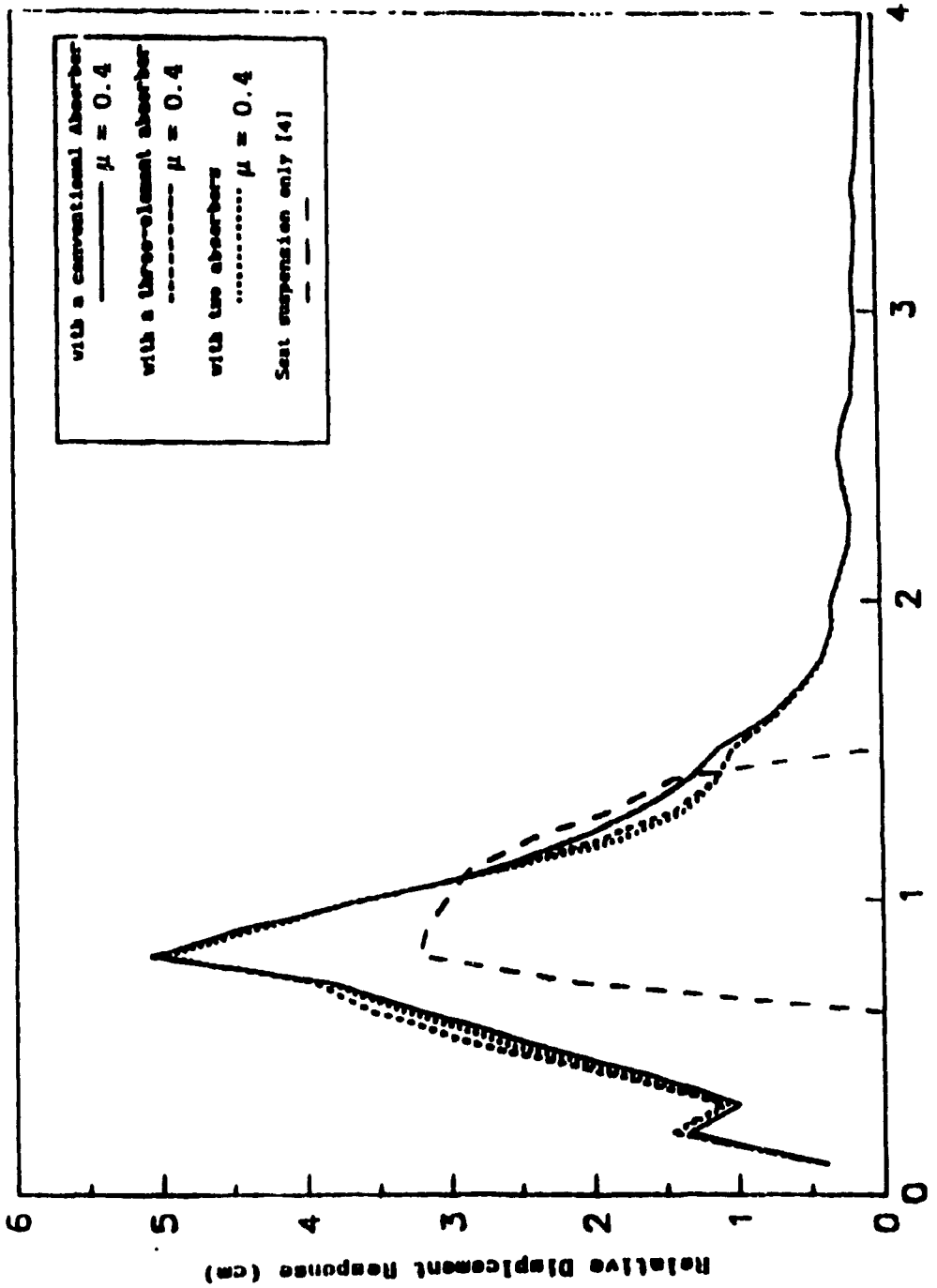

Fig.5.8 Relative Displacement Response of The Driver Mass with Different Cab and Seat Suspensions

5.7 Conclusions

In this chapter, a nonlinear direct search optimization algorithm is applied to investigate the effects of the relative displacement constraint and the absorber mass ratio on the ride performance as well as the optimal system parameters. The vibration isolation performance of different suspension systems are compared with respect to the acceleration and relative displacement responses of the driver mass. From the simulation results, the following conclusions can be drawn:

1. The upper bound of the relative displacement constraint must be chosen properly. The trade-off between better ride (smaller acceleration response) and better vehicle control (smaller relative displacement response) exists only when the relative displacement is within some limit. Below this limit, the optimization results will be affected by the relative displacement constraint. However, if the upper bound of the constraint is set beyond the limit, the relative displacement constraint will not be active and the optimization results are hardly optimal. The above results are obtained with the assumption of constant spring rate of the primary system.

2. The upper bound of the relative displacement constraint has strong influence on the adoption of the optimal main system damping but has no influence on the selection of the optimal tuning. Generally, the absorber damping ratio is small. The optimal absorber damping falls between 0.1 - 0.2.

3. Three-element absorber shows slightly superior performance over the conventional absorber. Two conventional absorbers also work slightly better than single conventional absorber for some settings of the relative displacement constraint.

4. Larger absorber mass ratios result in smaller attainable acceleration

and relative displacement response of the driver mass, and also, greater absorber mass requires both larger main system damping ratio and absorber damping ratio.

5. In order to achieve a good compromise between the ride performance and the weight of the system, the absorber mass ratio should be chosen less than 0.4.

6. All of the three types of lateral seat suspensions with absorber can provide excellent acceleration attenuation performance.

CHAPTER 6

Conclusions and Recommendations for Future Work

6.1 Conclusions

In this thesis, parametric study as well as parameter optimization of different schemes of lateral seat suspensions with dynamic vibration absorbers are conducted. From the simulation results, the following conclusions can be drawn:

The lateral ride can be significantly improved by the attachment of vibration absorber to the primary lateral seat suspension. The lateral seat suspensions with vibration absorber show better vibration isolation performance than the suspension without absorber. The low frequency vibration excitation can be effectively attenuated by the addition of vibration absorber without the need for lowering the stiffness value of the primary suspension.

Among the three different types of suspension systems, the seat suspension with a three-element absorber show the best vibration isolation performance. The lateral seat suspension with dual absorbers having the total mass equivalent to the single absorber also show better vibration reduction performance for some settings of the relative displacement constraint.

An increase in the absorber mass always results in the reduction of the motion response of both the driver and the absorber mass. However, the mass ratio greater than 0.4 is usually undesirable due to relatively very little ride improvement that can be achieved and large weight of the resultant system.

The selection of the absorber damping ratio is compromised due to the isolation performance around the tuned frequency and other frequencies away from the tuned frequency, especially at the system's second natural frequency. Small absorber damping ratio provides good acceleration isolation around the tuning frequency but poor acceleration response for excitation frequencies away from the tuned frequency. For reducing the relative displacement response of the absorber mass, greater absorber damping ratio is always desirable.

The natural frequency of the absorber should be tuned around the excitation frequency where intensive vibration inputs occur. Since the peak input excitation of the acceleration and the displacement do not occur at the same frequency, the selection of the tuning ratio become a compromise between the attenuation of the acceleration and the relative displacement response. From the point of acceleration attenuation, the tuning ratio should be around 1.5, however, reduction of the relative displacement response requires smaller tuning ratio. With the proper selection of the absorber tuning ratio, both acceleration and relative displacement responses of the driver mass can be reduced.

The selection of the main system damping ratio offers a compromise between low and high frequency performance. The importance of damping ratio on the isolation performance at each excitation frequency is weighted by the varying amplitudes of the excitation inputs.

The implementation of dual absorbers can effectively reduce the vibration response of driver mass without introducing large resonant response at system's natural frequencies.

6.2 Recommendations For Future Work

Although the attachment of a vibration absorber to a seat suspension can provide much better ride for the driver than the conventional seat suspension, the vibration level experienced by the driver is reduced only to the ISO-2.5 hour fatigue decreased proficiency limit. In order to provide the driver, a working environment with vibration level below the ISO recommended 8-hour fatigue decreased proficiency limit, two-stage vibration isolation (cab suspension and seat suspension) is necessary. Future research may be conducted towards the development and simulation of cab and seat suspension with vibration absorbers.

In order to verify the simulation results, experimental work on the lateral seat suspensions with a vibration absorber is recommended.

The limitation of a passive vibration absorber is its narrow vibration suppression bandwidth. Research efforts may be contributed towards the development of a semi-active or active absorbers for lateral seat suspensions, which can provide vibration suppression over a wider frequency range.

REFERENCES

1. Matthews, J., 1964, "Ride Comfort for Tractor Operators: Review of Existing Information," Journal of Agricultural Engineering, pp.3-31.

2. Roley, D.G., 1975, "Tractor Cab Suspension Performance Modeling," Ph.D. Thesis Univ. of California, Davis.

3. Rakheja, S. and Sankar, S., 1984, "Suspension Designs to Improve Tractor Ride: I. Passive Seat Suspension," Society of Automotive Engineers, Paper No. 841107.

4. Rakheja, S., 1983, "Computer Aided Dynamic Analysis and Optimal Design of Suspension Systems for Off-Road Tractors," Ph.D. Thesis, Concordia Univ.

5. Claar II, P.W., Buchele W.F., and Sheth, P.N., 1980, "Off-Road Vehicle Ride: Review of Concepts and Design Evaluation with Computer Simulation," International Off-Highway Vehicle Meeting and Exposition. MECCA, Milwaukee.

6. Crolla, D.A., 1981, "Off-Road Vehicle Dynamics," Vehicle System Dynamics, Vol. 10, pp.253 - 266.

7. Golich, H. and Weigelt, H., 1985, "Improvements of the Drivers Comfort and Safety By Means of Vibration Reduction," Ergonomics International, pp.220-222.

8. Rakheja, S., Sankar, S., and Afonso, M, 1989, "Cab Suspension for Off-Road Vehicles: A Review of the State-of the Art," CONCAVE Report 11-89, Concordia University.

9. Venkatesan, C. and Krishnan, R., 1975, "Harmonic Response of A Shock Mount Employing Dual-Phase Damping," Journal of Sound and Vibration, Vol.40, pp.409-413.

10. Snowdon, J.C., 1970, "Isolation from Mechanical Shock with a

Mounting System Having Nonlinear Dual Phase Damping," The Shock and Vibration Bulletin, No. 41, Part 2.

11. Stikleather, L.F. and Suggs, C.W., 1970, "An Active Seat Suspension System for Off-Road Vehicles," Transactions of the ASME, 13(1), pp.99-106.

12. Young, R.F. and Suggs, C.W., 1973, "Seat Suspension Systems for Isolation of Roll and Pitch in Off-Road Vehicles," Transactions of the ASAE, 16(5), pp.876-880.

13. Kyeong U.K., Dean L.H., and Donnell, R.H., 1985, "Ride Simulation of Passive, Active and Semi-active Seat Suspensions for Off-Road Vehicles," Transactions of the ASAE, pp.56-64.

14. Harris and Crede, 1976, "Shock and Vibration Handbook," Second Edition. McGraw-Hill Inc.

15. Den Hartog, J.P., 1956, "Mechanical Vibrations," McGraw-Hill, New York.

16. Thompson, A.G., 1981, "Optimum Tuning And Damping Of A Dynamic Vibration Absorber Applied To A Forced Excited And Damped Primary System," Journal of Sound and Vibration, 77(3), pp.403-415.

17. Randall, S.E., 1981, "Optimum Vibration Absorbers for Linear Damped Systems," Journal of Mechanical Design, Vol.103, pp.908-913.

18. Puksand, H., 1975, "Optimum Conditions for Dynamic Vibration Absorbers for Variable Speed Systems With Rotating or Reciprocating Unbalance," IJMEE, Vol.3, No.2 pp.145 - 152.

19. Kojima, H. and Saito, H., 1983, "Forced Vibrations of Beam with A Nonlinear Dynamic Vibration Absorber," Journal of Sound and Vibration, 88(4), pp.559-568.

20. Soom, A. and Ming-san, L., 1983, "Optimal Design of Linear and Nonlinear Vibration Absorbers for Damped Systems," Journal of Sound and

Vibration, Vol.105, pp.112-119.

21. Jordanov, I.N. and Cheshankov, B.I., 1988, "Optimal Design of Linear and Nonlinear Dynamic Vibration Absorbers," Journal of Sound and Vibration, 123(1), pp.157-170.

22. Ghoneim, H., and Metwalli, S.M. 83-DET-42, "Optimum Vehicle Suspension With a Damped Absorber," Journal of Mechanisms, Transmissions, and Automation in Design, pp. 1-8.

23. Hunt, J.B., 1979, "Dynamic Vibration Absorber," Mechanical Engineering Publications Ltd., London.

24 Shotwell, D.B., "Application of the Tuned and Damped Dynamic Absorber to Rubber-Tired Earthmoving Machines," ASME Preprint Paper No.67-Vibr-64 for Meeting 29-31 March 1967.

25 Inoh, T. and Aisaka, M., 1973, "Tuning Techniques for Controlling Heavy-Duty Truck Shake — Vertical, Tortional and Lateral," SAE Preprint Paper No.730650 for Meeting June 18-22.

26. International Organization for standardization, 1974, "Guide for Evaluation of Human Exposure to Whole Body Vibration," ISO 2631, 1974(E).

27. Newland, D.E., 1975, "An Introduction to Random Vibrations and Spectral Analysis," Longman Group Limited.

28. Hullender, D.A., 1979, "Generation Of A Random Time Series With A Specified Spectral Density Function," Proc. Joint Automatic Control Conference, Denver, Colo, June 17-21, Publ. by AICHE, New York, N.Y., 1979, pp.532-535.

29. Dhir, A., 1988, "Ride Dynamics of Heavy Vehicles Using local Equivalent Linearization Technique," Master Thesis, Concordia University.

30. Rakheja, S. and Sankar, S., 1984, "Suspension Design to Improve Tractor Ride: II. Passive Cab Suspension," Society of Automotive

Engineers, Paper No. 841108.

31. Craig, C.S., 1976, "On Using the ISO To Evaluate the Ride Quality of Broad-Band Vibration Spectra in Transportation Vehicles," Transactions of the ASME, pp.440-443.

32. Tambe, U.V., Chandrasekharappa, G. and Srirangarajan, H.R., 1988, "Voigt Dynamic Vibration Absorber," Journal of Sound and Vibration, 124(2), pp.381-384.

33. Hunt, J.B. and Nissen, J.C., 1982, "The Broadband Dynamic Vibration Absorber," Journal of Sound and Vibration, 83(4), pp.573-578.

34. Vakakis, A.F. and Paipetis, S.A., 1986, "The Effect of A Viscously Damped Dynamic Absorber On A Linear Multi-Degree-Of-Freedom System," Journal of Sound and Vibration, 105(1), pp.49-60.

35. Bapat, V.A. and Kumaraswamy, H.V., 1979, "Effect Of Primary System Damping On The Optimum Design Of An Untuned Viscous Dynamic Vibration Absorber," Journal of Sound and Vibration, 63(4), pp.469-474.

36. Thompson, A.G., 1980, "Auxiliary Mass Throw In A Tuned And Damped Vibration Absorber," Journal of Sound and Vibration, 70(4), pp.481-486.

37. Thompson, A.G., 1980, "Optimizing The Untuned Viscous Dynamic Vibration Absorber With Primary System Damping: A Frequency Locus Method," Journal of Sound and Vibration. 73(3), pp.469-472.

38. Bapat, V.A. and Kumaraswamy, H.V., 1979, "Effect Of Primary System Damping Of An Untuned Viscous Dynamic Vibration Absorber," Journal of Sound and Vibration, 63(4), pp.469 - 474.

39. Bapat, V.A. And Prabhu, P., 1979, "Optimum Design Of Lanchester Damper For A Viscously Damped Single Degree Of Freedom System By Using Minimum Force Transmissibility Criterion," Journal of Sound and

Vibration, 67(1) pp.113 - 119.

40. Snowdom, J.C., 1974, "Dynamic Vibration Absorbers That Have Increased Effectiveness," Transactions of ASME, pp.940-945.

41. Division of Mechanical Engineering, NSERC, 1987, "The Manual of Optimization Package PAROPT".

42. Lee, S., and Sinha, A., 1986, "Design of An Active Vibration Absorber. Journal of Sound and Vibration," Vol.109(2), pp.347-352.

43. Thompson, W., 1988, "Theory of Vibration With Applications," Prentice Hall.

44. Stephen, H.C., and William, D.M., 1963, "Random Vibration in Mechanical Systems," Academic Press, New York and London.
The United Kingdom and French Joint Meeting on Human Response to Vibration," Vandoeuvre, France, Sept.26-28.

45. Wang, B.P., Kitis, L., Pilkey, W.D. and Palazzolo, A., 1985, "Synthesis of Dynamic Vibration Absorbers," Journal of Vibration,. Acoustics, Stress, and Reliability in Design, Vol.107, pp.161-166.

46. Matthews, J., 1966, "Ride Comfort for Tractor Operators IV: Assessment of the Ride Quality of Seats," J. Agric. Engr. Res., Vol.11, pp.44-57.

47. Kitis, L., Wang, B.P. and Pilkey, W.D., 1983, "Vibration Reduction Over A Frequency Range," Journal of Sound and Vibration, 89(4), pp.559-569.

48. Ghonein, H. and Cheema, R.A., 85-DET-68. "On the Application of Optimum Damped Absorber to Vehicle Suspension," Journal of Mechanisms, Transmissions , and Automation in Design, pp.1-3.

49. Nobile, M.A.and Snowdon, J.C., 1977, "Viscously Damped Dynamic Absorbers Of Conventional And Novel Design," Journal of Acoustic Society of American, Vol.61 , No.5, pp. 1198 - 1208.

50. Hunt, J.B. and Nissen, J.C. 1982, "The Broadband Dynamic Vibration Absorber," Journal of Sound and Vibration, Vol.4, pp.573-578.